Excitations in the higher-lattice gauge theory model for topological phases. II. The (2+1)-dimensional case

Joe Huxford [1,2] and Steven H. Simon [1]

[1] *Rudolf Peierls Centre for Theoretical Physics, Clarendon Laboratory, Oxford OX1 3PU, United Kingdom*

[2] *Department of Physics, University of Toronto, Toronto, Ontario M5S 1A7, Canada*

(Received 6 August 2022; revised 18 October 2023; accepted 31 October 2023; published 12 December 2023)

In this work, the second paper of this series, we study the (2+1)-dimensional version of a Hamiltonian model for topological phases based on higher-lattice gauge theory. We construct the ribbon operators that produce the pointlike excitations. These ribbon operators are used to find the braiding properties and topological charge carried by the pointlike excitations. The model also hosts looplike excitations, which are produced by membrane operators. By considering a change of basis, we show that, in certain cases, some looplike excitations represent domain walls between patches corresponding to different symmetry-related ground states, and we find this symmetry. We also map the higher-lattice gauge theory Hamiltonian to the symmetry-enriched string-net model for symmetry-enriched topological phases described by Heinrich, Burnell, Fidkowski, and Levin [Phys. Rev. B **94**, 235136 (2016)], again in a subset of cases.

DOI: 10.1103/PhysRevB.108.245133

I. INTRODUCTION

In this series of papers, we are examining the commuting projector model for topological phases from Ref. [1], based on higher-lattice gauge theory (see also Refs. [2–7] for further work on these phases, as well as Refs. [8–10] for work on similar models). In the previous paper in this series, we discussed the higher-lattice gauge theory model in 3+1 dimensions [(3+1)D], but the model can also be defined in 2+1 dimensions [(2+1)D], as discussed in Ref. [1] (with a generalization of this (2+1)D model also studied in Ref. [7]). This lower-dimensional case exhibits interesting properties in its own right. Despite the spatial lattice being 2D, the model hosts looplike excitations. Furthermore, the ground state on a sphere is generally degenerate [1]. These features are both somewhat unusual, and are not found in generic models for (2+1)D topological phases. We will find that, in certain cases, both of these features can be explained by an additional, spontaneously broken, symmetry. The looplike excitations (or at least a subset of them) form domain walls between patches corresponding to the different ground states. In these cases, the model is therefore an example of a so-called "symmetry-enriched topological phase," or SET phase.

In an SET phase, in addition to long-range entanglement, there is an enforced symmetry [11,12]. This can be contrasted with a symmetry-protected topological phase (SPT phase), which is a short-range entangled phase where the degrees of freedom can be "disentangled" smoothly into a product state with a suitable local unitary evolution, but only by breaking the symmetry [12,13]. When considering additional enforced symmetries, the space of phases becomes even richer, and so there has been considerable interest in SET phases, and Hamiltonian models describing them [11,14–29]. One Hamiltonian model of particular interest is the symmetry-enriched string-net model of Ref. [16], which generalizes the Levin-Wen string-net model [30] to allow for an additional symmetry. In this symmetry-enriched string-net model, which we describe in more detail and relate to the higher-lattice gauge theory model in Sec. VIII, there are additional degrees of freedom on the plaquettes of the 2D lattice, with the symmetry affecting these degrees of freedom. In some cases this symmetry may permute the anyons of the model, converting one anyon type into another (although we do not find this feature for the higher-lattice gauge theory model).

Another interesting feature exhibited by the higher-lattice gauge theory model is condensation and confinement. This refers to the situation where some topological charges join the topological vacuum (trivial charge) [31–35]. During this process some charges become confined, so that it costs energy to separate an anyon from its associated antianyon. The theory of anyon condensation in (2+1)D is well developed [31–35], and commuting projector models that exhibit this property include the family examined in Ref. [36], which is a generalization of Kitaev's quantum double model [37]. Indeed, we will draw on the methods developed in Ref. [36] to explicitly show which topological sectors are confined. We do this by constructing the topological charge measurement operators and demonstrating that certain measurement operators are only compatible with confined excitations.

There are other advantages to considering the higher-lattice gauge theory model in (2+1)D, despite the existence of the (3+1)D model. The first advantage is theoretical: there already exists a well-understood structure for considering many topological phases in (2+1)D. Bosonic topological phases are believed to be characterized by modular tensor categories, along with the chiral central charge and other objects

relating to any symmetry present [15,26,27]. In addition, many features of topological phases in (2+1)D, including the previously mentioned condensation and confinement, have been extensively studied compared to their (3+1)D counterparts. This gives us a framework with which to understand the features of any particular topological phase, but it also means that any physics found outside the accepted structure would be an interesting challenge to existing knowledge. The other advantage is more pragmatic: there are by now many examples of experimentally observed (2+1)D topological phases, including fractional quantum Hall systems [38–42] as well as small fabricated systems [43]. It is therefore more realistic to suppose that a (2+1)D phase may be observed in experiment than a (3+1)D one (at least for the near future).

A. Structure of this paper

Here we briefly outline the layout of the rest of this paper. We begin in Sec. II by reminding the reader of some concepts and mathematical ideas discussed in Ref. [44]. Then in Secs. III and IV we start describing our results by presenting the *ribbon operators* in (2+1)D, for two of the special cases described in Ref. [44] and more concisely here in Sec. II (cases 1 and 3 from Table I). Ribbon operators create, annihilate, and move the quasiparticles of our theory, so these are the key to many of our other results. By obtaining these operators, we can work out the *fusion rules* of our theory, that is how we can bring multiple particles together and consider them as a single object. The ribbon operators can also be used to obtain the *braiding relations* of our theory, which describe what happens when we move the excitations around each other. We consider these braiding relations in Sec. V. Having looked at these ideas in fairly general cases, in Sec. VI we take two specific examples that highlight some of the important features of this model. In Sec. VII, we interpret various features of the (2+1)D model when a particular operator called $\triangleright$ (which we define in Sec. II) is trivial, by changing basis from group elements to irreps, and expose a symmetry in the model. We then use this basis to construct a mapping between some of the higher-lattice gauge theory models and the symmetry-enriched string-net construction from Ref. [16]. Finally, in Sec. IX we consider the *topological sectors* of the models. The topological sectors classify the conserved charges that the excitations carry. These sectors therefore determine what distinct species of anyon are present in the model. We examine how these sectors change when the model undergoes a *condensation-confinement* transition, where some charges join the topological vacuum and become trivial and other charges become confined.

The proofs for many of our results are relegated to the Supplemental Material [45]. In Sec. S-I, we calculate the commutation relations between the ribbon and membrane operators and the energy terms, therefore showing which energy terms are excited. Then, in Sec. S-II, we prove that the nonconfined ribbon operators are topological, meaning that the ribbon can be smoothly deformed without changing the action of the ribbon operator. Next, in Sec. S-III, we demonstrate the pattern of condensation for the magnetic excitations (i.e., which magnetic excitations are topologically trivial and can be produced by local operators). An explicit calculation of the braiding of the various excitations is presented in Sec. S-IV, while the measurement operators for topological charge are constructed in Sec. S-V. Then, in Sec. S-VI, we give some miscellaneous algebraic proofs that support Sec. VII of the main text. Finally, in Sec. S-VII, we show that, in certain cases, it is possible to construct the magnetic excitations of the model even when $\triangleright$ is nontrivial. In these cases, the magnetic and electric excitations have an interesting pattern of condensation and confinement that depends on which degenerate ground state we create the excitations from.

II. SUMMARY OF THE MODEL

Before describing our results, we would briefly like to review some ideas we covered in the previous paper in this series, Ref. [44], to prevent readers from needing to refer back to that work (or Ref. [1], where the model was originally defined) for definitions. The higher-lattice gauge theory model is based on a generalization of ordinary lattice gauge theory, where in addition to the ordinary (1-)gauge field, there is a second 2-gauge field which describes a gauge symmetry on the first gauge field itself. That is, while an ordinary gauge field describes a transformation of pointlike objects (matter) the higher gauge field describes a transformation of extended objects, such as the Wilson lines.

We work with a 2D lattice, where the (directed) edges are labeled by elements of a group G (the 1-gauge field) and the plaquettes (which have both an orientation and a distinguished vertex called the base point) are labeled by elements of a second group E (the 2-gauge field). These groups are part of a "crossed module" and each crossed module defines a different lattice model. A crossed module $(G, E, \partial, \triangleright)$ consists of the two previously mentioned groups, together with two maps $\partial : E \to G$ and $\triangleright : G \to \mathrm{Aut}(E)$. Here ∂ is a group homomorphism from E to G which controls the action of the 2-gauge transforms on the 1-gauge field, while $\triangleright$ is another homomorphism that maps elements of G to automorphisms on E (isomorphisms from E to itself) and controls the action of the 1-gauge transforms on the 2-gauge field. We write the automorphisms in the form $g\triangleright$ (so each $g\triangleright$ is a particular isomorphism), and we denote this map acting on an element e of E by $g \triangleright e$. The fact that $\triangleright$ is a homomorphism means that these maps have a group structure: $g_1 \triangleright (g_2 \triangleright e) = (g_1 g_2) \triangleright e$ for any elements $g_1, g_2 \in G$ and $e \in E$. In addition to restrictions put upon the maps $\triangleright$ and ∂ by them being homomorphisms, the two maps must also satisfy additional constraints, called the Peiffer conditions, in order for the parallel transport processes described by the gauge fields to be consistent [46,47]. These Peiffer conditions are

$$\partial(g \triangleright e) = g\partial(e)g^{-1}, \tag{1}$$

$$\partial(e) \triangleright f = efe^{-1}. \tag{2}$$

Definition 1. A crossed module is a collection $(G, E, \partial, \triangleright)$, where G and E are groups, and $\partial : E \to G$ and $\triangleright : G \to \mathrm{Aut}(E)$ are group homomorphisms satisfying the Peiffer conditions (1) and (2).

While the spatial dimensions are represented by a lattice, the time dimension is continuous with evolution controlled by a Hamiltonian. This Hamiltonian, as introduced in Ref. [1], is

a sum of commuting projector terms:

$$H = -\sum_{\text{vertices, } v} A_v - \sum_{\text{edges, } i} \mathcal{A}_i - \sum_{\text{plaquettes, } p} B_p, \tag{3}$$

where, unlike the version we used in Ref. [44], there are no blob (3-cell) terms because the 2D lattice has no 3-cells. Here the vertex term A_v is an average over the 1-gauge transforms at vertex v labeled by the different elements of G:

$$A_v = \frac{1}{|G|}\sum_{g\in G} A_v^g, \tag{4}$$

where A_v^g fluctuates the states of the surrounding edges i and also changes the state of any plaquette p for which v is the base point:

$$\begin{aligned} A_v^g : g_i &\to \begin{cases} g g_i & \text{if } v \text{ is the start of } i, \\ g_i g^{-1} & \text{if } v \text{ is the end of } i, \\ g_i & \text{otherwise,} \end{cases} \\ A_v^g : e_p &\to \begin{cases} g \triangleright e_p & \text{if } v \text{ is the base point of } p, \\ e_p & \text{otherwise.} \end{cases} \end{aligned} \tag{5}$$

From this definition, we see that $\triangleright$ describes how the (1-gauge) vertex transforms act on the surface labels that are based at that vertex. Geometrically, the vertex transform acts like parallel transport of that vertex across an edge, and so $\triangleright$ describes how the 2-gauge field changes under such parallel transport. Equivalently, it describes how the label of the field changes when we alter the base point of a plaquette or surface [1].

The individual vertex transforms satisfy the algebra $A_v^g A_v^h = A_v^{gh}$, which further leads to the result $A_v^g A_v = A_v$ (i.e., the vertex transforms can be absorbed into the corresponding vertex term). Because of this, the vertex term is a projector which projects onto states which are 1-gauge invariant at that vertex. This also means that the ground states (which are eigenstates of each vertex term with eigenvalue 1) can absorb vertex transforms (i.e., the ground state is 1-gauge invariant):

$$A_v^g |GS\rangle = A_v^g A_v |GS\rangle = A_v |GS\rangle = |GS\rangle$$

for all vertices v and elements $g \in G$. In fact we can absorb the vertex transform A_v^g into any state for which the vertex v is unexcited, not just the ground states.

Similarly, the edge term $\mathcal{A}_i$ is an average of the 2-gauge transforms at edge i labeled by the different elements of the group E:

$$\mathcal{A}_i = \frac{1}{|E|}\sum_{e\in E} \mathcal{A}_i^e. \tag{6}$$

Here $\mathcal{A}_i^e$ fluctuates the labels of the plaquettes adjacent to the edge i, and multiplies the label of edge i itself by $\partial(e)$:

$$\begin{aligned} \mathcal{A}_i^e : g_{i'} &\to \begin{cases} \partial(e) g_{i'} & \text{if } i = i', \\ g_{i'} & \text{otherwise,} \end{cases} \\ \mathcal{A}_i^e : e_p &\to \begin{cases} e_p\{g[v_0(p) - s(i)] \triangleright e^{-1}\} & \text{if } i \text{ is on } p \text{ and aligned with } p, \\ \{g[\overline{v_0(p) - s(i)}] \triangleright e\} e_p & \text{if } i \text{ is on } p \text{ and points against } p, \\ e_p & \text{otherwise.} \end{cases} \end{aligned} \tag{7}$$

Here $v_0(p)$ is the base point of plaquette p and $s(i)$ is the source of edge i (an edge points from its source vertex to its target vertex). $v_0(p) - s(i)$ is the path around the plaquette, following the circulation of the plaquette, from the base point of p to the source of i. On the other hand, $\overline{v_0(p) - s(i)}$ is the path from the base point to the source of i traveling against the circulation of the plaquette, as illustrated in Fig. 1.

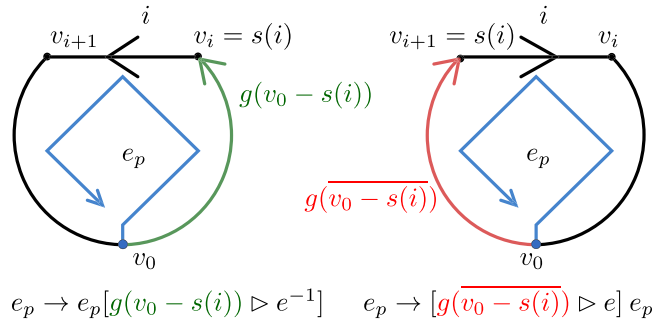

FIG. 1. (Copy of Fig. 22 from Ref. [44]) The path involved in the effect of the 2-gauge transform $\mathcal{A}_i^e$ on a plaquette p depends on whether the edge i is aligned with the p (as in the left case) or antialigned (as in the right case). If the edge is aligned with the plaquette, then the path $[v_0 - s(i)]$ in the transformation of the plaquette label is aligned with p, whereas if i is antialigned with p, then the path $[\overline{v_0 - s(i)}]$ is antialigned with p. Either way, the path is aligned with the edge i.

These edge transforms satisfy an algebra analogous to the vertex transforms. That is, we have $\mathcal{A}_i^e \mathcal{A}_i^f = \mathcal{A}_i^{ef}$. This again allows the individual transforms to be absorbed into the corresponding energy term: $\mathcal{A}_i^e \mathcal{A}_i = \mathcal{A}_i$. Because of this, the edge terms project to states which are 2-gauge invariant at that edge and in particular the ground state satisfies $\mathcal{A}_i^e |GS\rangle = |GS\rangle$ for all edges i and elements $e \in E$.

The two types of gauge transform satisfy the mutual algebra [1]

$$A_v^g \mathcal{A}_i^e = \begin{cases} \mathcal{A}_i^{g \triangleright e} A_v^g & \text{if } v \text{ is } s(i), \\ \mathcal{A}_i^e A_v^g & \text{otherwise.} \end{cases}$$

This means that the 2-gauge symmetry is not entirely 1-gauge symmetric, with the discrepancy described by $\triangleright$. Nonetheless, the overall energy terms $\mathcal{A}_i$ and A_v do commute because the $\triangleright$ action can be absorbed into the sum over elements of E in Eq. (6) for $\mathcal{A}_i$.

Finally, the plaquette term B_p enforces so-called fake flatness on the plaquette p [1]. A plaquette satisfies fake flatness if its boundary path element g_p is related to its plaquette label e_p by $\partial(e_p) g_p = 1_G$. B_p then projects onto the states

for which fake flatness of the plaquette p is satisfied. The plaquette term enters the Hamiltonian with a minus sign, so this leads to a reduction in energy for states satisfying fake flatness. This energy term commutes with both the 1-gauge transforms and 2-gauge transforms, so the Hamiltonian is indeed a commuting projector Hamiltonian. For readers familiar with Kitaev's quantum double model [37], which is based on lattice gauge theory, this plaquette term (and the vertex term from earlier) may seem familiar, except for the factor of $\partial(e_p)$. Whereas in the quantum double model, the plaquette term ensures that contractible closed loops have trivial label, in the higher-lattice gauge theory model such closed loops can have any label in the subgroup $\partial(E) \subset G$, provided that this label matches the surface label contained within the closed loop. Indeed, the edge transforms described by Eq. (7) ensure that the ground state contains closed loops with these nontrivial labels. As we will discuss in more detail later, this leads to some of the magnetic vortices associated to G becoming condensed, meaning they proliferate within the ground state.

This similarity to Kitaev's quantum double model extends beyond the plaquette term. Indeed, if we take the group E to be trivial, then the higher-lattice gauge theory model reduces to Kitaev's model [37], with the vertex and plaquette terms becoming the analogous terms from Kitaev's model and the edge terms becoming trivial. This is because the group E describes a higher gauge field that acts on the original gauge field and so taking it to be trivial recovers the ordinary lattice gauge theory described by Kitaev's model. For this reason, it will be useful to compare and contrast the features of the higher-lattice gauge theory model to those of the Kitaev quantum double model. As we go on, we will find many similarities with the quantum double model, but will also find interesting properties not present in Kitaev's model, such as looplike excitations, confinement, and a ground-state degeneracy on the sphere.

The final thing that we would like to discuss before getting to our results is the special cases of the model. As described in Ref. [44], there are some obstructions that prevent us from considering a general crossed module without restricting to fake flatness. In particular, in the most general case the edge energy terms are not invariant under changes to the branching structure of the lattice and moving the base point of a plaquette all the way around the plaquette changes the plaquette label. In (2+1)D, we are only able to consider two special cases fully (rather than the three in (3+1)D, although we consider some additional cases in Sec. VI A and in Sec. S-VII in the Supplemental Material [45]). These are the cases when $\triangleright$ is trivial, but we do not restrict the Hilbert space, and the case of a general crossed module, but where we restrict the Hilbert space to only include fake-flat configurations (where configurations are basis states for which each edge and plaquette is labeled by an appropriate group element). These two special cases are shown in Table I. In the (3+1)D case we were also able to deal with the case where E is Abelian and ∂ maps to the center of G, but $\triangleright$ is general and fake flatness is not enforced on the level of the Hilbert space (case 2 in Table I). However in the (2+1)D model we were not able to construct the magnetic (fake-flatness violating) excitations in this case (at least not generally, although see Sec. VI A 3 and Sec. S-VII A in the Supplemental Material [45] for a construction in some cases). We note that restricting to the case where $\triangleright$ is trivial also simplifies the group E and the map ∂. The first Peiffer condition $\partial(g \triangleright e) = g\partial(e)g^{-1}$ (for all $g \in G$ and $e \in E$) becomes $\partial(e) = g\partial(e)g^{-1}$, which implies that all elements $\partial(e)$ are in the center of G. Furthermore, the second Peiffer condition $\partial(e) \triangleright f = efe^{-1}$ (for each pair $e,\ f \in E$) becomes $f = efe^{-1}$, which implies that the group E is Abelian.

TABLE I. A summary of the special cases of the model in (2+1)D. Note that case 2, which is a generalization of case 1 and was examined closely for the (3+1)D case in Ref. [44], will not be considered here for the (2+1)D case.

Case	E	$\triangleright$	$\partial(E)$	Full Hilbert space
1	Abelian	Trivial	$\subset$ center(G)	Yes
2	Abelian	General	$\subset$ center(G)	Yes
3	General	General	General	No

III. RIBBON OPERATORS WHEN $\triangleright$ IS TRIVIAL

The creation and movement of the topological excitations in the (2+1)D model are governed by ribbon operators. The name ribbon operators [37] originates from the fact that, in order to produce a pair of excitations, we typically have to act along a ribbon whose end points lie at the positions of the excitations. We must act along a ribbon, rather than just locally at the location of our excitations, because the excitations may carry a conserved charge, called *topological charge* [48]. Because this charge is conserved, we cannot create a single charge-carrying excitation, and can instead only transport charge along a path by producing two excitations with opposite charge at the ends of the path. To do so we must act along the entire path, hence the requirement for an operator with linearly extended support. In addition to being linearly extended, the width of the creation operator may also be small but finite, hence the name ribbon operators, rather than string operators. These ribbon operators underpin most of our other results, and so we will start by constructing them and looking at how they interact with the energy terms.

As we mentioned in Sec. I, due to the consistency issues described in Ref. [44] (in Sec. I F), we restrict to the special cases described in Table I. The first case that we look at is the one where $\triangleright$ is trivial (that is $g \triangleright e = e\ \forall\ g \in G,\ e \in E$). In this case we find two simple types of pointlike excitations: excitations that violate the vertex terms (electric excitations) and excitations that violate the plaquette terms (magnetic excitations). These excitations are analogous to the electric and magnetic excitations of the Kitaev quantum double model [37], as we will see in the next sections. We can also fuse these two types of excitation to produce dyonic excitations, which excite both the vertices and plaquettes at the ends of the ribbon.

A. Electric excitations

The first excitations that we look at are the electric excitations, corresponding to violations of the vertex energy terms.

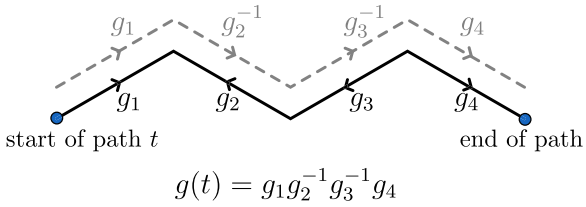

FIG. 2. (Copy of Fig. 37 from Ref. [44]) An electric ribbon operator measures the value of a path and assigns a weight to each possibility, creating excitations at the two ends of the path. In order to find the group element associated to the path, we must first find the contribution of each edge to the path. In this example, the edges along the path are shown in black. Some of the edges are antialigned with the path and so we must invert the elements associated to these edges to find their contribution to the path. This is represented by the gray dashed lines, which are labeled with the contribution of each edge to the path.

In Sec. I we explained that the vertex terms enforced 1-gauge symmetry on their lower-energy eigenstates. Therefore, the electric excitations correspond to violations of this gauge symmetry.

To study these excitations, we first construct their associated ribbon operators, which produce the excitations at the ends of a ribbon. The electric ribbon operator acts along a path made of connected edges from the lattice. This ribbon operator measures the group element associated to that path and then assigns a weight to each possible value. We define an operator $\hat{g}(t)$ which measures the group element of a path t, where the path element is the product of the elements associated to the edges along the path (or the inverse of the edge element if an edge is antialigned with the path, as shown in Fig. 2). Then the electric ribbon operators applied on a path t are given by

$$\hat{S}^{\vec{\alpha}}(t) = \sum_{g \in G} \alpha_g \delta(\hat{g}(t), g), \tag{8}$$

where α_g are coefficients which describe the ribbon operator. These operators commute with all of the plaquette energy terms because both the ribbon operators and the plaquette terms are diagonal in the basis described by group elements (where the basis states are those for which each edge is labeled by an element of G and each plaquette is labeled by an element of E). These ribbon operators also commute with all of the vertex terms, except for the two at the ends of the path. This is because the vertex transform only affects the labels of paths starting or ending at that vertex, not paths that just pass through the vertex. As we show in Sec. S-I A in the Supplemental Material [45], if a path passes through a vertex, then the vertex transform A_v^g gives a factor of g^{-1} to the contribution to the path label from the edge on which the path enters the vertex, and a factor of g to the contribution from the edge on which the path leaves the vertex, which cancel. This means that the only vertex transforms that affect the path element are the ones applied on the two ends of the path, and so only the vertex energy terms at these ends may fail to commute with the ribbon operator.

If our ribbon operator commutes with particular energy terms, it means that the ribbon operator does not excite those energy terms. Therefore, the operator may excite the two vertices at the ends of the path, but not any other vertices or plaquettes. Notice that we have not yet mentioned the edge terms. We will see later in this section that the edge terms are significant and provide a mechanism for the confinement of some of the electric particles.

Looking at the expression for our ribbon operators, given in Eq. (8), we see that there is a $|G|$-dimensional space of electric operators because we have a coefficient for each group element. An appropriate basis for this space has basis vectors labeled by the irreducible representations of the group G. For these basis vectors, the coefficients are given by matrix elements of the irreps:

$$S^{R,a,b}(t) = \sum_{g \in G} [D^R(g)]_{ab} \delta(\hat{g}(t), g), \tag{9}$$

where $[D^R(g)]$ is the matrix representation of g in representation R, while a and b are the indices of the matrix. The fact that the operators labeled by the possible R, a and b in this way do indeed form a basis for the space of electric ribbon operators follows from the grand orthogonality theorem of representation theory (a proof that such a change of basis from group elements to irreps is allowed is given in Ref. [49], for example). We expect (and show in Sec. S-V C 1 in the Supplemental Material [45]) that the *topological sectors* of pure electric excitations are labeled by these irreps. A topological sector is a group of particle types that carry the same conserved charge, called topological charge. Any degrees of freedom within the sector (such as the matrix indices a and b here) describe nonconserved, local quantities. These local quantities may be changed by local operators, but to change the topological charge of an excitation we must transport that topological charge away using a ribbon operator. A particularly important idea related to topological charge is that there must be a so-called vacuum topological charge, which is carried by the ground state. We can see this reflected in the electric ribbon operators. When R is the trivial irrep, given by $D^{1_R}(g) = 1 \; \forall \; g \in G$, the ribbon operator is given by

$$\sum_{g \in G} \delta(\hat{g}(t), g) = 1,$$

which is just the identity operator. Naturally, the identity operator does not produce any excitations, and so will not excite the two vertices at the end points of the path. In fact, of the electric ribbon operators labeled by the irreps of G, only the electric ribbon labeled by the trivial irrep fails to excite the two vertices. This suggests that the irrep labels the topological charge and the trivial irrep corresponds to the vacuum charge. This is true for pure electric excitations, but the picture is more complicated when we also allow for magnetic excitations. Nonetheless, the trivial irrep labels the case where the electric part of the topological charge is trivial and labels the vacuum if the magnetic part is also trivial.

Those familiar with Kitaev's quantum double model [37] may notice that these ribbon operators are exactly the same as the ribbon operators corresponding to the electric excitations in the Kitaev quantum double model. However, in the higher-lattice gauge theory case, these electric excitations have an additional feature: they may be *confined*. By confined, we mean that when we create a pair of excitations from the vacuum, there is an energy cost for pulling the pair apart.

This energy grows with the length of the ribbon operator we apply to move them. In this model, the mechanism for this confinement is through the edge terms of the Hamiltonian. Unlike in the Kitaev quantum double model, there are energy terms associated to the edges of our lattice that allow the edges to be excited. We find that some of the electric operators excite every edge along the path that they act on, so that the energy cost of the ribbon operator has a component proportional to the length of the ribbon.

In order to determine which electric excitations are confined, we need to consider how the edge terms interact with the path element measured by the ribbon operators. Recall from Sec. I that an edge transform $\mathcal{A}_i^e$ changes the label of the edge i on which the operator is applied by the element $\partial(e)$. Because a ribbon operator measures the group element of a path on the lattice, the ribbon operator can be sensitive to this change in path element and so will not commute with the edge transform in general. However, the element $\partial(e)$ is not a general element of G, but instead lies in the image of ∂. This means that the potential noncommutativity of the ribbon operators and edge transforms is controlled by the map ∂. For example, if ∂ mapped only to the identity element of G, then the factor $\partial(e)$ would be trivial and so the edge transform would not affect the path element, meaning that all of the ribbon operators would commute with the edge transforms. Even when ∂ is nontrivial, not every electric ribbon operator is sensitive to factors in the image of ∂. Considering the general electric ribbon operator given in Eq. (8), we can divide the ribbon operators into a class of confined ribbon operators and a class of unconfined ones. As we prove in Sec. S-I A of the Supplemental Material [45], a ribbon operator is unconfined if the coefficients α_g satisfy

$$\alpha_g = \alpha_{g\partial(e)} \quad \text{for all } g \in G \text{ and } e \in E. \tag{10}$$

That is, the ribbon operator is unconfined if α_g is only a function of the coset of $\partial(E)$ in G and not of elements within the coset. On the other hand, a ribbon operator is confined in orthogonal cases, where the coefficients within each coset sum to zero:

$$\sum_{e\in E} \alpha_{g\partial(e)} = 0 \; \forall \; g \in G. \tag{11}$$

A general ribbon operator will have coefficients that can be split into a sum of two parts, the first being a function of coset only and the second summing to zero over a coset. This pattern of confinement is the same as that for the related four-dimensional (4D) field theory discussed in Ref. [8], where the electric operators are confined if they can detect factors in a subgroup $\pi_1(H)$ [equivalent to $\partial(E)$ here].

Another way to look at which ribbon operators are confined is to use the irrep basis described in Eq. (9), for which it is easy to separate the confined and unconfined excitations. Because the image of ∂ is a (normal) subgroup of G, each irreducible representation of G gives us a representation of $\partial(E)$, by restricting the irrep to the subgroup. That is, for each irrep R of G we have a representation of $\partial(E)$, R_∂, defined by $R_\partial(h) = R(h)$ for $h \in \partial(E)$. If this representation is trivial, then the electric ribbon operator is not sensitive to changes to the path element in $\partial(E)$ and so is not sensitive to the edge transform, therefore commuting with the transform (and the edge energy term). On the other hand, if the ribbon operator carries some nontrivial irrep of the image of ∂, then applying the edge term (which is an average of the edge transforms with each label in E) applies factors to the path element which average over the elements in the image of ∂. Because averaging over a nontrivial irrep gives zero by the orthogonality theorem, this leads to the edge energy term annihilating the state produced by the ribbon operator. This means that the edge energy terms along the ribbon are excited by the ribbon operator, and so the corresponding excitations are confined.

For example, consider the quaternion group $\mathbb{Q}_8$. This group has elements $1, -1, i, -i, j, -j, k$, and $-k$. The group has a two-dimensional irrep with corresponding matrices given by $\pm\mathbf{1}_2$ and $\pm i\sigma_l$ (for l=1, 2, 3), where σ_l are the three Pauli matrices. $\mathbb{Q}_8$ has a $\mathbb{Z}_2$ subgroup $\{1, -1\}$. By restricting the two-dimensional irrep to these elements, we get the matrices $\pm\mathbf{1}_2$, which form a (reducible) representation of the subgroup $\mathbb{Z}_2$. As we see in this $\mathbb{Q}_8$ example, the restricted representation R_∂ need not be an *irreducible* representation of $\partial(E)$. However, when $\triangleright$ is trivial, $\partial(E)$ is in the center of G (and so the subgroup is Abelian). This means that, from Clifford's theorem [50], the restricted representation R_∂ branches into copies of one particular (1D) irrep of $\partial(E)$, $R_\partial^{\text{irr.}}$. Because $\partial(E)$ is in the center of G, this can also be understood from Schur's lemma, which enforces that the matrices in the restricted irrep must be scalar multiples of the identity matrix. As an example of this branching, in the $\mathbb{Q}_8$ example above, the 2D irrep gives us two copies of the nontrivial irrep of $\mathbb{Z}_2$, which has phases $\{1, -1\}$ representing the two elements of $\mathbb{Z}_2$. If the irrep $R_\partial^{\text{irr.}}$ is trivial, so that $R_\partial^{\text{irr.}}(g) = 1$ for all $g \in \partial(E)$, then the excitations labeled by the irrep R are unconfined. On the other hand, if the irrep $R_\partial^{\text{irr.}}$ is nontrivial (as in the example above) then the excitations labeled by R are confined. A similar argument holds when $\triangleright$ is not trivial [so that $\partial(E)$ is not in the center of G], though in that case $R_\partial^{\text{irr.}}$ need not be 1D, and rather than copies of $R_\partial^{\text{irr.}}$ we will have different irreps related to $R_\partial^{\text{irr.}}$ by conjugation, as we can deduce from Clifford's theorem [50].

Having obtained the ribbon operators that produce the electric excitations, we can make use of them to examine the properties of these excitations. One important property is the set of *fusion* rules of the excitations. To understand fusion, recall that our excitations carry some conserved charge. Then, given two such excitations, we can bring them close together and ask what their total charge is. We say that the two charges fuse to the total charge. To find the fusion properties we consider applying two electric operators in sequence on the same path. This corresponds to the process where we produce a pair of excitations and separate them using a ribbon operator, before producing another pair of excitations and moving them to the locations of the first pair, i.e., to the ends of the same ribbon. Then we want to ask what total charge is located at each end of the ribbon. Applying these ribbon operators, we have that

$$\sum_{g\in G}[D^{R_1}(g)]_{ab}\delta(g,\hat{g}(t))\sum_{k\in G}[D^{R_2}(k)]_{cd}\delta(k,\hat{g}(t)) = \sum_{g\in G}\sum_{k\in G}[D^{R_1}(g)]_{ab}[D^{R_2}(k)]_{cd}\delta(g,\hat{g}(t))\delta(k,\hat{g}(t))$$

$$= \sum_{g\in G}\sum_{k\in G}[D^{R_1}(g)]_{ab}[D^{R_2}(k)]_{cd}\delta(g,k)\delta(k,\hat{g}(t))$$
$$= \sum_{g\in G}[D^{R_1}(g)]_{ab}[D^{R_2}(g)]_{cd}\delta(g,\hat{g}(t)).$$

As described previously in this section, the irreps R_1 and R_2 label conserved charges, while the matrix indices describe internal degrees of freedom. By allowing a, b, c, and d to vary here (which moves us through the internal spaces of the individual sectors), we see all possible results from fusing the charges labeled by R_1 and R_2. The result is the tensor product of the irreps $R_1 \otimes R_2$, with four matrix indices. This tensor product is a representation but not necessarily an irreducible one. However, we can then decompose this representation into irreps. The resulting irreps will describe the possible charges resulting from fusion. The fusion of the electric excitations is therefore described by the decomposition of products of irreps of the group G [i.e., the electric excitations are described by the fusion category Rep(G), although the nonconfined excitations form a subcategory].

For fusion it is not strictly necessary to have the ribbon operators acting on the same path. It is sufficient to bring the excitations close together. However, when the paths do not align, we cannot simply write the product of ribbon operators as a single ribbon operator, and so we must use another method to find the charge of the two excitations. We consider how to find the charge of a general set of excitations in a different way in Sec. IX. Having said that, there are cases where we can combine operators on different paths simply. This occurs when the path s has the same start and end points as t, and s can be deformed smoothly into t without crossing any excitations. In this case, due to the plaquette constraints satisfied by unexcited regions of the lattice, the group elements assigned to the paths s and t only differ by an element of $\partial(E)$. For the unconfined excitations, this has no effect because such excitations are described by trivial representations of $\partial(E)$. This illustrates a general point: the ribbon operators associated to nonconfined excitations in our model are topological, in the sense that deforming the ribbons over a region with no excitations does not affect the result of acting with the operator. This is proven for each ribbon and membrane operator in the Supplemental Material (see Sec. S-II) [45].

B. Magnetic excitations

The next type of excitation that we examine is called the magnetic excitation, due to the similarity with the magnetic excitation in the Kitaev quantum double model [37]. The magnetic excitations are "flux" excitations, corresponding to excited plaquette terms. They are called magnetic excitations because they are associated to closed loops with nontrivial flux (1-holonomy), just like the magnetic field in the Aharanov-Bohm effect. Just as with the electric excitations, the ribbon operators that produce the magnetic excitations are the same as those in the Kitaev quantum double model [37]. To find the ribbon operators for the magnetic excitations, we consider trying to excite a plaquette term. Recall from Sec. I that the plaquette term measures the path around the plaquette and checks if it is compatible with the surface element of the

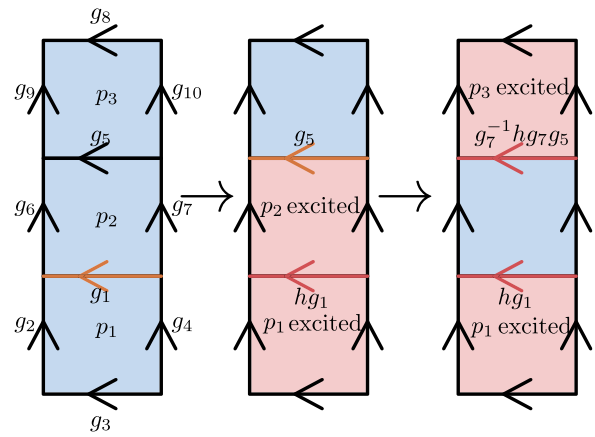

FIG. 3. If we consider trying to produce a single-plaquette excitation by changing an edge label (here g_1) we instead excite two plaquettes, as shown in the second diagram. Changing further edges (here the edge labeled by g_5 in the second diagram) just pushes these excitations apart, as shown in the third diagram.

plaquette. Denoting the path around plaquette p, starting at the base point of p and matching the orientation of the plaquette, by $r(p)$, the plaquette term is $\delta(\partial(e_p)g(r(p)), 1_G)$. Starting in the ground state, to excite such a term we can either change the plaquette label or the edge labels of the edges that make up the path $r(p)$. The former case is considered in Sec. III C. Here we consider the latter approach. We consider trying to change a single edge on a plaquette, by multiplying it by some group element in G. However, each edge is shared by two plaquettes, so performing this operation will excite two plaquettes rather than one. For example, consider the situation in Fig. 3. In the left image we have one of the configurations in the ground state, satisfying the plaquette constraints. Then we multiply the edge label g_1 by an element h (which will label our magnetic ribbon operator) to give hg_1. Looking at the bottom plaquette (p_1), initially

$$\partial(e_{p_1})g(r(p_1)) = \partial(e_{p_1})g_1g_2^{-1}g_3^{-1}g_4 = 1_G.$$

Then after our operator acts, we have

$$\begin{aligned}\partial(e_{p_1})g(r(p_1)) &= \partial(e_{p_1})hg_1g_2^{-1}g_3^{-1}g_4\\ &= h\partial(e_{p_1})g_1g_2^{-1}g_3^{-1}g_4\\ &= h1_G\\ &= h,\end{aligned}$$

where we used the fact that $\partial(e_{p_1})$ is in the center of G due to $\triangleright$ being trivial (see Sec. II). Looking at Fig. 3, we see that changing g_1 will also excite the plaquette p_2, as shown in the middle diagram, because the corresponding edge is shared by the two plaquettes p_1 and p_2. Therefore, we consider trying to correct the plaquette holonomy of p_2, to leave p_2 unexcited, by changing another edge label. To do this, we try multiplying the edge label g_5 by some element x. The plaquette holonomy of p_2 was originally given by

$$\partial(e_{p_2})g(r(p_2)) = \partial(e_{p_2})g_5g_6^{-1}g_1^{-1}g_7 = 1_G.$$

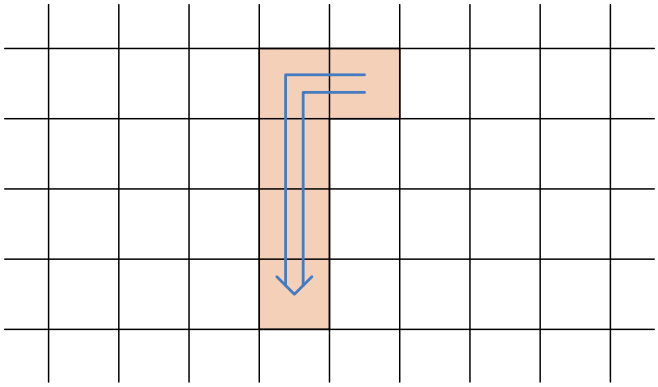

FIG. 4. An example of a dual path on a lattice. This dual path includes the shaded plaquettes, which take the role usually held by vertices on a path. Note that the path passes through, rather than along, the edges of the lattice.

After changing the two edges, we have instead that

$$\begin{aligned}\partial(e_{p_2})g(r(p_2)) &= \partial(e_{p_2})xg_5g_6^{-1}g_1^{-1}h^{-1}g_7\\ &= x\partial(e_{p_2})g_5g_6^{-1}g_1^{-1}(g_7g_7^{-1})h^{-1}g_7\\ &= x\big[\partial(e_{p_2})g_5g_6^{-1}g_1^{-1}g_7\big]g_7^{-1}h^{-1}g_7\\ &= x1_Gg_7^{-1}h^{-1}g_7\\ &= xg_7^{-1}h^{-1}g_7. \end{aligned} \tag{12}$$

We see that for this to give 1_G (and so to leave the plaquette unexcited), we need to choose $x = g_7^{-1}hg_7$. We note that the value of x needed depends on the edge label g_7 and therefore depends on the state that the ribbon operator is acting on. This action reduces to multiplying both edges by h when G is Abelian, but in the non-Abelian case we need to keep track of additional edge labels.

While this action leaves the plaquette p_2 unexcited, because the second edge that we changed is also shared by two plaquettes, a third plaquette (p_3 in the figure) must now be excited. Therefore, we have simply separated the two plaquette excitations that we initially produced and cannot remove the second excitation (at least not without moving it back to the first excitation), indicating that the magnetic excitations are produced in pairs.

Looking at Fig. 3, we note that the edges that we changed (the ones labeled by g_5 and g_1) are bisected by a path between the two excited plaquettes. Indeed, generally to create two plaquette excitations we must act on all edges that are bisected by a path that connects those two plaquettes. This path exists on the dual lattice: it travels between the centers of plaquettes and bisects the edges of the lattice. This is in contrast with a path on the direct lattice, which passes from vertex to vertex along the edges of the lattice. Therefore, we call this path the dual path of the ribbon operator. A simple example of such a dual path is shown in Fig. 4.

We already mentioned that the factor $x = g_7^{-1}hg_7$ by which we must change the second edge in our simple example (see Fig. 3) is not a constant, but instead depends on the edge label g_7. The edge labeled by g_7 lies on a path between the two excited plaquettes, but on the direct lattice rather than the dual lattice. Generally, to define our magnetic ribbon operator we must define both a direct path, which passes from vertex to vertex along the edges of the lattice, and a dual path, which passes between plaquettes and so cuts through edges on the lattice. For example, in Fig. 3 the direct path is the edge labeled by g_7, while the dual path passes from plaquette p_1 to plaquette p_2 and cuts through the edges labeled by g_1 and g_5. The space between the dual and direct paths forms a ribbon, which is the origin of the name ribbon operator [37]. We give an example of a ribbon, along with its corresponding direct and dual paths, in Fig. 5.

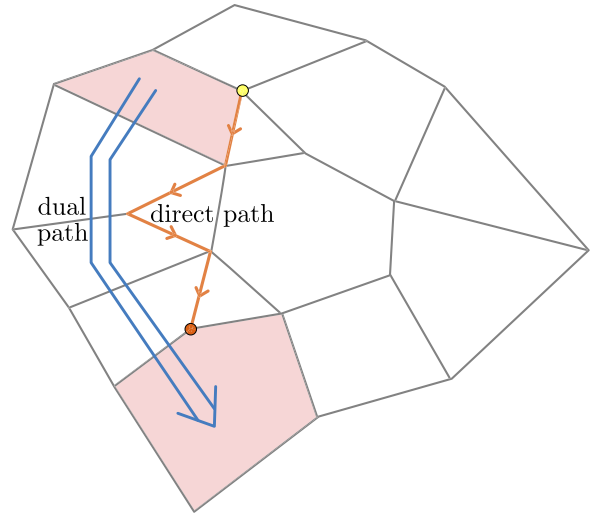

FIG. 5. An example of the dual and direct paths. The dual path is the (blue) double arrow between the shaded plaquettes and the direct path is the (orange) solid line between the two vertices shown by circles. The edges cut by the dual path of the magnetic ribbon operator have their labels changed by the operator.

Having given a rough motivation and description of the magnetic ribbon operator, we will now be more specific about its action. As we just described, when defining our ribbon operator we must specify a dual path, which connects the two plaquettes to be excited. We must also give a direct path, which runs from a specified start point (which we usually take to lie on the first excited plaquette) and a vertex on the second excited plaquette. Which edges are affected by the multiplication from the ribbon operator depends on the dual path, but precisely which factor they are multiplied by depends on the label of an appropriate section of the direct path. A magnetic ribbon operator $C^h(t)$, labeled by an element h of G and acting on a ribbon t, affects the label g_i of an edge i cut by the dual ribbon according to

$$C^h(t) : g_i = \begin{cases} g(\tilde{t}_i)^{-1}hg(\tilde{t}_i)g_i & \text{if edge } i \text{ points away from the direct path,}\\ g_ig(\tilde{t}_i)^{-1}h^{-1}g(\tilde{t}_i) & \text{if } i \text{ points towards the direct path,}\end{cases} \tag{13}$$

given that $\tilde{t}_i$ is the path from the start point of the direct path up to the edge i.

As an example of the action of the magnetic ribbon operator, consider Fig. 6. We see that the cut edges are either left multiplied by some element in the conjugacy class of h, or right multiplied by some element in the conjugacy class of h^{-1}, depending on whether the edge points into or out of the

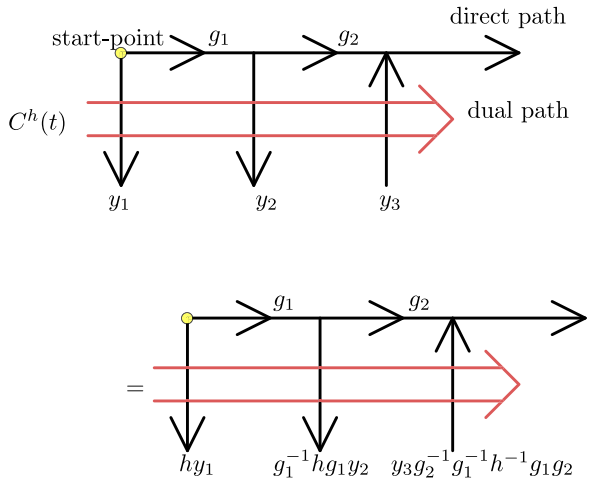

FIG. 6. An explicit example of the action of the magnetic ribbon operator on the edges. The action on the edges cut by the dual path (the vertical edges) depends on the labels of the edges on the direct path (horizontal line) and on the orientation of the affected edges.

ribbon. The element within the conjugacy class is determined by the direct path from the start of the ribbon to the edge being cut. The reason that this dependence on the direct path is necessary is that it ensures that plaquettes along the ribbon (apart from at the ends of our ribbon) are not excited, as we saw in our earlier example.

As we have discussed already, the ribbon operator has the effect of exciting the two plaquettes at the end of the ribbon (the shaded ones in Fig. 5). However, this is not the only excitation that may be produced by the ribbon operator. The first vertex on the direct path, which we call the start point of the ribbon operator (the yellow circle in Fig. 5), may be excited. The reason that this start point may be excited is the dependence of the action of the magnetic ribbon operator on the direct path. As shown in Fig. 6 and Eq. (13), the ribbon operator multiplies the element of each edge cut by the dual path by an element $g(\tilde{t}_i)^{-1}hg(\tilde{t}_i)$ or its inverse, where $\tilde{t}_i$ is the path from the start point to the edge being changed, and $g(\tilde{t}_i)$ is the group element assigned to that path. If we apply a vertex transform at the start point, then we will change this path element, and so the vertex transform will not commute with the ribbon operator. Specifically, the action of the vertex transform A_v^g takes the path element $g(\tilde{t}_i)$ to $gg(\tilde{t}_i)$, which means that the factor $g(\tilde{t}_i)^{-1}hg(\tilde{t}_i)$ in the action of the ribbon operator becomes $g(\tilde{t}_i)^{-1}g^{-1}hgg(\tilde{t}_i)$. We can think of this as replacing the label h of the ribbon operator by $g^{-1}hg$ and so our ribbon operator $C^h(t)$ becomes $C^{g^{-1}hg}(t)$ instead. In terms of a commutation relation, we have

$$C^h(t)A_v^g = A_v^g C^{g^{-1}hg}(t), \tag{14}$$

where v is the start point of t, and so generally the vertex transform at the start point does not commute with the ribbon operator. To determine whether the vertex is excited, we need to look at the vertex energy term, which is an average over the vertex transforms: $A_v = \frac{1}{|G|}\sum_{g\in G} A_v^g$. Applying this to our commutation relation (14), we have

$$A_v C^h(t) = \frac{1}{|G|}\sum_{g\in G} C^{ghg^{-1}}(t)A_v^g. \tag{15}$$

Now we need to use this to evaluate the state produced by acting with the ribbon operator on the ground state, to see if the vertex is excited. Because A_v is a projector, with eigenvalue one for the lower-energy state and eigenvalue zero for the higher-energy state, the expression $A_vC^h(t)\,|GS\rangle$ will give zero if the vertex is excited and $C^h(t)\,|GS\rangle$ if it is not excited. To evaluate this expression we can first use the fact that the ground state is an eigenstate of the vertex term to pull out a factor of A_v, to obtain

$$A_vC^h(t)|GS\rangle = A_vC^h(t)A_v|GS\rangle.$$

We can then use the commutation relation between the ribbon operator and vertex term given in Eq. (15) to find that

$$A_vC^h(t)|GS\rangle = \frac{1}{|G|}\sum_{g\in G} C^{ghg^{-1}}(t)A_v^gA_v|GS\rangle.$$

Then, using the fact that $A_v^gA_v = A_v$ (as described in Sec. II) we have

$$\begin{aligned} A_vC^h(t)|GS\rangle &= \frac{1}{|G|}\sum_{g\in G} C^{ghg^{-1}}(t)A_v|GS\rangle \\ &= \frac{1}{|G|}\sum_{g\in G} C^{ghg^{-1}}(t)|GS\rangle, \end{aligned} \tag{16}$$

where we used the relation $A_v|GS\rangle = |GS\rangle$ in the final step. We therefore obtain an average over the ribbon operators that have label in the conjugacy class of h. We see that the magnetic ribbon operator does not generally produce an eigenstate of A_v when acting on the ground state, and so the start-point vertex is not generally in an excited or unexcited state. In order to construct ribbon operators that leave the vertex in a definite energy state, we must construct a linear combination of magnetic ribbon operators with different labels h. A general magnetic operator on the path t is given by $C_{\vec{\alpha}}(t) = \sum_{h\in G}\alpha_hC^h(t)$, where $\vec{\alpha}$ is a set of coefficients. Using Eq. (16) with this linear combination, we obtain

$$\begin{aligned} A_vC_{\vec{\alpha}}(t)|GS\rangle &= A_v\sum_{h\in G}\alpha_hC^h(t)|GS\rangle \\ &= \frac{1}{|G|}\sum_{g\in G}\sum_{h\in G}\alpha_hC^{ghg^{-1}}(t)|GS\rangle. \end{aligned}$$

Replacing the dummy index h with $h' = ghg^{-1}$, we have

$$\begin{aligned} A_vC_{\vec{\alpha}}(t)|GS\rangle &= \frac{1}{|G|}\sum_{g\in G}\sum_{h'\in G}\alpha_{g^{-1}h'g}C^{h'}(t)|GS\rangle \\ &= \sum_{h'\in G}\left(\frac{1}{|G|}\sum_{g\in G}\alpha_{g^{-1}h'g}\right)C^{h'}(t)|GS\rangle. \end{aligned} \tag{17}$$

Then, the coefficients $\vec{\alpha}$ determine whether or not the start point is excited. If the coefficients α_h are a function of conjugacy class, so that $\alpha_h = \alpha_{xhx^{-1}}\ \forall\ h, x \in G$, then the start-point vertex is not excited. For example, we could have the operator $C_{[h]}(t) = \sum_{x\in G}C^{xhx^{-1}}(t)$, which is an equal sum over

all elements of the conjugacy class of h. In this case the expression $\frac{1}{|G|}\sum_{g\in G}\alpha_{g^{-1}h'g}$ in Eq. (17), which averages over elements in the conjugacy class of h', just gives us $\alpha_{h'}$ because the coefficients are already a function of conjugacy class (specifically, $\alpha_{h'}$ is one if h' is in the same class as h and zero otherwise). Therefore, the vertex term commutes with such a linear combination of magnetic ribbon operators and so the start-point vertex would be unexcited. On the other hand, if the coefficients for the elements of each conjugacy class sum to zero, then the vertex is excited. That is, the vertex is definitely excited if $\sum_{g\in G}\alpha_{g^{-1}h'g^{-1}}=0$ for each h' in G, as we can see from Eq. (17). For example, consider the case where we have a conjugacy class with two elements x and y, and we have a superposition over only these two elements: $aC^x(t)+bC^y(t)$. If $a+b=0$, then the vertex is excited.

Generally, any linear combination of basis magnetic ribbon operators can be written as a sum of two parts, the first of which is a function of conjugacy class and the second of which has coefficients which sum to zero within each conjugacy class. This is because, given coefficients a_g for the elements within a conjugacy class $[g_1]$, we can extract the average coefficient to obtain the part which is a function of conjugacy class, while the remainder will sum to zero. That is, we write

$$\sum_{g\in[g_1]} a_g C^g(t) = \langle a\rangle \sum_{g\in[g_1]} C^g(t) + \sum_{g\in[g_1]} (a_g-\langle a\rangle) C^g(t), \quad (18)$$

where $\langle a\rangle$ is the mean coefficient for that conjugacy class. The first term has the same coefficient for each operator in the conjugacy class, and the coefficients in the second term sum to zero by the definition of the mean. Therefore, our space of ribbon operators can be decomposed in terms of ribbon operators that excite the start point and ones that do not.

From considering the start-point excitations, we can see that conjugacy classes of G are important when considering the magnetic ribbon operators. These conjugacy classes are also important for considering the conserved topological charge of the excitations, along with their braiding. We can think of the magnetic excitation as being labeled by a conjugacy class and some internal degrees of freedom which describe the coefficients within the conjugacy class. The topological sectors will be unions of these classes, as we will discuss in Sec. III E, while the internal degrees of freedom contribute to the braiding of the magnetic excitations around each other together with the conjugacy class.

Now that we have found the ribbon operators for the magnetic excitations, we can consider fusion of the magnetic excitations. If we apply two magnetic ribbon operators, labeled by g and h, on the same ribbon in sequence, we get gh or hg depending on the order in which we apply them (note that these are in the same conjugacy class and so the resulting excitations are in the same sector). That is, we have

$$C^g(t)C^h(t) = C^{gh}(t), \quad (19)$$

when combining two ribbons of the form shown in Fig. 6.

In addition to considering ribbon operators that are purely magnetic or purely electric, we can consider ribbons made by applying both a magnetic and electric ribbon on the same space (that is, the electric ribbon is placed on the direct path of the magnetic one). We write this as $F^{h,g}(t)=\delta(g,g(t))C^h(t)$, following the notation used by Kitaev in Ref. [37]. Note that, while the magnetic part acts on a ribbon t, the electric operator only acts on the direct path of that ribbon. Nonetheless, following Kitaev's notation, we will use t as the argument for the electric part as well, and hope that it is clear which part of the ribbon is relevant for the electric operator. These more general ribbon operators obey the fusion rules

$$F^{h_1,g_1}(t)F^{h_2,g_2}(t) = \delta(g_1,g_2)F^{h_1h_2,g_1}(t). \quad (20)$$

Note that the electric part is not labeled by an irrep, so to recover the familiar fusion of electric excitations from Sec. III A we must take appropriate linear combinations of these ribbon operators.

C. Single-plaquette multiplication operators

In Sec. III B, we mentioned that there are two ways to produce excitations of the plaquette energy terms. In addition to exciting the plaquettes by changing the edges around them (as we did to produce the magnetic excitations), we can change the plaquette label itself. This can be done simply by multiplying a single-plaquette label e_p by a group element e (note that when E is Abelian we do not need to worry about the order of multiplication). We denote the operator that does this to a plaquette p by $M^e(p)$ and refer to such operators as "single-plaquette multiplication operators." If e is in the kernel of ∂, applying the operator $M^e(p)$ does not change $\partial(e_p)$. Because the plaquette condition $\partial(e_p)g(\text{boundary})=1_G$ only depends on e_p through $\partial(e_p)$, this means that no plaquette excitation is formed. On the other hand, if e is not in the kernel, this operator causes a fake-flatness violation and so we have an excitation of a single plaquette p (no other plaquettes are affected). Because this excitation is formed on its own by a local operator, the excitation does not correspond to a nontrivial anyon (it cannot carry nontrivial topological charge).

From the fact that the single-plaquette multiplication operators, much like the magnetic ribbon operators, produce plaquette excitations, we may suppose that there is a connection between the two types of operator. Indeed, as we show in Sec. S-III in the Supplemental Material [45], some of the magnetic ribbon operators act on the ground state in the same way as a pair of single-plaquette multiplication operators applied on the two plaquettes at the ends of the ribbon. Specifically, this is true for magnetic ribbon operators whose labels lie in $\partial(E)$. The single-plaquette multiplication operators act on the plaquettes, whereas the ribbon operator acts on the edges of the lattice, but for these particular ribbon operators the difference between the two types of action is a series of edge transforms that act trivially on the ground state. This means that the action of such a magnetic ribbon operator on the ground state is equivalent to that of local operators (the single-plaquette multiplication operators) at the ends of the ribbon. This indicates that the excitations produced by such a ribbon operator are equivalent to those produced by the (local) single-plaquette multiplication operators and so are not topologically protected (the excitations must carry trivial topological charge). Such an excitation is called *condensed* (we will discuss the concept of condensation further in Sec. III E). Recalling from Sec. III B [see Eq. (19)] that the fusion rule for magnetic ribbons is $C^g(t)C^h(t)=C^{gh}(t)$,

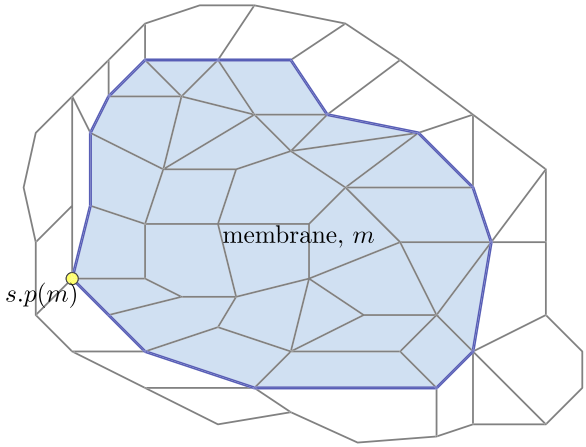

FIG. 7. Consider an E-valued membrane operator applied on a fragment of the lattice. We measure the surface label of the membrane (shaded area) and apply a weight to each possibility. This excites the edges on the boundary of the membrane (solid blue edges). If $\triangleright$ is nontrivial, we must choose a base point for the surface, which we call the start point of the membrane (here represented by the yellow dot).

we have that $C^g(t)C^{\partial(e)}(t) = C^{g\partial(e)}(t)$. Then because $C^{\partial(e)}(t)$ is equivalent to the action of local operators when acting on the ground state, we see that $C^g(t)$ and $C^{g\partial(e)}(t)$ are equivalent up to some local operators (again, when acting on the ground state). This indicates that the magnetic excitations labeled by g and $g\partial(e)$ belong to the same topological sector. The sectors are therefore not just given by conjugacy classes of G, unlike in Kitaev's quantum double model [37], but instead are given by unions of conjugacy classes that are related by multiplication by elements of $\partial(E)$. We can think of these unions as conjugacy classes of cosets of $\partial(E)$ in G. This is because a class that includes an element g includes all elements of each coset $xgx^{-1}\partial(E)$ for each $x \in G$ (i.e., the elements of cosets corresponding to elements of the conjugacy class of g in G). Because $\partial(E)$ is a normal subgroup, these cosets can also be written as $xg\partial(E)x^{-1}$.

D. Loop excitations

In addition to the features of confinement and condensation (which can be seen in other extensions to the Kitaev quantum double model, such as the models studied in Ref. [36]), there are additional looplike excitations, despite the (2+1)D nature of the model. These loop excitations are formed by excited edges, with these edges connecting together to give us a loop. To construct the excitations, we must act with an operator that has support across an extended surface, rather than just on a ribbon. Such an operator is called a *membrane operator*, and produces excitations along the boundary of the membrane, as shown in Fig. 7.

The membrane operators for our loop excitations, which we will call E-valued membrane operators, act by measuring the total group element assigned to the surface (calculated using the rules for composing surfaces given in Ref. [1]) and then applying a weight based on the group element measured. The operator that measures the total surface element of the membrane m is denoted by $\hat{e}(m)$ and can be expressed as

$$\hat{e}(m) = \prod_{\text{plaquettes } p\in m} g(\text{s.p.}(m) - v_0(p)) \triangleright e_p^{\sigma_p},$$

where $v_0(p)$ is the base point of plaquette p, s.p.(m) is the start point of the membrane (which is the base point with respect to which we measure the surface label), and σ_p is $+1$ or -1 to account for the relative orientations of p and m (1 if p and m are aligned, -1 otherwise). For a general crossed module, the order of multiplication and the paths [s.p.$(m) - v_0(p)$] must be determined using the rules for composing surfaces. In the present case, where $\triangleright$ is trivial (case 1 in Table I), the expression for the surface label simplifies to

$$\hat{e}(m) = \prod_{\text{plaquettes } p\in m} e_p^{\sigma_p},$$

and because E is Abelian when $\triangleright$ is trivial, the order of multiplication is arbitrary. The membrane operator is then

$$L^{\vec{\gamma}}(e) = \sum_{e\in E} \gamma_e \delta(e, \hat{e}(m)), \tag{21}$$

where γ_e is some set of coefficients. Allowing these coefficients to vary gives us a space of possible membrane operators. This space is (much like the space of electric ribbon operators) conveniently spanned by irreducible representations, this time of E. In the case where $\triangleright$ is trivial, the group E must be Abelian and so these irreps are 1D. We therefore do not need to include matrix indices for our basis vectors, as we did for the electric operators in Eq. (9). Then the basis operator labeled by irrep μ of E is

$$L^{\mu}(m) = \sum_{e\in E} \mu(e)\delta(e, \hat{e}(m)). \tag{22}$$

Note that we use greek letters to represent irreps of E throughout this paper, in order to differentiate them from the irreps of G, which we represent with upper case roman letters (typically R).

In a similar way to the fusion of particles, we can fuse two loops by applying their membrane operators on the same surface. The membrane operators obey a similar algebra to the electric ribbon operators. We have

$$\begin{aligned} L^{\mu}(m)L^{\nu}(m) &= \sum_{e\in E} \mu(e)\delta(e, \hat{e}(m)) \sum_{f} \nu(f)\delta(f, \hat{e}(m)) \\ &= \sum_{e\in E} \mu(e)\delta(e, \hat{e}(m)) \sum_{f} \nu(f)\delta(f, e) \\ &= \sum_{e\in E} \mu(e)\nu(e)\delta(e, \hat{e}(m)) \\ &= L^{\mu\cdot\nu}(m), \end{aligned} \tag{23}$$

from which we see that two excitations labeled by irreps fuse by multiplication of those irreps. Because the irreps are 1D, the result of this fusion is an irrep (rather than generically being a reducible representation as for the general case). This means that there is only one possible fusion channel (unlike for the electric excitations where we had branching into multiple irreps). Such fusion is called *Abelian* [48].

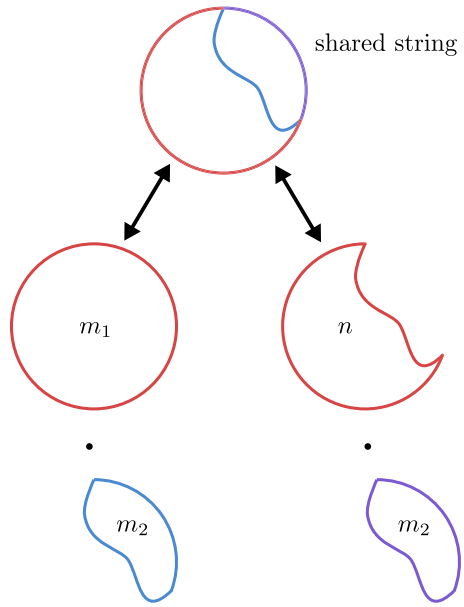

FIG. 8. Consider applying two E-valued membrane operators on two membranes m_1 and m_2 (enclosed within the red and blue loops on the left side of the image), where one membrane (m_2) is contained within the other (m_1) and the two membranes share part of their boundary. Then applying both of these membrane operators results in the situation shown in the top of the image, where the common boundary is represented by the thicker purple line at the top right. We can decompose this product of membrane operators as two membrane operators acting on the membranes n and m_2 shown on the right of the image, which do not share any area. Then the only operator acting near the previously shared boundary is the membrane operator acting on the region m_2 enclosed by the (purple) string in the bottom right of the image, and the label of this membrane operator can be obtained from the labels of the original membrane operators by using the fusion rules from Eq. (23).

Unlike point particles, looplike excitations are extended, and do not need to be fused along their entire length. That is, we can consider a case where parts of the loops fuse into a combined string and then split further along the loops' boundary, as shown in Fig. 8. For example, this can occur if the two membrane operators that produce the loops share part, but not all, of the membrane with each other. Consider the case where we have two membrane operators $L^\mu(m_1)$ and $L^\nu(m_2)$ applied on membranes m_1 and m_2, for which m_2 is entirely contained within m_1. Further, in order to fuse the strings produced along the boundaries of the membranes, we consider the case where the boundary of m_2 includes some of the boundary of m_1, as shown in Fig. 8. Then some of the excited edges, those on the shared boundary of the two membranes, are excited due to the combined action of the two membrane operators, and so should correspond to a fused string. We therefore expect this part of the string to correspond to an irrep $\mu \cdot \nu$, just as for the case of complete fusion discussed above. This can be shown directly by explicitly considering the action of the two membrane operators on the shared parts of the membrane and the parts exclusively in m_1 (i.e., not in m_2). We will refer to this latter part of the membrane as n. Then we can write the surface element of m_1 in terms of the elements of the shared and exclusive parts as $\hat{e}(m_1) = \hat{e}(m_2)\hat{e}(n)$. This allows us to rewrite the product of membrane operators as

$$\begin{aligned} &L^\mu(m_1)L^\nu(m_2) \\ &\quad= \sum_{e\in E} \mu(e)\delta(e, \hat{e}(m_1)) \sum_f \nu(f)\delta(f, \hat{e}(m_2)) \\ &\quad= \sum_{e\in E} \mu(e)\delta(e, \hat{e}(m_2)\hat{e}(n)) \sum_f \nu(f)\delta(f, \hat{e}(m_2)) \\ &\quad= \sum_{e\in E} \mu(e)\delta(\hat{e}(m_2)^{-1}e, \hat{e}(n)) \sum_f \nu(f)\delta(f, \hat{e}(m_2)). \end{aligned}$$

Then we can use the fact that we are applying $\delta(f, \hat{e}(m_2))$ to replace the element $\hat{e}(m_2)^{-1}$ in the other Kronecker delta with f^{-1}. This gives us

$$\begin{aligned} &L^\mu(m_1)L^\nu(m_2) \\ &\quad= \sum_{e\in E} \mu(e)\delta(f^{-1}e, \hat{e}(n)) \sum_f \nu(f)\delta(f, \hat{e}(m_2)) \\ &\quad= \sum_{e'=f^{-1}e} \mu(fe')\delta(e', \hat{e}(n)) \sum_f \nu(f)\delta(f, \hat{e}(m_2)) \\ &\quad= \sum_{e'\in E} \mu(e')\delta(e', \hat{e}(n)) \sum_f \mu(f)\nu(f)\delta(f, \hat{e}(m_2)), \end{aligned}$$

where we used the fact that μ is an irrep of E to write $\mu(e'f) = \mu(e')\mu(f)$. Then we note that $\mu(f)\nu(f) = (\mu \cdot \nu)(f)$ and so

$$\begin{aligned} &L^\mu(m_1)L^\nu(m_2) \\ &\quad= \sum_{e'\in E} \mu(e')\delta(e', \hat{e}(n)) \sum_f (\mu \cdot \nu)(f)\delta(f, \hat{e}(m_2)) \\ &\quad= L^\mu(n)L^{\mu\cdot\nu}(m_2). \end{aligned}$$

Now only the operator $L^{\mu\cdot\nu}(m_2)$ acts on the part of the membrane near the boundary shared by m_1 and m_2 (i.e., near the fused string), and so we see that, as we expect from the fusion rules given in Eq. (23), this part of the boundary corresponds to the irrep $\mu \cdot \nu$.

While it is convenient to label the looplike excitations with irreps, some of these irreps label condensed excitations. The reason that some of the loop excitations are condensed can be seen fairly clearly without detailed calculation. Consider a closed electric ribbon operator placed on the path around the boundary of some membrane m. This operator is sensitive to the path element around the boundary. However, due to fake flatness, when acting on the ground state this path element is related to the surface element by $\partial[(e(m)]g(\text{boundary}) = 1_G$. That is, the path element can resolve information about $e(m)$ up to elements of the kernel of ∂. This means that any membrane operators that cannot resolve elements within the kernel (i.e., excitations labeled by irreps that trivially restrict to the kernel) are equivalent to electric ribbon operators placed on the boundary of the membrane. However, the boundary operator is *local* to the excitation: it only acts near the excited loop. We contrast this with the case we have considered so far, where to create a large loop we need to act on an entire membrane bounded by it. This is local in a slightly different sense to the usual meaning because rather than the operators

having no linear extent, operating on only a few degrees of freedom, the operators instead act on a region extended in one dimension (a loop). However, the boundary operators are local in the sense that they only act in a region that is close to the loop excitation (the region has potentially large extension only in the same direction as the loop). This fact is particularly important in the (3+1)D case, which we will study in a future paper (Ref. [51]), where the looplike excitations are truly topological excitations and so the fact that the excitations can be produced by an operator on the boundary of a membrane means that the membrane operator cannot move topological charge across the membrane. Any charge must only be moved along the support of the operator, and the fact that the membrane operator is equivalent to an operator on the boundary (when acting on the ground state) means that charge can only be moved along the boundary of the membrane. This means that the excitations cannot carry looplike charge and so are condensed. The picture in (2+1)D is a little different, however. In Sec. VII we will see that the loop excitations in (2+1)D, at least when $\triangleright$ is trivial, are related to a symmetry of the model. This symmetry is spontaneously broken when $\ker(\partial)$ is a nontrivial group and the uncondensed excitations then represent domain walls between different ground states of the model [with the ground states labeled by different irreps of $\ker(\partial)$]. On the other hand, if $\ker(\partial)$ is trivial then all of the E-valued loops are labeled by irreps with trivial representations of the kernel and so all of the E-valued loop excitations are condensed.

E. Condensation and confinement

When discussing our excitations in Sec. III A, we noted that some of the electric excitations are confined. Whereas unconfined excitations cost no energy to separate, the confined excitations have an energy cost proportional to the length of the ribbon operator producing them. In this model, this energy cost is due to the edges along the ribbon being excited. We found in Sec. III A that the confined excitations are the electric excitations whose labeling representation has nontrivial restriction to the subgroup $\partial(E)$. We also discussed the idea that some of our magnetic excitations were equivalent to local operators in Sec. III C, and we described such excitations as condensed. This is a general feature exhibited by certain topological models [31,32] and is particularly important when we consider transitions between topological phases.

Given a topological phase, we can cause a transition by allowing some of the (bosonic) topological charges to join the ground state. That is, some of the topologically nontrivial excitations become trivial, with their conserved charge joining the vacuum sector, just as we already discussed for some of our excitations. This process is known as condensation (hence our use of the term condensed excitations). When this happens, any excitations that originally braid nontrivially with the condensing charges must become confined [31,32] in the condensed phase. The ribbon operators of such confined excitations can no longer be topological because their nontrivial interaction with the vacuum means that we cannot freely deform the ribbons through space. This restriction manifests in the confinement of the excitations.

We can see this process in the context of the higher-lattice gauge theory models. In the case of the higher-lattice gauge theory model with $\triangleright$ trivial, there can be several models with the same groups E and G (but different ∂) and so with the same Hilbert space on a given lattice. We can therefore consider transitions between these models. In particular, we have the model $(G, E, \partial \to 1_G, \triangleright \to \mathrm{id})$, for which $\partial(e) = 1_G \; \forall \; e \in E$. This means that the image of ∂ only contains the identity element, which in turn means that all irreps of this image are trivial. This means that there is no confinement of the electric excitations and no condensation of the magnetic excitations. We refer to this model as the uncondensed model. However, we can then consider "switching ∂ on" by changing ∂ to map onto some larger subgroup of G and considering this new higher-lattice gauge theory model. In doing this, we condense the magnetic excitations with label in the image of the new ∂. We will see in Sec. V A that these excitations braid nontrivially with the electric excitations that carry nontrivial representations of this subgroup, which results in these electric excitations being confined.

We also saw that some of our loop excitations were condensed. When we go from our uncondensed $(G, E, \partial \to 1_G, \triangleright \to \mathrm{id})$ case to a more general ∂, we condense the loop excitations whose irreps restrict to trivial representations of the kernel of ∂. That is, any irreps that have $\mu(e_K) = 1$ for every e_K in the kernel of ∂ are associated to condensed excitations. As we will see in Sec. VII, the uncondensed loop excitations are associated to domain walls related to a symmetry of the model, so it is more appropriate to consider the condensation in that context rather than as condensation of a topological charge.

IV. RIBBON OPERATORS WHEN $\triangleright$ IS NONTRIVIAL

So far we have dealt with the case where $\triangleright$ is trivial. We also consider the case where $\triangleright$ is nontrivial but we restrict to fake-flat configurations (configurations that satisfy the plaquette constraints). In this case, many of the excitations are largely the same as in the $\triangleright$ trivial case discussed in Sec. III, and so we will not repeat results from that section. Instead, we will describe the differences between the two cases. The biggest difference is that we do not allow any magnetic excitations in the fake-flat case because the magnetic excitations violate fake flatness. The other difference is that the loop excitations gain an extra feature. Consider the E-valued membrane operator for a loop excitation, which measures the total surface label of the membrane. As discussed in Ref. [1], the label of a surface depends on its base point when $\triangleright$ is nontrivial. Therefore, when we specify the membrane operator we must specify the base point of the surface that we measure. We call this base point the start point of the membrane operator. In addition to the edge excitations, the membrane operator may excite this start-point vertex. Recall that the vertex transform A_v^g acting on the base point of a plaquette takes that plaquette label from e_p to $g \triangleright e_p$. This is also true for a general surface made up of multiple plaquettes (as we show in Sec. S-I C in the Supplemental Material [45]). This means that the vertex operator at the start-point of our membrane will affect the surface element of the membrane, and so may not commute with our membrane operator. Denoting our membrane

operator (acting on a membrane m) by $\sum_{e\in E}\gamma_e\delta(\hat{e}(m),e)$ and the start point of this operator by s.p,, we have that

$$\begin{aligned}\sum_{e\in E}\gamma_e\delta(\hat{e}(m),e)A^g_{s.p}&=A^g_{s.p}\sum_{e\in E}\gamma_e\delta(g\triangleright\hat{e}(m),e)\\&=A^g_{s.p}\sum_{e\in E}\gamma_e\delta(\hat{e}(m),g^{-1}\triangleright e)\\&=A^g_{s.p}\sum_{e'=g^{-1}\triangleright e}\gamma_{g\triangleright e'}\delta(\hat{e}(m),e').\end{aligned}$$

This indicates that the E-valued membrane operator only commutes with the vertex transform $A^g_{\text{s.p.}}$ at the start point when the set of coefficients γ_e satisfy $\gamma_{g\triangleright e}=\gamma_e$ for all $e\in E$. Then the start-point vertex is not excited when this condition is satisfied for all $g\in G$ and it is excited in orthogonal cases. Explicitly, after the action of a membrane operator $\sum_{e\in E}\gamma_e\delta(e,\hat{e}(m))$ the start-point vertex is not excited (indicating that the operator is gauge invariant) if the coefficients for the membrane operator satisfy

$$\gamma_e=\gamma_{g\triangleright e}\quad\forall\, g\in G, \tag{24}$$

and it is excited if the coefficients satisfy

$$\sum_{g\in G}\gamma_{g\triangleright e}=0\quad\forall\, e\in E. \tag{25}$$

All possible sets of coefficients can be written as a sum of two sets of coefficients: one set satisfying Eq. (24) and one set satisfying Eq. (25), in a similar way to how the coefficients for magnetic ribbon operators could be split into parts that were functions of conjugacy class and parts that gave zero when summed over a conjugacy class [as shown in Eq. (18)]. This is simply because, given an arbitrary set of coefficients, we can separate the part which is invariant under $\triangleright$ action from the rest, analogous to separating symmetric and antisymmetric parts of a matrix. Explicitly, for an arbitrary set of coefficients γ_e we have

$$\gamma_e=\frac{1}{|G|}\sum_{g\in G}\gamma_{g\triangleright e}+\left(\gamma_e-\frac{1}{|G|}\sum_{g\in G}\gamma_{g\triangleright e}\right),$$

where the first term satisfies Eq. (24) and the second term satisfies Eq. (25). This means that we can construct a basis where each basis element corresponds to either the excited case or the unexcited case.

This excitation of the start point of the E-valued membrane operator is, as already mentioned, similar to how the magnetic ribbon operator can excite its start point, depending on what linear combination of magnetic ribbon operators is taken. In the case of the magnetic ribbon operators, it is the conjugacy classes that are the significant objects for determining when the start point is excited. For the E-valued membrane operators, instead of conjugation it is the action of $\triangleright$ that matters. We can define an equivalence relation by $e\sim f$ if and only if there exists an element $g\in G$ such that $e=g\triangleright f$ (reflexivity, symmetry, and transitivity all follow from the group properties of the map $\triangleright$), so much like how G is partitioned by conjugacy classes, there is a partition of E by "$\triangleright$ classes." The vertex at the start point is not excited if the coefficients of the membrane operators are functions of $\triangleright$ class (that is, group elements in a particular $\triangleright$ class all have the same coefficient). This is similar to how the magnetic excitations have no vertex excitations if their operator has coefficients that are a function of conjugacy class.

To better understand these $\triangleright$ classes, it may be useful to go through an example. Consider the crossed module ($G=\mathbb{Z}_2, E=\mathbb{Z}_3, \partial\to 1_G, \triangleright$), where, denoting the elements of G by 1 and -1, the map $\triangleright$ is defined by $-1\triangleright e=e^{-1}$ and $1\triangleright e=e$ for all $e\in E$. Denoting the elements of $E=\mathbb{Z}_3$ by 1_E, ω_E, and ω_E^2, we can write the action of $-1\triangleright$ explicitly as $-1\triangleright 1_E=1_E$, $-1\triangleright\omega_E=\omega_E^2$, and $-1\triangleright\omega_E^2=\omega_E$. We therefore see that ω_E and ω_E^2 are in the same $\triangleright$ class because they are related by the action of $-1\triangleright$. On the other hand, 1_E is in a $\triangleright$ class of its own because it is left invariant by any $\triangleright$ action. Therefore, there are two $\triangleright$ classes. In this case the condition for the start-point vertex of an E-valued membrane operator not to be excited is that the coefficients of ω_E and ω_E^2 in the membrane operator are the same, while the conditions for the vertex to be definitely excited are that the coefficients of ω_E and ω_E^2 must sum to zero and the coefficient of 1_E must be zero.

So far, we have been considering the E-valued membrane operators in a basis labeled by elements of E. However, in a similar way to the $\triangleright$ trivial case, it is useful to use irreducible representations to form a basis for our membrane operators. Unlike the $\triangleright$ trivial case, however, E need not be Abelian and so these irreps do not have to be 1D. Therefore, we also need to include the matrix indices for the representation in our basis membrane operators. We define

$$L^{\mu,a,b}(m)=\sum_{e\in E}[D^\mu(e)]_{ab}\delta(e,\hat{e}(m)), \tag{26}$$

where $D^\mu(e)$ is the matrix representation of e for irrep μ and a and b are its indices. Under an edge transform $\mathcal{A}_i^f$, the surface label $e(m)$ transforms in the same way as individual plaquettes (see Fig. 1) and so transforms as $e(m)\to[g(t)\triangleright f]e(m)$ or $e(m)\to e(m)[g(t)\triangleright f^{-1}]$ for some path element $g(t)$ (as we consider in more detail in Sec. S-I C in the Supplemental Material [45]). This means that we expect our individual edge transforms $\mathcal{A}_i^f$ to affect our membrane operator as

$$\begin{aligned}&\sum_{e\in E}[D^\mu(e)]_{ab}\delta(e,\hat{e}(m))\\&\quad\to\sum_{e\in E}[D^\mu([g\triangleright f]e)]_{ab}\delta(e,\hat{e}(m))\\&\quad=\sum_{e\in E}\sum_{c=1}^{|\mu|}[D^\mu(g\triangleright f)]_{ac}[D^\mu(e)]_{cb}\delta(e,\hat{e}(m)),\end{aligned}$$

where some details of the transformation (such as the label of g, and whether $g\triangleright f$ or its inverse appears) may depend on the branching structure of the lattice and details of the membrane operator. Regardless of the precise form of the transformation, we see that the edge transforms mix labels within a representation (it mixes operators labeled by different indices c within the representation). These edge transforms are local operators. From the fact that the local operator $\mathcal{A}_i^f$ can change the matrix indices, we see that, as we may expect, the matrix elements do not label distinct topological charges, but instead describe

local degrees of freedom. In addition, there is some mixing of different labels due to the vertex transforms. While edge transforms only mix excitations with different indices but the same irreps, vertex transforms mix different representations within a class of representations that we call a "▷-Rep class" of representations. To explain what we mean by this, consider the object

$$D^{g\triangleright\mu}(e) := D^{\mu}(g \triangleright e).$$

This defines a representation $g \triangleright \mu$ because

$$\begin{aligned} D^{g\triangleright\mu}(ef) &= D^{\mu}(g \triangleright (ef)) = D^{\mu}((g \triangleright e)\,(g \triangleright f)) \\ &= D^{\mu}(g \triangleright e) D^{\mu}(g \triangleright f) = D^{g\triangleright\mu}(e) D^{g\triangleright\mu}(f). \end{aligned}$$

We say that two representations μ and α are in the same ▷-Rep class if $g \triangleright \mu = \alpha$ for some $g \in G$. This is an equivalence relation because of the group properties of the ▷ map. We can define this equivalence relation simply in the case of 1D reps, but for higher-dimensional reps we need to be careful because each irrep is related to a set of equivalent irreps which we can generate by conjugating the matrix representation by a constant matrix. Then it could be possible for the $g\triangleright$ action on an irrep to give an irrep that is equivalent to one of our irreps, but in a different form. In most cases, we will either be dealing with the case where E is Abelian or will only care about subgroups in the center of E (specifically the kernel of ∂). In this case conjugation is trivial and the irreps are unaffected. However, to be concrete, in the non-Abelian case we should talk about classes of characters, or define the ▷-Rep classes to account for conjugation.

Having discussed these ▷-Rep classes, we can now see how they relate to the action of the vertex transform. The action of the vertex transform on an E-valued membrane operator is to take $L^{\mu,a,b}(m) = \sum_{e\in E}[D^{\mu}(e)]_{ab}\delta(e, \hat{e}(m))$ to

$$\begin{aligned} &\sum_{e\in E}[D^{\mu}(e)]_{ab}\delta(e, g^{-1} \triangleright \hat{e}(m)) \\ &\quad = \sum_{e'=g\triangleright e}[D^{\mu}(g^{-1} \triangleright e')]_{ab}\delta(e', \hat{e}(m)) \\ &\quad = \sum_{e'\in E}[D^{g^{-1}\triangleright\mu}(e')]_{ab}\delta(e', \hat{e}(m)) \\ &\quad = L^{g^{-1}\triangleright\mu,a,b}(m), \end{aligned}$$

which is labeled by another irrep in the same ▷-Rep class as μ. The fact that vertex operators link excitations labeled by irreps within these classes suggests that we should group the membrane operators into ▷-Rep classes of representations of E. However, just as we discussed in the ▷ trivial case in Sec. III D, some of the E-valued loops are condensed, which means that some membrane operators labeled by different irreps are in fact equivalent up to operators on the boundary of the membrane. Just as in the ▷ trivial case, the condensed E-valued loops are those labeled by irreps that have trivial restriction to the kernel of ∂. This follows from the same reasoning as for the ▷ trivial case: an electric ribbon around the boundary of a surface can measure the surface element up to an element of the kernel when that surface satisfies fake flatness. This condensation of the excitations corresponding to irreps with trivial restriction to the kernel means that we should group the looplike excitations into ▷-Rep classes of irreps of the kernel of ∂. These groupings will fuse in a non-Abelian way because two ▷-Rep classes of irreps can potentially fuse to more than one ▷-Rep class. This is true even if the irreps themselves are 1D (in fact, irreps of the kernel are always 1D because the kernel is Abelian), so that an Abelian group E does not necessarily give Abelian fusion.

As an example, consider the crossed module $(\mathbb{Z}_2, \mathbb{Z}_3, \partial \to 1_G, \triangleright)$ that we used earlier in this section. Here the map ▷ is defined by $-1_G \triangleright e = e^{-1}$ for any $e \in \mathbb{Z}_3$ (while $1_G\triangleright$ is the identity map). The group $\mathbb{Z}_3$ has three irreps. The trivial one, which we call 1_R, is invariant under the ▷ action [because $1_R(g \triangleright e) = 1$ regardless of g], and so is in a ▷-Rep class of its own. The other two irreps, which we denote by α_R and α_R^2, are defined by $\alpha_R(\omega_E) = e^{\frac{2\pi i}{3}}$, $\alpha_R(\omega_E^2) = e^{\frac{4\pi i}{3}}$, and $\alpha_R^2(e) = \alpha_R(e^{-1})$ (where ω_E and ω_E^2 are the two nontrivial elements of E). We therefore see that

$$-1_G \triangleright \alpha_R(e) = \alpha_R(-1_G \triangleright e) = \alpha_R(e^{-1}) = \alpha_R^2(e),$$

and so α_R and α_R^2 belong to the same ▷-Rep class. Now consider an E-valued membrane operator made from a combination of the α_R and α_R^2 irreps:

$$L^{\vec{A}}(m) = A_1 L^{\alpha_R}(m) + A_2 L^{\alpha_R^2}(m),$$

where A_1 and A_2 are nonzero coefficients. If we fuse two copies of this membrane operator, we obtain

$$\begin{aligned} &L^{\vec{A}}(m)L^{\vec{A}}(m) \\ &\quad = \big(A_1 L^{\alpha_R}(m) + A_2 L^{\alpha_R^2}(m)\big)\big(A_1 L^{\alpha_R}(m) + A_2 L^{\alpha_R^2}(m)\big) \\ &\quad = A_1^2 L^{\alpha_R}(m)L^{\alpha_R}(m) + A_2^2 L^{\alpha_R^2}(m)L^{\alpha_R^2}(m) \\ &\qquad + 2A_1A_2 L^{\alpha_R}(m)L^{\alpha_R^2}(m). \end{aligned}$$

Using the fusion rules given in Eq. (23), we have

$$\begin{aligned} L^{\alpha_R}(m)L^{\alpha_R}(m) &= L^{\alpha_R\alpha_R}(m) = L^{\alpha_R^2}(m), \\ L^{\alpha_R^2}(m)L^{\alpha_R^2}(m) &= L^{\alpha_R^2\alpha_R^2}(m) = L^{\alpha_R}(m), \end{aligned}$$

and

$$L^{\alpha_R}(m)L^{\alpha_R^2}(m) = L^{\alpha_R\alpha_R^2}(m) = L^{1_R}(m).$$

Therefore,

$$L^{\vec{A}}(m)L^{\vec{A}}(m) = A_1^2 L^{\alpha_R^2}(m) + A_2^2 L^{\alpha_R}(m) + 2A_1A_2 L^{1_R}(m).$$

We see that the fusion product includes contributions from the ▷-Rep class containing α_R and α_R^2, but also a term corresponding to the trivial ▷-Rep class, indicating that the fusion is non-Abelian.

V. BRAIDING

In (2+1)D, one major feature of topological phases of matter is that the excitations may support *braiding statistics* that generalize the familiar bosonic and fermionic exchange phases [48,52–54]. When one point particle is taken on a path all the way around another (which would give a trivial transformation for either fermions or bosons) it can result in a transformation that is a general phase, or even some more complicated transformation. Before we discuss the braiding

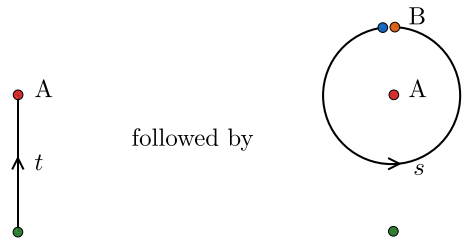

FIG. 9. We can create the situation where a particle B braids around A by first producing A and then moving B around it with ribbon operators.

results for this model, we should first explain how we find the braiding relations. We mentioned earlier how the ribbon operators produce and move excitations. This lets us recast braiding in terms of commutation relations of the ribbon operators. Consider the following situation, as shown in Fig. 9. We create a pair of excitations and move one of them (A) far away from the other, using a ribbon operator on a path t. Then we produce another pair of excitations and move one of these (B) around A, by acting with a ribbon operator on a new path s.

Now consider applying the operators in the other order, acting on s first, as shown in Fig. 10. This moves B around empty space and then creates the other pair and moves A into the region of interest. Therefore, no braiding has occurred, because no particle moved around another.

In the first case (shown in Fig. 9), B braided with A but in this second case (Fig. 10) it has not. However, in the two cases the particles end up in the same places and have moved through the same space. Comparing the two (by working out the commutation relation of the two ribbon operators used to perform the movement) therefore isolates the effect of braiding B around A from any other details and gives the braiding relation.

A. The $\triangleright$ trivial case

We first look at braiding in the case where $\triangleright$ is trivial. In this case, the nontrivial braiding involves only the electric and magnetic excitations, and not the looplike excitations. This is because the braiding relations can be calculated from commutation relations, and the electric and magnetic operators both commute with the E-valued membrane operators. We can see this from the fact that the electric and magnetic ribbons act only on the edge labels, whereas the membrane operators only act on the surface labels.

We also have trivial braiding between two electric excitations. The braiding is trivial because the electric ribbons are

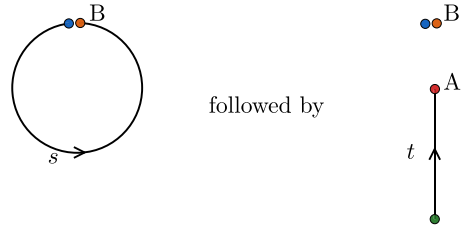

FIG. 10. By applying the ribbon operators in the other order, we move particle B through empty space rather than around A.

diagonal in the configuration basis (i.e., the basis where each edge is labeled by a group element in G and each plaquette by a group element in E), so that they all commute with each other. On the other hand, braiding an electric excitation with a magnetic excitation is not trivial. When the start points of the operators are the same, electric operators transform under braiding with magnetic excitations according to the representation of the electric excitation and the group element of the magnetic one. For braiding of an electric excitation labeled by irrep and matrix indices $\{R, a, b\}$ with a magnetic excitation labeled by h, we have (as we show in Sec. S-IV A of the Supplemental Material [45])

Electric-magnetic braiding

$$S^{R,a,b}(t)C^h(r)|GS\rangle = C^h(r)\sum_{c=1}^{|R|}[D^R(h)]_{ac}S^{R,c,b}(t)|GS\rangle. \quad (27)$$

We can understand this relation by considering that the magnetic excitation sets up a flux labeled by h. When the electric excitation crosses the magnetic ribbon, it is acted on by this flux, so that the path measured by the electric excitation gains an additional factor of h. When we consider the irrep basis, this leads to the factor of $[D^R(h)]_{ac}$. We see that different indices within the representation of the electric excitation are mixed by this braiding. Note that the precise formula depends on the orientation of the braiding procedure, so there may be an inverse on h compared to the result in Eq. (27). This braiding between the electric and magnetic excitations is the same as in the Kitaev quantum double model [37] because the ribbon operators have the same commutation relations as the corresponding operators in that model. In Ref. [37], the commutation relations are calculated by using the group element basis for the electric part of the ribbon, rather than the irrep basis. Then to obtain the relation given above we simply need to take appropriate linear combinations of the operators used in Ref. [37].

One interesting case of the braiding relation given in Eq. (27) is where we take h to be an element of $\partial(E)$. In this case, as we discussed in Sec. III C, the magnetic excitation is condensed. Taking $h = \partial(e)$, the braiding relation becomes

$$\begin{aligned} &S^{R,a,b}(t)C^{\partial(e)}(r)|GS\rangle \\ &\quad = \sum_{c=1}^{|R|}[D^R(\partial(e))]_{ac}C^{\partial(e)}(r)S^{R,c,b}(t)|GS\rangle. \end{aligned}$$

When $\triangleright$ is trivial, $\partial(E)$ is in the center of G (see Sec. II), and so $[D^R(\partial(e))]$ must be a scalar multiple of the identity from Schur's lemma. The braiding relation therefore simplifies to

$$\begin{aligned} &S^{R,a,b}(t)C^{\partial(e)}(r)|GS\rangle \\ &\quad = \sum_{c=1}^{|R|}[D^R(\partial(e))]_{11}\delta_{ac}C^{\partial(e)}(r)S^{R,c,b}(t)|GS\rangle \\ &\quad = [D^R(\partial(e))]_{11}C^{\partial(e)}(r)S^{R,a,b}(t)|GS\rangle. \end{aligned} \quad (28)$$

The diagonal element $[D^R(\partial(e))]_{11}$ can be considered as an irrep of $\partial(E)$ (the irrep branching from the restricted

representation we described in Sec. III A), and the braiding is only nontrivial if this irrep is nontrivial. As we described in Sec. III A, this irrep of $\partial(E)$ being nontrivial is also the condition for an electric excitation to be confined. We therefore see that the only electric excitations that braid nontrivially with the condensed magnetic excitations are the confined excitations, as we expect.

The final nontrivial braiding is between two magnetic excitations, with this braiding only being nontrivial when the group G is non-Abelian. Under braiding, two magnetic ribbons with the same start point transform by conjugation. When the end of one ribbon (the end is a quasiparticle) is taken all the way around one of the other quasiparticles (not enclosing any other quasiparticle), the label of each is conjugated by the product of the labels of each quasiparticle. If we then consider ribbon operators that are linear combinations of operators labeled by elements in a certain conjugacy class, then the braiding results in mixing within this conjugacy class. In particular, note that if one of the magnetic ribbons is an equal superposition of all fluxes in a conjugacy class (meaning it carries no start-point excitation, as discussed in Sec. III B), conjugation has no effect because it just permutes these fluxes within their conjugacy class. If the ribbon is not an equal superposition, then it transforms in some other, more complex, way. This means that the degrees of freedom within a conjugacy class of the flux are nonconserved internal degrees of freedom that describe how they braid with other fluxes, as we mentioned in Sec. III B. Again, this braiding is the same as the braiding of the equivalent excitations in Kitaev's quantum double model [37], so we will not go into too much detail here (although the detailed results are discussed in Sec. S-IV B in the Supplemental Material [45]).

The nontrivial braiding relations that we have discussed so far hold only when the ribbon operators have the same start point. This is because the theory is generally non-Abelian. In a non-Abelian anyon theory, the braiding between two anyons depends on what fusion channel they are in [48]. That is, the braiding operator R_c^{ab} for two anyons a and b depends on their total anyonic charge c. The excitations are generally only in a definite fusion channel (as opposed to some operator superposition) when the ribbons used to create them share a start point. Therefore, they only have a definite braiding transformation under the same circumstances.

The notion of definite braiding only occurring when our operators have a "start point" at the same location also has an interpretation in terms of the gauge theory picture. In non-Abelian gauge theory, fluxes are associated with some closed loop [55]. This closed loop has a definite start point and moving this start point should be accompanied by some change of basis. Therefore, to compare two fluxes (such as when we want to fuse or braid them), they need to be defined with the same start point. If we start with two fluxes that have different start points, we therefore need to write one of these fluxes in terms of a flux based at the other start point (i.e., work out its label with respect to a different start point). In our lattice theory, the flux label corresponding to a new start point is the original flux label conjugated by a path element operator (not just a fixed group element), so the flux does not have definite label with respect to that new start point.

B. The fake-flat case

When we restrict to fake-flat configurations, but allow $\triangleright$ to be nontrivial (case 3 in Table I in Sec. II), we do not have the magnetic excitations. In addition the E-valued loops and the electric ribbons still braid trivially, due to the fact that both are diagonal in the configuration basis. Therefore, there is no nontrivial braiding in this case. There is nontrivial commutation between the E-valued membrane operators and the single-plaquette multiplication operators (which is also the case in the $\triangleright$ trivial case). However, this does not correspond to braiding because the single-plaquette operators are local operators and have no interpretation in terms of moving excitations.

While restricting to fake-flatness rules out any magnetic excitations, the signatures of these missing excitations are still present in the model. If we consider a manifold with noncontractible cycles, such as a torus, then some ground states contain closed loops with labels outside of $\partial(E)$ (just like we would expect around a noncondensed magnetic excitation). If we apply an electric ribbon operator around such a cycle t, then this is equivalent to producing a pair of electric excitations and passing one of them around the cycle. We can use this to find the transformation from moving the excitation around the handle. Consider comparing an electric ribbon operator that produces and separates a pair of excitations along a small path s, to one that produces and separates the pair along s, but then further moves the excitation at the end of s around the noncontractible cycle t. That is, we compare a ribbon operator applied on s to one applied on the composite path st. If the ribbon operators are labeled by irrep R of G, with matrix indices a and b, then the latter ribbon operator is given by

$$S^{R,a,b}(s\cdot t)=\sum_{g\in G}(D^R(g))_{ab}\delta(g,\hat{g}(s\cdot t)).$$

We can then separate the path element $\hat{g}(s\cdot t)$ into two parts, corresponding to s and t: $\hat{g}(s\cdot t)=\hat{g}(s)\cdot\hat{g}(t)$. This tells us that

$$\begin{aligned}S^{R,a,b}(s\cdot t)&=\sum_{g\in G}(D^R(g))_{ab}\delta(g,\hat{g}(s)\cdot\hat{g}(t))\\&=\sum_{g\in G}(D^R(g))_{ab}\delta(g\hat{g}(t)^{-1},\hat{g}(s))\\&=\sum_{g'=g\hat{g}(t)^{-1}\in G}[D^R(g'\hat{g}(t))]_{ab}\delta(g',\hat{g}(s)).\end{aligned}$$

We can then split the matrix element $[D^R(g'\hat{g}(t))]_{ab}$ into contributions from g' and $\hat{g}(t)$, to give

$$S^{R,a,b}(s\cdot t)=\sum_{g'\in G}\sum_{c=1}^{|R|}(D^R(g'))_{ac}[D^R(\hat{g}(t))]_{cb}\delta(g,\hat{g}(s)).$$

Recognizing $\sum_{g'\in G}(D^R(g'))_{ac}\delta(g,\hat{g}(s))$ as the electric ribbon operator $S^{R,a,c}(s)$ on the ribbon s, we have

$$S^{R,a,b}(s\cdot t)=\sum_{c=1}^{|R|}[D^R(\hat{g}(t))]_{cb}S^{R,a,c}(s),$$

TABLE II. The notation used for the two groups $\mathbb{Z}_2$ and $\mathbb{Z}_3$ in this section.

	G	E
Group	$\mathbb{Z}_2$	$\mathbb{Z}_3$
Elements	$\{1, -1\}$	$\{1_E, \omega_E, \omega_E^2\}$
Irreps	$\{1_R^G, -1_R^G\}$	$\{1_R, \alpha_R, \alpha_R^2\}$

so that moving the excitation around t induces a transformation that mixes the ribbon operators labeled by different matrix indices for the irrep R, by (right-) matrix multiplication by $D^R[\hat{g}(t)]$ (note the similarity to the transformation we predicted in Sec. II in Ref. [44], except that right multiplication is required to ensure correct composition, rather than left multiplication). Here $\hat{g}(t)$ is an operator, and cycles (including noncontractible ones) in the ground state are not generally in an eigenstate of this path measurement operator (that is, the cycles are in a linear combination of states with different labels), so this transformation is not usually a simple one. In Sec. S-IV C of the Supplemental Material [45], we discuss in more detail the circumstances where we can simplify this transformation. We find that, for ground states where $\hat{g}(t)$ is minimally mixed, and where we annihilate the two excitations at the end of the ribbon operator, the transformation can be described by the character of the irrep R.

VI. PARTICULAR EXAMPLES

It may be useful to consider some simple examples in more detail to see the interesting features of the higher-lattice gauge theory model. Therefore, we will look at two examples that each highlight a particular feature of the model.

A. $\mathbb{Z}_2$, $\mathbb{Z}_3$ model

The first features to highlight are the loop excitations and how these excitations are related to the ground-state degeneracy. For simplicity we first look at these in the absence of condensation and confinement. A convenient model with which to examine these features is described by the crossed module $(\mathbb{Z}_2, \mathbb{Z}_3, \partial \to 1_G, \triangleright)$ (which we used as an example in Sec. IV, but define again here for reference). To distinguish the elements of the two groups, we will write the elements of $G = \mathbb{Z}_2$ as ± 1 and those of $E = \mathbb{Z}_3$ as 1_E, ω_E, and ω_E^2. Then $\triangleright$ is defined by

$$1 \triangleright e = e \forall\, e \in E, \quad -1 \triangleright 1_E = 1_E,$$
$$-1 \triangleright \omega_E = \omega_E^2, \quad -1 \triangleright \omega_E^2 = \omega_E.$$

This can be summarized as $1 \triangleright e = e$, $-1 \triangleright e = e^{-1}$. One simple way to generalize this crossed module slightly is to replace the group $\mathbb{Z}_3$ with $\mathbb{Z}_n$, where n is odd, and define $\triangleright$ by $-1 \triangleright e = e^{-1}$. However, the features of such a model are very similar to the $\mathbb{Z}_3$ case, so we only present the $\mathbb{Z}_3$ case here. The properties of this crossed module and the notation used in this section are summarized in Tables II and III to refer back to as necessary.

In addition to choosing this particular crossed module, we also choose a specific lattice, a fragment of which is shown in Fig. 11. In this lattice we have one kind of vertex, two types of edge (horizontal and vertical) and one kind of plaquette. The actions of the corresponding operators are shown in Fig. 12.

TABLE III. The result of each map acting on the elements of E. The final line shows the general action of each map.

e	$\partial(e)$	$1 \triangleright e$	$-1 \triangleright e$
1_E	1_G	1_E	1_E
ω_E	1_G	ω_E	ω_E^2
ω_E^2	1_G	ω_E^2	ω_E
General $e \in E$	1_G	e	e^{-1}

It will be convenient to consider a change of basis, to simplify the action of the operators. For the plaquette elements we change variables from group elements to irreps. We denote the three irreps of $\mathbb{Z}_3$ by 1_R, α_R, and α_R^2. The 1D irreps form a group under the multiplication defined by $(\mu_1\mu_2)(e) = \mu_1(e)\mu_2(e)$ for irreps μ_1 and μ_2. 1_R is the identity element for this group, while α_R and α_R^2 are inverses to each other. We can then define states for the plaquette degrees of freedom using these irreps:

$$|1_R\rangle = \frac{1}{\sqrt{3}}\left(|1_E\rangle + |\omega_E\rangle + |\omega_E^2\rangle\right),$$
$$|\alpha_R\rangle = \frac{1}{\sqrt{3}}\left(|1_E\rangle + \omega|\omega_E\rangle + \omega^2|\omega_E^2\rangle\right),$$
$$|\alpha_R^2\rangle = \frac{1}{\sqrt{3}}\left(|1_E\rangle + \omega^2|\omega_E\rangle + \omega|\omega_E^2\rangle\right),$$

where ω is $e^{2\pi i/3}$. We now wish to see how the various energy terms act in this new basis. First, we consider the vertex transforms, as defined in Eq. (5) in Sec. II. We consider the state of the degrees of freedom around a particular vertex, using the notation $|e, g_1, g_2, g_3, g_4\rangle$ defined in Fig. 13. We suppress any labels corresponding to the degrees of freedom in the rest of our lattice (because these other degrees of freedom are unaffected by the vertex transform). Then the corresponding state where the plaquette is labeled by an irrep μ of E is given

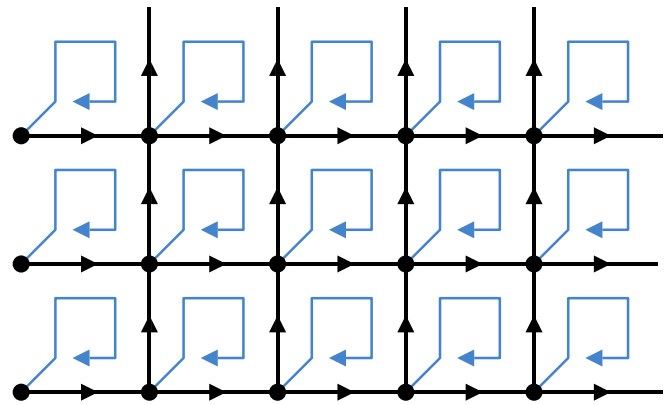

FIG. 11. This image shows a fragment of the lattice used for our example model. The (blue) circulating arrows represent the plaquettes, which are based at the vertices (shown as small black circles) that are attached to the arrows.

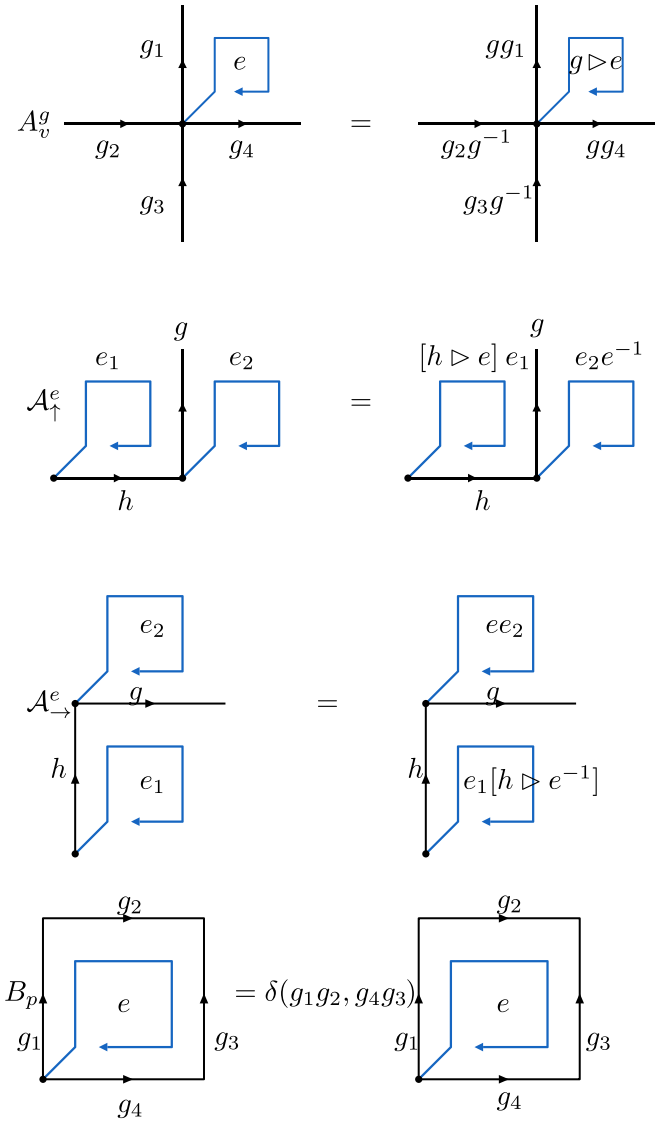

FIG. 12. Here we indicate the action of the vertex transforms, edge transforms, and plaquette term of the example model.

by

$$|\mu, g_1, g_2, g_3, g_4\rangle = \frac{1}{\sqrt{3}} \sum_{e \in \mathbb{Z}_3} \mu(e) |e, g_1, g_2, g_3, g_4\rangle.$$

From the definition of the vertex transforms [Eq. (5)], we know that the vertex transform labeled by the identity element of G is the identity operator. On the other hand, the vertex transform A_v^{-1} acts on this new basis as

$$\begin{aligned}
&A_v^{-1} |\mu, g_1, g_2, g_3, g_4\rangle \\
&\quad = A_v^{-1} \frac{1}{\sqrt{3}} \sum_{e \in \mathbb{Z}_3} \mu(e) |e, g_1, g_2, g_3, g_4\rangle \\
&\quad = \frac{1}{\sqrt{3}} \sum_{e \in \mathbb{Z}_3} \mu(e) |-1 \triangleright e, -1 \cdot g_1, -1 \cdot g_2, -1 \cdot g_3, -1 \cdot g_4\rangle \\
&\quad = \frac{1}{\sqrt{3}} \sum_{e \in \mathbb{Z}_3} \mu(e) |e^{-1}, -1 \cdot g_1, -1 \cdot g_2, -1 \cdot g_3, -1 \cdot g_4\rangle \\
&\quad = \frac{1}{\sqrt{3}} \sum_{e' = e^{-1}} \mu(e'^{-1}) |e', -1 \cdot g_1, -1 \cdot g_2, -1 \cdot g_3, -1 \cdot g_4\rangle \\
&\quad = \frac{1}{\sqrt{3}} \sum_{e' \in \mathbb{Z}_3} \mu(e')^{-1} |e', -1 \cdot g_1, -1 \cdot g_2, -1 \cdot g_3, -1 \cdot g_4\rangle \\
&\quad = \frac{1}{\sqrt{3}} \sum_{e' \in \mathbb{Z}_3} \mu^{-1}(e') |e', -1 \cdot g_1, -1 \cdot g_2, -1 \cdot g_3, -1 \cdot g_4\rangle \\
&\quad = |\mu^{-1}, -1 \cdot g_1, -1 \cdot g_2, -1 \cdot g_3, -1 \cdot g_4\rangle. \qquad (29)
\end{aligned}$$

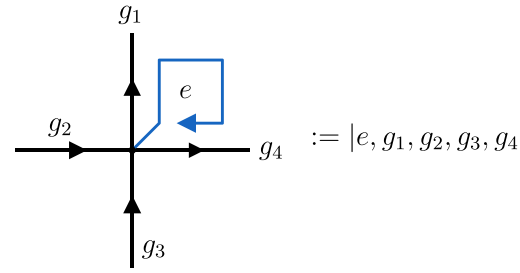

FIG. 13. We wish to consider the effect of a vertex transform on the degrees of freedom around the vertex as we change basis. It is therefore useful to have a simple notation for the state of the degrees of freedom affected by the vertex transform in the original basis, which we define here.

Next we consider the edge terms, starting by considering the edge terms for the vertical edges $\mathcal{A}_\uparrow$. In Fig. 14 we define the state $|e_1, e_2, g, h\rangle$ for the degrees of freedom near the edge. Again, for simplicity we suppress labels corresponding to the degrees of freedom on the rest of our lattice, which are unaffected by the edge term.

As described in Eq. (6) in Sec. II, the edge energy terms are given by averages of different edge transforms, where the edge transforms are defined in Eq. (7). That is, the edge energy term is given by $\mathcal{A}_\uparrow = \frac{1}{|E|} \sum_{f \in E} A_\uparrow^f$. Then the action of the edge term in the new basis is

$$\begin{aligned}
&\mathcal{A}_\uparrow |\mu_1, \mu_2, g, h\rangle \\
&\quad = \frac{1}{3} \sum_{e_1, e_2 \in \mathbb{Z}_3} \mathcal{A}_\uparrow \mu_1(e_1) \mu_2(e_2) |e_1, e_2, g, h\rangle \\
&\quad = \frac{1}{3} \sum_{e_1, e_2 \in \mathbb{Z}_3} \left(\frac{1}{3} \sum_{f \in E} \mathcal{A}_\uparrow^f \right) \mu_1(e_1) \mu_2(e_2) |e_1, e_2, g, h\rangle
\end{aligned}$$

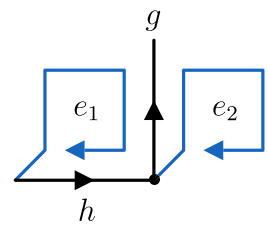

FIG. 14. We introduce notation to represent the state of the degrees of freedom around the vertical edges of our lattice (here the one labeled by g).

$$= \frac{1}{9} \sum_{e_1,e_2\in\mathbb{Z}_3} \mu_1(e_1)\mu_2(e_2) \sum_{f\in E} |[h \triangleright f]e_1, e_2 f^{-1}, g, h\rangle$$
$$= \frac{1}{9} \sum_{f,e_1',e_2'\in\mathbb{Z}_3} \mu_1([h \triangleright f^{-1}]e_1')\mu_2(e_2' f)|e_1', e_2', g, h\rangle, \quad (30)$$

where we replaced the dummy indices e_1 and e_2 with $e_1' = [h \triangleright f]e_1$ and $e_2' = e_2 f^{-1}$ in the last step. We can then use the fact that μ_1 and μ_2 are irreps to split off the contribution from f from the contributions of e_1' and e_2' in Eq. (30) to obtain

$$\begin{aligned}\mathcal{A}_\uparrow|\mu_1, \mu_2, g, h\rangle &= \frac{1}{9} \sum_{f,e_1',e_2'\in\mathbb{Z}_3} \mu_1(h \triangleright f^{-1})\mu_2(f)\mu_1(e_1')\mu_2(e_2') \\ &\times |e_1', e_2', g, h\rangle \\ &= \frac{1}{3} \sum_{f\in\mathbb{Z}_3} \mu_1(h \triangleright f^{-1})\mu_2(f)|\mu_1, \mu_2, g, h\rangle. \end{aligned} \quad (31)$$

The above equation includes the quantity $\mu_1(h \triangleright f^{-1})$. Because we are working with irreps, rather than group elements, it is useful to consider the $h\triangleright$ as acting on the irrep rather than the group, just as we did in Sec. IV for the E-valued membrane operators. Consider a general expression $\mu(g \triangleright e)$, where μ is an irrep of E and g is a general group element of G. We see that this will give us a new irrep of E acting on e, $\mu'(e)$, with the resulting irrep depending on g:

$$\begin{aligned} 1_R(g \triangleright e) &= 1 = 1_R(e), \\ \alpha_R(1 \triangleright e) &= \alpha_R(e), \\ \alpha_R^2(1 \triangleright e) &= \alpha_R^2(e), \\ \alpha_R(-1 \triangleright e) &= \alpha_R(e^{-1}) = \alpha_R^{-1}(e) = \alpha_R^2(e), \\ \alpha_R^2(-1 \triangleright e) &= \alpha_R^2(e^{-1}) = (\alpha_R^2)^{-1}(e) = \alpha_R(e). \end{aligned}$$

Therefore, we can write $\mu(g \triangleright e)$ as a group element acting on an irrep, by defining the irrep $g \triangleright \mu$ according to

$$\mu(g \triangleright e) = [g \triangleright \mu](e).$$

We say that irreps that are related by this $\triangleright$ action, for some value of $g \in G$, are in the same $\triangleright$-Rep class. For this crossed module, α_R and α_R^2 are in the same $\triangleright$-Rep class (they are related by the action $-1\triangleright$), while the trivial irrep is in a class of its own. We note that the composition rule for this action on the irreps is generally reversed:

$$\begin{aligned}[(gh) \triangleright \mu](e) &= \mu[(gh) \triangleright e] = \mu[g \triangleright (h \triangleright e)] \\ &= [g \triangleright \mu](h \triangleright e) = [h \triangleright (g \triangleright \mu)](e), \end{aligned} \quad (32)$$

although this does not matter in this case because G is Abelian. Under this definition of the $\triangleright$ action on the irreps, for an arbitrary irrep μ of E, we have $1 \triangleright \mu = \mu$ and $-1 \triangleright \mu = \mu^{-1}$.

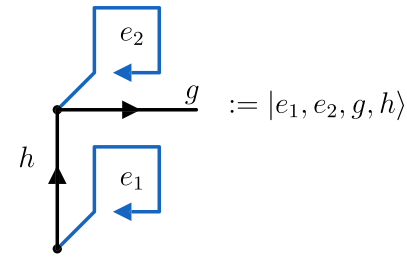

FIG. 15. We introduce notation to describe the state of the degrees of freedom affected by a horizontal edge transform.

Returning to our calculation of the action of the edge terms, we can insert the relation

$$\mu_1(h \triangleright f^{-1}) = [h \triangleright \mu_1](f^{-1})$$

into our expression for the action of $\mathcal{A}_\uparrow$ from Eq. (31) to obtain

$$\begin{aligned}\mathcal{A}_\uparrow|\mu_1, \mu_2, g, h\rangle &= \frac{1}{3} \sum_{f\in\mathbb{Z}_3} [h \triangleright \mu_1(f^{-1})]\mu_2(f)|\mu_1, \mu_2, g, h\rangle \\ &= \delta(\mu_2, h \triangleright \mu_1)|\mu_1, \mu_2, g, h\rangle, \end{aligned} \quad (33)$$

where the last equality follows from standard orthogonality relations for irreps of groups. We see that the edge transform enforces that the irreps labeling the plaquettes separated by the edge must be related by the action of $h\triangleright$ in the low-energy state, where h labels the edge separating the base points of the two plaquettes.

Next we consider the other type of edge energy term $\mathcal{A}_\rightarrow$, corresponding to the horizontal edges of our lattice, for which we will find a similar result. As with the vertex transform and other edge transform, we use a simplified notation to describe the degrees of freedom in the support of this energy term, as shown in Fig. 15. Then, following the same procedure as for the vertical edge energy terms, we have the following action for this horizontal edge energy term [again using the definition of the edge transforms from Eq. (7) and averaging them to obtain the edge term]:

$$\begin{aligned}\mathcal{A}_\rightarrow|\mu_1, \mu_2, g, h\rangle &= \frac{1}{9} \sum_{e_1,e_2,f\in\mathbb{Z}_3} \mu_1(e_1)\mu_2(e_2)\mathcal{A}_\rightarrow^f|e_1, e_2, g, h\rangle \\ &= \frac{1}{9} \sum_{e_1,e_2,f\in\mathbb{Z}_3} \mu_1(e_1)\mu_2(e_2)|e_1[h \triangleright f^{-1}], f e_2, g, h\rangle \\ &= \frac{1}{9} \sum_{e_1',e_2',f\in\mathbb{Z}_3} \mu_1(e_1'[h \triangleright f])\mu_2(e_2' f^{-1})|e_1', e_2', g, h\rangle \\ &= \frac{1}{3} \sum_{f\in\mathbb{Z}_3} \mu_1(h \triangleright f)\mu_2(f^{-1})|\mu_1, \mu_2, g, h\rangle \\ &= \delta(\mu_2, h \triangleright \mu_1)|\mu_1, \mu_2, g, h\rangle. \end{aligned} \quad (34)$$

Again we see that the irreps labeling the plaquettes separated by the edge must be related by the $\triangleright$ action of the label of the edge separating their base points. This suggests that the plaquette labels must be different to account for the effect of choosing different base points (recall that moving the base

point of a plaquette has a similar $\triangleright$ action on the plaquette label). That is, if we had chosen the plaquettes to have the same base points, the irreps labeling them would be the same in the low-energy space. Indeed, we shall see that this is true when we consider this in more detail in Sec. VI A 5.

The last energy term to consider is the plaquette term, which is described in the group element basis in the bottom of Fig. 12. In a general higher-lattice gauge theory model, the plaquette term B_p depends on the plaquette label e_p only through $\partial(e_p)$. This means that in the example model under consideration, where ∂ maps to the identity element 1_G, the plaquette term does not act on the plaquette labels, and so it acts exactly the same in the basis where the plaquettes are labeled by irreps as in our original basis where they were labeled by group elements. That is, the plaquette term is satisfied if the boundary of the plaquette has total label 1_G, and gives zero otherwise.

1. Ground states

Having considered the various energy terms of this example model, we wish to use them to examine the ground states. The number of ground states will generally depend on the topology of the manifold. Our fragment of lattice can be completed to a variety of manifolds, depending on the boundary conditions of our lattice. We want to keep the discussion general, but it may be useful to have the sphere in mind. Typically, topological models on the sphere have a unique ground state, in the absence of symmetry. In order to close the lattice we have been considering into a sphere, we may need to include additional vertices that do not look like the ones in the fragment of lattice shown in Fig. 11. However, the general features of the different energy terms will still be preserved when we include such vertices.

Now consider the restrictions for states in the ground-state sector. Flatness constraints (the plaquette terms) restrict our choice of configuration, by restricting the allowed edge labels. Then given a set of edge labels, the plaquette labels (in representation basis) are restricted by the edge transforms. We can see from Eqs. (33) and (34) that the edge transforms fix the labels μ_1 and μ_2 of neighboring plaquettes to be related by $\mu_2 = h \triangleright \mu_1$, where h labels the edge separating the base points of the two plaquettes. To see how this determines the allowed plaquette labels, consider taking one of these plaquettes and choosing a particular irrep μ_1 to label it. If we choose μ_1 to be the trivial irrep 1_R, then the label μ_2 of an adjacent plaquette must satisfy $\mu_2 = 1_R$ because $h\triangleright$ acts trivially on the trivial irrep for any group label $h \in G$. Then by iteration, this will be true for any plaquette connected to the first by a path on the dual lattice. Therefore, for a path-connected manifold, once we choose one plaquette to be labeled by 1_R, all of the other plaquette labels must also take that value.

Next we look at the case where we choose the irrep label μ_1 of the first plaquette to be $\mu_1 = \alpha_R$ or α_R^2 instead of 1_R. Then the label μ_2 of an adjacent plaquette could be either α_R or α_R^2, but which one is fixed by the edge configuration (the labels of the two plaquettes match if the edge connecting their base points is labeled by 1 and are opposite if the edge is labeled by -1). Again, all path-connected plaquettes will be fixed in this way. By iterating the relationship that two adjacent plaquettes

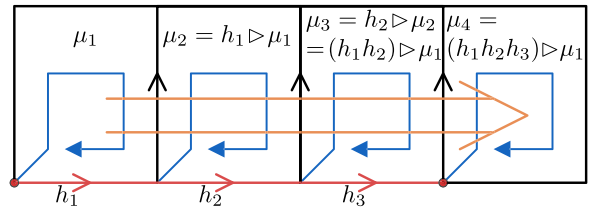

FIG. 16. The edge terms relate the labels of neighboring plaquettes, so that the labels μ_1 and μ_2 of plaquettes 1 and 2 in the figure are related by $\mu_2 = h_1 \triangleright \mu_1$. By iterating this relation, we can relate the labels of distant plaquettes, such as plaquettes 1 and 4 in the figure, as long as they are connected by a ribbon (here the direct path of the ribbon is the thicker red edges at the bottom and the dual path is the large orange arrow in the middle).

1 and 2 labeled μ_1 and μ_2 must satisfy $\mu_2 = h \triangleright \mu_1$, where h is the label of the edge connecting the base points of plaquette 1 and plaquette 2, we can find the relationship between any two plaquettes connected by a path (see Fig. 16 for an example). For a plaquette 1 with base point at the start of path t and plaquette n with base point at the end of the path, we must have $\mu_n = g(t) \triangleright \mu_1$, where $g(t)$ is the label of path t. If there are multiple paths between two plaquettes, we must ask if these different paths always give consistent conditions on the two irreps. In order to answer this question, consider two such paths t_1 and t_2 between the two plaquettes. Because these two paths share the same start and end points, we can construct a closed path $s = t_1 t_2^{-1}$ by concatenating one with the inverse of the other. If the two paths t_1 and t_2 can be smoothly deformed into one another, then the closed path s is contractible and so must satisfy fake flatness in the ground state. For a general crossed module, fake flatness enforces that the label of the closed path is related to the label e_s of the surface enclosed by that path by $\partial(e_s)g(s) = 1_G$. In the case of this specific $\mathbb{Z}_2$, $\mathbb{Z}_3$ model, however, ∂ maps to the identity element of G and so $\partial(e_s)$ is always 1_G. Therefore, $g(s) = g(t_1)g(t_2)^{-1} = 1_G$, meaning that the labels $g(t_1)$ and $g(t_2)$ of the two paths are the same, and so the two paths give consistent conditions $\mu_n = g(t_1) \triangleright \mu_1 = g(t_2) \triangleright \mu_1$. Of course, this relies on the two paths being related by a smooth deformation, which means that the closed path s is contractible. However, if this is not so and the closed path is noncontractible, then the closed path s can have either label ± 1. If it has the label -1, then we have $g(t_1) = -1 \cdot g(t_2)$, which leads to the two conditions

$$\mu_n = g(t_2) \triangleright \mu_1$$

and

$$\mu_n = [-1 \cdot g(t_2)] \triangleright \mu_1,$$

which together imply that $\mu_1 = -1 \triangleright \mu_1$ in order for the two conditions to be consistent and all of the edge terms to be satisfied. This can only be true if $\mu_1 = 1_R$, not if $\mu_1 = \alpha_R$ or α_R^2. We therefore see that, if there are noncontractible paths, not all edge configurations are compatible with choosing the first plaquette label to be α_R or α_R^2 (specifically, a configuration is incompatible with this choice if there are closed paths with nontrivial label).

From this procedure of fixing the edge configurations, then making a particular choice for the label of one plaquette,

we might think that on the sphere we have three choices of plaquette configurations per edge configuration, one for each irrep of E. However, this is not quite true because some of the resulting sets of plaquette labels are connected by the energy terms. If we apply $\prod_{\text{all } v} A_v^{-1}$, the product of vertex transform A_v^{-1} on every vertex of the lattice, the edge labels are unchanged because we act on both ends of the edge, so that $g \to -1 \cdot g \cdot -1 = g$. On the other hand, we apply a transform on the base point of each of the plaquettes precisely once, so all of the plaquette labels are affected by the $\triangleright$ action from the vertex transform. This means that the label μ_p of each plaquette p transforms as $\mu_p \to -1 \triangleright \mu_p$ [from Eq. (29)]. This leaves the identity irrep unchanged, and so does not affect the state arising from an initial choice of $\mu_1 = 1_R$. On the other hand, if we took a nontrivial irrep as the label of the first plaquette, then this plaquette swaps label from α_R to α_R^2 or vice versa. In addition, all of the other plaquettes swap their labels between these two irreps. The state resulting from this is the same state we would have if we had chosen the other label for the first plaquette and then used that to determine the label of all of the other plaquettes. Then, because each ground state is invariant under the vertex transforms, the ground state satisfies $\prod_{\text{all } v} A_v^{-1}|GS\rangle = |GS\rangle$. This means that the two plaquette configurations arising from choosing the label of the first plaquette to be $\mu_1 = \alpha_R$ or α_R^2 for a given edge configuration must appear with equal amplitude in the ground state (the configurations are connected by the vertex terms). Therefore, the ground states produced from the two initial choices of plaquette label are not distinct.

This means that, for each edge configuration, we have a choice of only two distinct plaquette configurations, corresponding to the two $\triangleright$-Rep classes of the crossed module. From these configurations, we can generate a ground state by acting with a product of all of the vertex energy terms. Given that the plaquette labels are fixed by our initial choice (to be 1_R or an entangled combination of α_R and α_R^2) and the vertex transforms commute with this fixing, we can forget about the plaquettes after making that choice. Then the problem reduces to finding the ground state of Kitaev's quantum double model. This gives us two parts to our ground-state sector, one for the normal Kitaev quantum double model in a tensor product with 1_R at each plaquette and one for the quantum double model entangled with a more complicated plaquette set. In the case where our manifold is the sphere, this gives us a ground-state degeneracy of two, rather than giving a ground-state degeneracy of one as we may expect for a generic topological phase on a sphere. However, the different ground states can be detected locally (by measuring the $\triangleright$-Rep class of the plaquette label in a single location), so the degeneracy on the sphere is not topologically protected. Note that the result for the ground-state degeneracy agrees with a more general calculation given in Ref. [1], as expected.

2. Excitations

In this model, we have the usual electric excitations of the Kitaev quantum double model, and these particles behave exactly as in the quantum double model [37]. On the other hand, we find loop excitations which are not present in Kitaev's quantum double model. To understand these loop excitations it is convenient to change how we label the plaquettes. Instead of considering the plaquette labels to belong to the plaquette itself, we put them on the vertex that the plaquette is based at, as shown in Fig. 17.

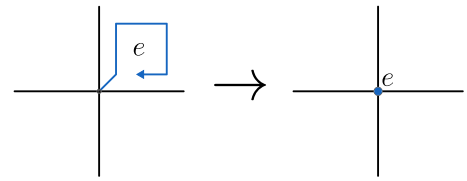

FIG. 17. We imagine the label of a plaquette to be placed at the base point of that plaquette.

Next we note that the edge transform corresponding to an edge i does not change the label of that edge because $\partial(e) = 1_G$ for all $e \in E$ in this example model. However, the action of the edge transform on the plaquettes does depend on a nearby edge, as indicated by Eqs. (33) and (34). Specifically, the action of the edge transform depends on the edge connecting the base points of the plaquettes affected by the edge transform. It is therefore convenient to relabel our operators to reflect the edge that matters for its action. Then the edge term $\mathcal{A}_\rightarrow$ becomes $\mathcal{Z}_\uparrow$ (applied on the edge down and to the left of the original horizontal edge) and $\mathcal{A}_\uparrow$ becomes $\mathcal{Z}_\rightarrow$ (again applied on the edge down and to the left of the vertical edge), and we now refer to the new labeled edges as being excited or not. The action of these operators can be written more compactly now that we no longer keep track of the extra edge. The action of these new edge transforms is defined in Figs. 18 and 19.

Now that we have relabeled our edge transforms, we see that they enforce that the (now vertex) labels at either end of the edge that we act on are related by the $\triangleright$ action of the edge label. We can think of adjacent vertices satisfying this relation as being linked. Then violating an edge transform can be thought of as "breaking" the link between vertices. Given a vertex and its neighbors (as shown in Fig. 20), we can excite the edges connecting the vertex to its neighbours by changing the label of that vertex. These excited edges are cut by a loop in the dual lattice, shown in Fig. 21 as a red dashed line, indicating that we have produced a looplike excitation. Note that in our original construction (where we use the original edge transforms $\mathcal{A}_i$), we would have placed the excited loop on the direct lattice, up and to the right of where we place it here. We can fix one of the broken bonds between the vertex and its neighbors by changing the label of a neighboring vertex so that the edge condition between the two vertices is satisfied, restoring the link between them. However, changing the label of this neighboring vertex will break more

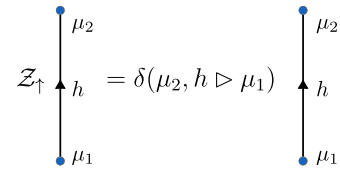

FIG. 18. Our new vertical edge operator.

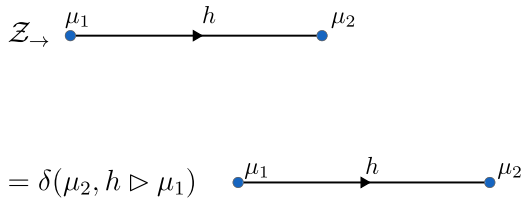

FIG. 19. Our new horizontal edge operator.

links on the neighboring vertex, as shown in Fig. 22. This simply changes the shape of the excited loop.

Recall that when we looked at the ground states, after fixing the edge labels we built the plaquette labels by starting at one plaquette and making the other plaquettes agree with that first one (in the sense that all of the edges connecting the plaquettes are satisfied). Similarly, to build the loop excitation, we start by changing one plaquette label, now living at a vertex, and then make the other labels within the loop agree with that vertex by ensuring that all links within this region are satisfied. That is, the region within the excited loop satisfies the same conditions as the ground state (although the bonds crossing the boundary of the loop are not satisfied). This means that we can think of the loop as a domain wall between two regions representing different ground states or ground-state-like configurations. This is most clear when we start in the ground state where all of the vertex labels are 1_R. Then to create the loop excitation we multiply one vertex label by α_R or α_R^2 and make all of the other vertices within the loop agree with that label (so that the edge terms within the loop are satisfied). However, recalling the general case (see Sec. III D), the loop excitation may have an excited vertex term at the start point of the membrane operator unless the membrane operator assigns equal weight to all surface elements within a particular class of elements. In this particular model, to avoid a vertex excitation we must take an equal superposition of the cases where we multiply the first label by α_R (then make all of the others agree) and the case where we multiply the first label by α_R^2 (then make all of the others agree). The loop then corresponds to a domain wall between the 1_R ground state and the ground state made of a combination of α_R and α_R^2 because the vertex labels within the loop are those that we would expect in the state made from α_R and α_R^2 and those outside are those we expect in the 1_R state. By extending this membrane operator over the entire lattice, we can move from the 1_R ground state to the other ground state. On the other hand, the privileged vertex will be excited if we take an orthogonal superposition of the two states built from α_R and α_R^2 (i.e., we take the state built from starting with the first vertex in the state α_R and making the other vertices agree and then make a linear combination by subtracting the state built from starting with that vertex in the state α_R^2).

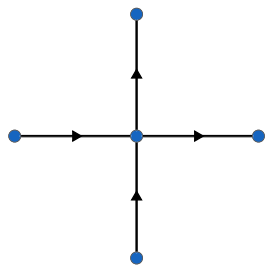

FIG. 20. A vertex and its neighbors, connected by edges.

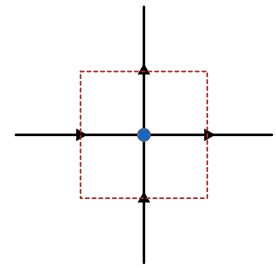

FIG. 21. Changing the label of a vertex in the ground state breaks its bonds with the neighboring vertices, resulting in the edges connecting the vertex to its neighbors becoming excited.

3. *Magnetic excitations*

As we described in Sec. II, we are not typically able to construct the magnetic excitations in (2+1)D when $\triangleright$ is nontrivial. For this simple model, however (and some generalizations, as we describe in Sec. S-VII A in the Supplemental Material [45]), and with this fixed branching structure, we are able to find these excitations. In fact, the ribbon operator that produces the magnetic excitation in the $(\mathbb{Z}_2, \mathbb{Z}_3)$ model has exactly the same form as the ones used in Sec. III B for the $\triangleright$ trivial case (and indeed for Kitaev's quantum double model [37]). However, unlike in the $\triangleright$ trivial case, the properties of the magnetic excitations depend on which ground state we create them from, as we shall see shortly. In order to reveal these properties, we consider applying the magnetic ribbon operator on a basis state in the basis where the plaquettes are labeled by irreps of E (but the edges are still labeled by group elements of G), as shown in Fig. 23.

We want to consider the commutation relations between the ribbon operator and the different energy terms. The magnetic ribbon operator only acts on the edges of the lattice, and it does so in the same way as in the case where $\triangleright$ is trivial. This means that it has the usual commutation relations with the vertex terms (which commute with it because $G = \mathbb{Z}_2$ is Abelian) and the plaquette terms (which commute with it, except at the two end plaquettes), both of which act on the edges of the lattice in the same way as in the $\triangleright$ trivial case. On

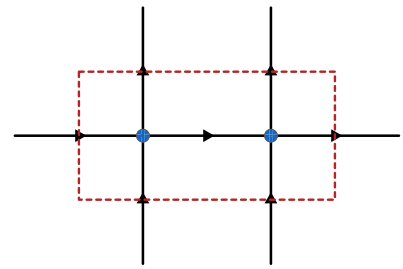

FIG. 22. Attempting to fix a broken bond may lead to more excited edges, thereby expanding or changing the shape of the looplike excitation.

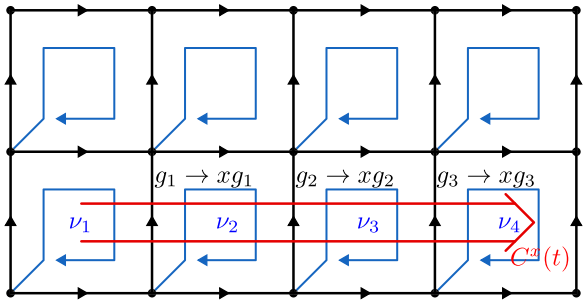

FIG. 23. We consider the action of the usual magnetic ribbon operator, in the basis where the plaquettes are labeled by irreps of E and the edges by elements of G. The ribbon operator acts only on the edges of the lattice, and because G is Abelian this action is simple [without the dependence on the path element of sections of the direct path seen in the more general case, as described by Eq. (13)]. In this example, all of the edges cut by the ribbon point in the same direction (upwards), so the action of the ribbon operator $C^x(t)$ is to multiply each edge label by x (if an edge pointed the opposite way with respect the ribbon, it would have its label multiplied by x^{-1} instead).

the other hand, the action of the edge term on the plaquettes depends on the edge labels [see Eq. (33)], unlike in the $\triangleright$ trivial case, and so there is some potential noncommutativity here. Looking at Eq. (33), we see that the edge transforms that may fail to commute with the magnetic ribbon operator are those whose action on the plaquette labels depends on an edge label of an edge that is cut by the ribbon operator (e.g., if the edge label h in Fig. 14 is changed by the ribbon operator, then that edge transform may fail to commute). If we are using the $\mathcal{Z}_\rightarrow$ and $\mathcal{Z}_\uparrow$ edge terms, then this means that edge transforms applied on the edges cut by the ribbon operator may fail to commute, whereas for the original $\mathcal{A}_i$ edge operators, it is the edge transforms on the edges up and to the right of the cut edges that may fail to commute (recall from Sec. VI A 2, and in particular Figs. 18 and 19, that the $\mathcal{Z}$ edge term on an edge is equivalent to the original $\mathcal{A}$ term on the edge above and to the right). This is illustrated in Fig. 24.

Having determined which edge transforms may fail to commute, we now look explicitly at the commutation rela-

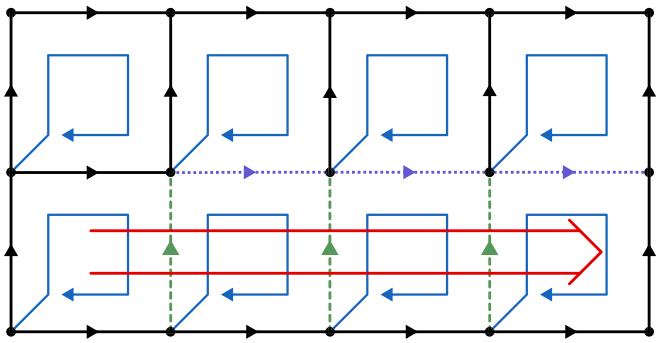

FIG. 24. The edge terms that may be excited are those whose action on the plaquette labels depends on the edges cut by the ribbon operator (the green dashed edges). That means that the edge terms on the purple dotted edges may be excited if we are using the original A_i edge terms, or the edge terms on the dashed green edges themselves may be excited if we are using the altered $\mathcal{Z}_\uparrow$ edge terms.

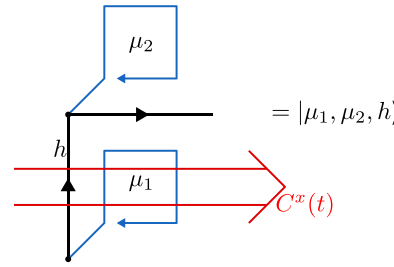

FIG. 25. We wish to consider the commutation relation between the edge transforms and magnetic ribbon operator. To do so we consider the degrees of freedom affected by the edge transforms indicated in Fig. 24, and provide a shorthand for the associated state.

tions. To do so we must consider the degrees of freedom around one of the edges cut by the magnetic ribbon, and so we will use the shorthand illustrated in Fig. 25. Then the action of the edge term $\mathcal{Z}_\uparrow$ on this state is (from Fig. 18)

$$\mathcal{Z}_\uparrow|\mu_1, \mu_2, h\rangle = \delta(\mu_2, h \triangleright \mu_1)|\mu_1, \mu_2, h\rangle,$$

whereas the action of the magnetic ribbon operator $C^x(t)$ on these degrees of freedom is

$$C^x(t)|\mu_1, \mu_2, h\rangle = |\mu_1, \mu_2, xh\rangle.$$

This means that applying the edge term and then the magnetic ribbon operator gives

$$C^x(t)\mathcal{Z}_\uparrow|\mu_1, \mu_2, h\rangle = \delta(\mu_2, h \triangleright \mu_1)|\mu_1, \mu_2, xh\rangle,$$

whereas applying the magnetic ribbon operator and then the edge term gives

$$\mathcal{Z}_\uparrow C^x(t)|\mu_1, \mu_2, h\rangle = \delta(\mu_2, (xh) \triangleright \mu_1)|\mu_1, \mu_2, xh\rangle.$$

In order to determine whether the ribbon operator excites the edge, we consider the product

$$\mathcal{Z}_\uparrow C^x(t)\mathcal{Z}_\uparrow,$$

which first projects to the case where the edge is initially unexcited, then acts with the ribbon operator and then projects again. If the ribbon operator excites the edge, then this product will give zero. On the other hand, if the ribbon operator leaves the edge unexcited, then we will obtain $C^x(t)\mathcal{Z}_\uparrow$ (because the second projection is trivial). We find that

$$\begin{aligned}
&\mathcal{Z}_\uparrow C^x(t)\mathcal{Z}_\uparrow|\mu_1, \mu_2, h\rangle \\
&\quad = \mathcal{Z}_\uparrow\delta(\mu_2, h \triangleright \mu_1)|\mu_1, \mu_2, xh\rangle \\
&\quad = \delta(\mu_2, (xh) \triangleright \mu_1)\delta(\mu_2, h \triangleright \mu_1)|\mu_1, \mu_2, xh\rangle \\
&\quad = \delta(h \triangleright \mu_1, (xh) \triangleright \mu_1)\delta(\mu_2, h \triangleright \mu_1)|\mu_1, \mu_2, xh\rangle \\
&\quad = \delta(\mu_1, x \triangleright \mu_1)\delta(\mu_2, h \triangleright \mu_1)|\mu_1, \mu_2, xh\rangle \\
&\quad = \delta(x \triangleright \mu_1, \mu_1)C^x(t)\mathcal{Z}_\uparrow|\mu_1, \mu_2, h\rangle. \qquad (35)
\end{aligned}$$

This indicates that whether the edge is excited or not depends on the term $\delta(x \triangleright \mu_1, \mu_1)$. Taking x to be the only nontrivial element -1 of $G = \mathbb{Z}_2$, and using the rule $-1 \triangleright \mu(e) = \mu(-1 \triangleright e)$ with the definition of $\triangleright$ given in Table III ($-1 \triangleright e = e^{-1}$), we see that

$$-1 \triangleright \mu(e) = \mu(e^{-1}) = \mu^{-1}(e).$$

Therefore,

$$\delta(-1 \triangleright \mu_1, \mu_1) = \delta\big(\mu_1^{-1}, \mu_1\big).$$

This Kronecker delta is satisfied (and so the edge is not excited) if $\mu_1 = 1_R$, and is not satisfied (implying an excited edge) if μ_1 is α_R or α_R^2. A general state will not be an eigenstate of this operator and so does not give us a well-defined energy for the edge. However, the ground states that we constructed in Sec. VI A 1 (which form a basis for the ground-state sector) will. To see this, recall that we found two unique ground states on the sphere. In the first, every plaquette was labeled by the trivial irrep 1_R. In this case, the plaquette label will always satisfy the Kronecker delta in Eq. (35), and so the edge will never be excited by the ribbon operator. This is true for each edge, and so the magnetic excitation is not confined. On the other hand, in the second ground state every irrep is in some combination of the states α_R and α_R^2 (entangled with the states of each other irrep). Regardless of which of these states the plaquette is in (or how it is entangled), the plaquette will therefore not satisfy $\delta(\mu_1^{-1}, \mu_1)$ and so the edge will be excited. This will be true for every edge cut by the ribbon operator (or the edges above and to the right if we use the original edge terms $\mathcal{A}_i$). This gives an energy cost that grows with the length of the ribbon, and so we see that the magnetic ribbon operator is confined. However, unlike the confinement of the electric excitations that we have seen previously, this confinement depends on which ground state we create the magnetic excitation from. While we have only been considering a specific crossed module here, this feature is more generic, as we explain in Sec. S-VII A in the Supplemental Material [45].

4. Condensation

Given that we have a confined magnetic excitation in one of the ground states, we also expect to see some condensation in that ground state, in the form of a condensed electric excitation (because confined excitations arise due to nontrivial braiding with condensed excitations). Recall from Sec. III E that we use the term condensed excitation to refer to an excitation which carries trivial topological charge (usually after some condensation-confinement transition). If we can find some local operator that reproduces the action of the electric ribbon operator on the ground state, then we know that the corresponding electric excitation is condensed. Consider an electric ribbon operator applied on a path t in the lattice. Because of how we have chosen our lattice, the two end points of the path will be the base points for two plaquettes, p_1 and p_2, as illustrated in Fig. 26. As we showed in Sec. VI A 1, in the ground state the labels of these two plaquettes in the irrep basis are related by the action of $g(t)\triangleright$. That is, if the labels of p_1 and p_2 are μ_1 and μ_2, respectively, then $\mu_2 = g(t) \triangleright \mu_1$. Now consider the bilocal operator $\delta(\hat{\mu}_1, \hat{\mu}_2)$, where $\hat{\mu}_i$ measures the value of plaquette i. In the ground state labeled by the trivial irrep, this operator acts as the identity because both plaquettes are labeled by the trivial irrep. However in the α_R/α_R^2 ground state this is not the case. Instead, this Kronecker delta is one when the path element $g(t)$ separating the plaquettes is 1_G and zero when the path element is -1_G (because $-1_G \triangleright \alpha_R = \alpha_R^2$). Therefore, when acting on the ground state

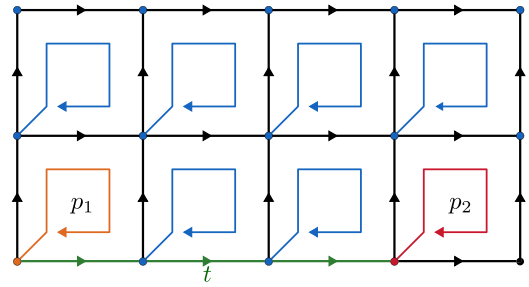

FIG. 26. Given an electric ribbon operator applied on a path t, the two ends of the ribbon are the base points for some plaquettes p_1 and p_2. In the ground state, the labels μ_1 and μ_2 of the plaquettes are related by $\mu_2 = g(t) \triangleright \mu_1$, where $g(t)$ is the path element of path t. Locally measuring the two plaquette labels therefore gives information about the path element $g(t)$, and so can reproduce some of the supposedly nonlocal electric ribbon operators on t, indicating that the corresponding electric excitations are condensed.

$|\alpha_R/\alpha_R^2\rangle$, we have

$$\delta(\hat{\mu}_1, \hat{\mu}_2)\big|\alpha_R/\alpha_R^2\big\rangle = \delta(\hat{g}(t), 1_G)\big|\alpha_R/\alpha_R^2\big\rangle,$$

which is just an electric ribbon operator acting on the ground state. We can also construct

$$\delta\big(\hat{\mu}_1, \hat{\mu}_2^{-1}\big)\big|\alpha_R/\alpha_R^2\big\rangle = \delta(\hat{g}(t), -1_G)\big|\alpha_R/\alpha_R^2\big\rangle.$$

This means that a general electric ribbon operator

$$a\delta(\hat{g}(t), 1_G) + b\delta(\hat{g}(t), -1_G)$$

(where a and b are arbitrary coefficients) can be reproduced (when acting on this particular ground state) by the bilocal operator

$$a\delta(\hat{\mu}_1, \hat{\mu}_2) + b\delta\big(\hat{\mu}_1, \hat{\mu}_2^{-1}\big).$$

This indicates that the electric excitations are condensed (although when $G = \mathbb{Z}_2$ there is only one independent electric excitation in the first place because there are two orthogonal electric ribbon operators, of which one is the trivial operator). In the α_R/α_R^2 ground state, where the nontrivial magnetic excitation is confined, the only nontrivial electric excitation is condensed (as we may expect from the idea that the confined excitation should braid nontrivially with the condensed one). On the other hand, there is no condensation or confinement in the 1_R ground state. Just like the confinement of magnetic excitations, this ground-state-dependent condensation occurs in the (2+1)D theory for other crossed modules, as we show in Sec. S-VII B in the Supplemental Material [45].

5. Alternate lattice

Returning to the discussion of the ground states, we can make a further simplification to the model that will make the structure of the ground states more obvious. Instead of basing every plaquette at the bottom left corner of the plaquette, we can base every plaquette at a single special vertex v_0 (in order to do this in a consistent way, we must have no noncontractible loops in the lattice). Because the choice of base point is analogous to a choice of gauge, this is equivalent to choosing all of the surface elements to be in the same gauge. This should therefore simplify certain expressions. Apart from the choice

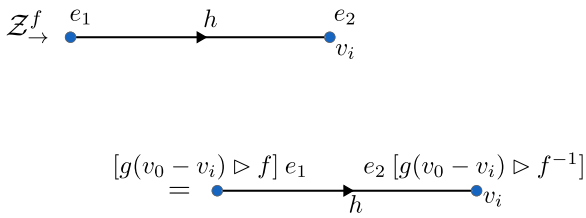

FIG. 27. The action of the horizontal edge operator $\mathcal{Z}^f_{\rightarrow}$ in the group-valued basis. Here $g(v_0 - v_i)$ is the path element from a privileged vertex in our lattice v_0 to v_i, the vertex at the end of the edge that is being transformed.

of base point, we proceed as before, replacing the plaquette labels with representations using a change of basis and placing the plaquette labels at the vertex down and to the left of the plaquette (although we note that the plaquette labels are no longer based at that vertex).

We start by considering the edge transforms on this new lattice. Just as before, the edge transforms do not affect the edge on which they are applied, and so it is convenient to instead associate them with the edge joining the two plaquette labels that they affect. That is, we define new operators $\mathcal{Z}^f_{\rightarrow} = A^f_{\uparrow}$ and $\mathcal{Z}^f_{\uparrow} = A^f_{\rightarrow}$, similar to the operators $\mathcal{Z}_{\uparrow}$ and $\mathcal{Z}_{\rightarrow}$ defined in Figs. 18 and 19, except for individual edge transforms rather than edge energy terms. The action of $\mathcal{Z}^f_{\rightarrow}$ on the group element basis is illustrated in Fig. 27 (and we can obtain the action of $\mathcal{Z}^f_{\uparrow}$ by rotating the figure 90° anticlockwise). The associated energy terms $\mathcal{Z}_{\rightarrow}$ and $\mathcal{Z}_{\uparrow}$ are obtained by averaging these transforms over all elements $f \in E$ as usual. For instance

$$\mathcal{Z}_{\rightarrow} = \frac{1}{|E|} \sum_{f \in E} \mathcal{Z}^f_{\rightarrow}.$$

Then for the action in the representation basis, we have

$$\begin{aligned}
&\mathcal{Z}_{\rightarrow} |\mu_1, \mu_2\rangle \\
&= \left(\frac{1}{|E|} \sum_{f \in E} \mathcal{Z}^f_{\rightarrow} \right) \left(\frac{1}{|E|} \sum_{e_1, e_2 \in E} \mu_1(e_1)\mu_2(e_2) |e_1, e_2\rangle \right) \\
&= \frac{1}{9} \sum_{e_1, e_2, f \in \mathbb{Z}_3} \mu_1(e_1)\mu_2(e_2) \\
&\quad \times |[g(v_0 - v_i) \triangleright f]e_1, [g(v_0 - v_i) \triangleright f^{-1}]e_2\rangle \\
&= \frac{1}{9} \sum_{e_1, e_2, f' = g(v_0 - v_i) \triangleright f} \mu_1(e_1)\mu_2(e_2) |f' e_1, f'^{-1} e_2\rangle \\
&= \frac{1}{9} \sum_{f' \in \mathbb{Z}_3} \sum_{e'_1 = f' e_1} \sum_{e'_2 = f'^{-1} e_2} \mu_1(f'^{-1} e'_1)\mu_2(f' e'_2) |e'_1, e'_2\rangle \\
&= \frac{1}{3} \sum_{f' \in \mathbb{Z}_3} \mu_1(f'^{-1})\mu_2(f') \frac{1}{3} \sum_{e'_1, e'_2 \in \mathbb{Z}_3} \mu_1(e'_1)\mu_2(e'_2) |e'_1, e'_2\rangle \\
&= \frac{1}{3} \sum_{f' \in \mathbb{Z}_3} \mu_1(f'^{-1})\mu_2(f') |\mu_1, \mu_2\rangle \\
&= \delta(\mu_1, \mu_2) |\mu_1, \mu_2\rangle.
\end{aligned}$$

Note that the edge label h is not present in this expression. The two irrep labels on either end of the edge are forced to be the same in the low-energy state, rather than being related by the action $h \triangleright$. In order to obtain this result, we implicitly used flatness to make sure that all paths with the same end points have the same label (the same rather than the same up to an element of $\partial(E)$ because $\partial(E)$ is trivial), provided that all such paths can be deformed into one another (the manifold is simply connected). The vertical edge transform gives something similar, enforcing that the irrep labels at the two ends of the vertical edge are the same. By fixing each plaquette to have the same base point, we have removed the impact of the edge labels on the edge transforms. The vertex transforms are also simplified because now only the vertex transform at the privileged point v_0 affects the surface labels, with the other vertex transforms only affecting the edge labels. This is because vertex transforms only affect plaquettes if that vertex is the base point of the plaquette, and we have chosen all of the plaquettes to have the same base point. The vertex transform $A^g_{v_0}$ at the privileged base point now takes all of the (group-valued) plaquette labels e_p to $g \triangleright e_p$. On the other hand, the vertex transforms at the other vertices do not change the surface labels, so they act exactly like the vertex transforms in Kitaev's quantum double model [37]. The other energy terms to consider are the plaquette terms. These energy terms are unaffected by changing the base point. As shown in Fig. 12, the plaquette term in the example model checks that the boundary of the plaquette is labeled by the identity element of G. If we move the base point of the plaquette along an edge labeled by g, then the label of the boundary of the plaquette is conjugated by g. However, this has no effect because the identity is preserved by conjugation (and besides the group G is Abelian in this case).

We can consider the ground-state degeneracy in the same way that we did before we changed the base points of the plaquettes, provided that the manifold is simply connected. That is, the plaquette terms again determine the allowed edge configurations and the edge terms then determine the allowed plaquette configurations for each edge configuration. Then we fluctuate the configurations by applying the vertex terms. However, when all of the plaquettes have the same base point it is easier to interpret the different ground states. This is because the edge terms now enforce that all of the plaquettes have the same irrep label in the ground state. In addition, only the vertex transform at the privileged vertex fluctuates these irreps and it simply flips between the labels α_R and α_R^2 for every plaquette. This means that there are always two choices for the plaquettes in the ground state (again assuming that there are no noncontractible paths). Either every plaquette is labeled by 1_R, or the plaquettes are in a linear combination of a product state where all plaquettes are in the $\mu = \alpha_R$ state and a product state where all plaquettes are in the $\mu = \alpha_R^2$ state.

6. Topological phase

Having considered the properties of the $\mathbb{Z}_2, \mathbb{Z}_3$ model, we can try to identify its topological phase. We found that the ground states of this model on the sphere can be split into two sectors, which can be distinguished locally. Namely, one sector has all plaquettes labeled by the trivial irrep of $\mathbb{Z}_3$,

while the other involves a combination of the two nontrivial irreps. In the former sector the ground state is equivalent to that of the toric code, and the excitations also have the same properties as the toric code. We therefore identify the topological phase in this sector as that of the toric code. For the other sector, we found that the magnetic excitation is confined, while the electric excitation is condensed. This implies that the topological phase for this sector is trivial.

From the ground state labeled by the trivial irrep, we can obtain the other ground state by applying a membrane operator over the entire lattice. However, we do not regard this operator as a symmetry because it only commutes with the Hamiltonian in the ground-state space (which is why the properties of the excitations are different in the two sectors). It therefore appears that the model contains two separate, but related, phases that happen to have degenerate ground states that are not protected by a true symmetry. We expect that this is a general feature of the models with $\triangleright$ nontrivial, although the inability to construct the magnetic excitations for general models makes it difficult to classify these phases.

B. $\mathbb{Z}_4$, $\mathbb{Z}_4$ model

The next example is the model based on the crossed module ($G = \mathbb{Z}_4$, $E = \mathbb{Z}_4$, $\partial \to \mathbb{Z}_2$, $\triangleright$ trivial). This example is intended to highlight the condensation and confinement aspect of the model. We denote the elements of $\mathbb{Z}_4$ by 1, i, -1, and $-i$. Then we define the map ∂ as follows: $\partial(1) = \partial(-1) = 1$ and $\partial(i) = \partial(-i) = -1$. This map preserves the group product, as we can see from the following relations:

$$\partial(\pm 1 \cdot \pm 1) = 1 = 1 \cdot 1 = \partial(\pm 1) \cdot \partial(\pm 1),$$
$$\partial(\pm 1 \cdot \pm i) = -1 = 1 \cdot -1 = \partial(\pm 1) \cdot \partial(\pm i),$$
$$\partial(\pm i \cdot \pm i) = 1 = -1 \cdot -1 = \partial(\pm i) \cdot \partial(\pm i).$$

Therefore, ∂ is indeed a group homomorphism. We can see that ∂ maps $\mathbb{Z}_4$ onto the $\mathbb{Z}_2$ subgroup of $\mathbb{Z}_4$: $(1, -1)$. Having chosen ∂ in this way, we now choose $\triangleright$ to be trivial. The crossed module then satisfies the Peiffer conditions, as we now verify directly. The first Peiffer condition, Eq. (1) in Sec. II, requires that $\partial(g \triangleright e) = g\partial(e)g^{-1}$ for all $g \in G$ and $e \in E$. This is true because $\triangleright$ is trivial and G is Abelian:

$$\partial(e) \overset{\triangleright \text{ trivial}}{=} \partial(g \triangleright e), \ \partial(e) \overset{G \text{ Abelian}}{=} g\partial(e)g^{-1}$$
$$\Rightarrow \partial(g \triangleright e) = g\partial(e)g^{-1}.$$

The second Peiffer condition, Eq. (2) in Sec. II, states that $\partial(e) \triangleright f = efe^{-1}$ for all e, $f \in E$. This is true for this example model because $\triangleright$ is trivial and E is Abelian:

$$f \overset{\triangleright \text{ trivial}}{=} \partial(e) \triangleright f, \ f \overset{E \text{ Abelian}}{=} efe^{-1}$$
$$\Rightarrow \partial(e) \triangleright f = efe^{-1}.$$

Because the maps ∂ and $\triangleright$ satisfy the homomorphism conditions and the Peiffer conditions, the collection of objects $(\mathbb{Z}_4, \mathbb{Z}_4, \partial, \triangleright)$ is a valid crossed module and so this crossed module defines a higher-lattice gauge theory model. We note that there is a related model with the same groups G and E and where $\triangleright$ is again trivial, but where $\partial : E \to 1_G$, as discussed in Sec. III E. In this case, because $\triangleright$ and ∂ are both trivial, the edge and plaquette labels completely decouple in the Hamiltonian. Furthermore, the excitations in that model are neither condensed nor confined. We will therefore refer to that model as the unconfined model and the model with $\partial \to \mathbb{Z}_2$ as the confined model in this section. We can think of the confinement and condensation in the confined model as arising from a condensation-confinement transition between the unconfined and confined models.

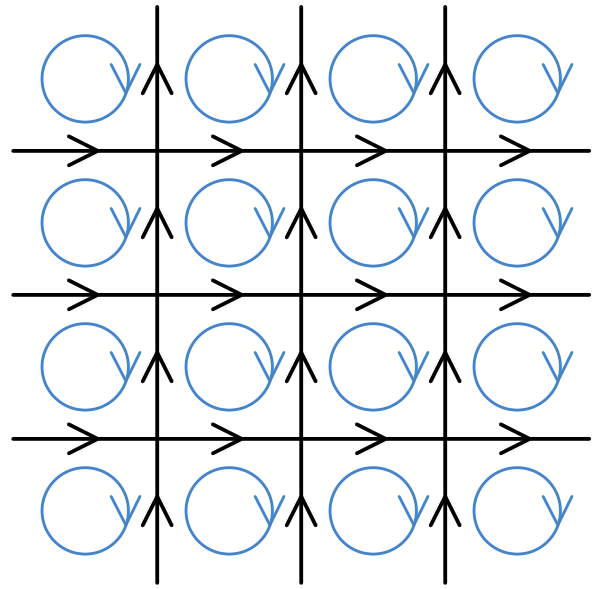

FIG. 28. A square lattice, with oriented edges and plaquettes.

Returning to the confined model where ∂ maps onto the $\mathbb{Z}_2$ subgroup, we now need to choose a lattice. We take a square lattice, as we did in the previous example. Because $\triangleright$ is trivial, we do not need to specify the base point of each plaquette, so we simply draw the plaquettes as oriented loops with no other feature. A fragment of this lattice is shown in Fig. 28. There are two kinds of edges in this lattice: vertical edges and horizontal edges. Each vertical edge has the same environment (i.e., the same objects surrounding it) and each horizontal edge has the same environment. Similarly, there is only one kind of plaquette because we have chosen each plaquette to have the same orientation, and one kind of vertex. Because of this, in later figures we may not draw the circulation of the plaquette at all and simply put a label in the middle of the plaquette. For now, we will not worry about the boundary of this lattice and simply assume that there is a sensible way to close it into a sphere or other desired manifold, although this may necessitate introducing vertices or plaquettes with different environments.

With the lattice fixed, we next consider the operators that make up the Hamiltonian: vertex transforms, edge transforms, and plaquette terms. Because of the simple lattice and crossed module, the action of these operators can be expressed relatively concisely, as shown in Fig. 29.

1. Excitations

We can now consider the excitations of this example model, starting with the purely electric ones. To examine the excitations, we construct the ribbon operators that produce them. As we discussed in Sec. III A, these can be labeled

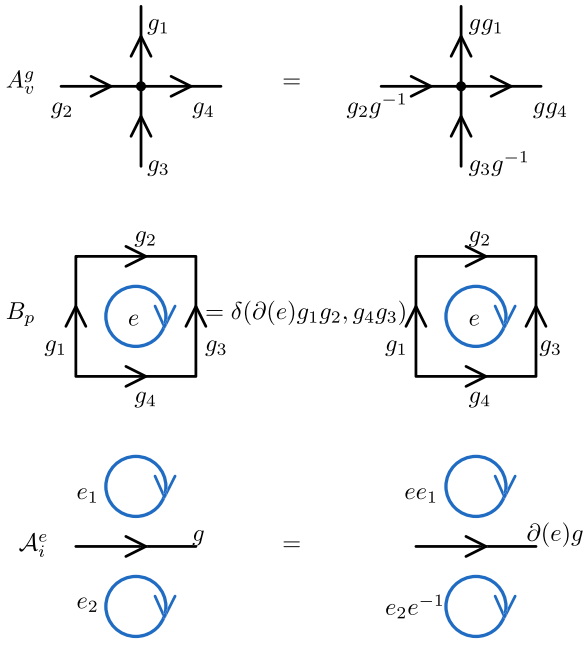

FIG. 29. The gauge transforms and plaquette terms in this example model. We can obtain the action of the vertical edge transform by rotating the bottom diagrams by 90° anticlockwise.

by irreps of the group G. Because $\mathbb{Z}_4$ is Abelian, the irreps (shown in Table IV) are 1D, which means that we do not need to give matrix indices in order to specify an electric ribbon operator. Then the basis operators for the space of electric ribbon operators are given by

$$\hat{S}^R(t) = \sum_{g\in G} R(g)\delta(g, \hat{g}(t)),$$

where R is an (1D) irrep of G, so that $R(g)$ is the representation of the element g, and t is the path on which we apply the operator. We discussed this construction for more general models in Sec. III A.

These ribbon operators commute with the plaquette terms because both types of operator are diagonal in the basis labeled by group elements on each edge. The ribbon operators also have the same commutation relations with the vertex operators as the equivalent operators in Kitaev's quantum double model [37]. Namely, the ribbon operators commute with all vertex operators except those at the two end points of t, which are excited by the ribbon operator (except for the ribbon operator labeled by the trivial irrep, which is just the identity operator). To see this, we first note that, as discussed in Sec. III A, the vertex transform only affects the labels of paths that start or end at that vertex, not those that just pass through it. This is because under the action of a gauge transform A_v^g the path obtains a factor g^{-1} from entering the vertex and a factor g from leaving the vertex, which cancel. Therefore, the ribbon operator will commute with all vertex transforms except those at the start and end of the path, just as we discussed for a more general case in Sec. III A. Then for the starting vertex operator, we have the commutation relation

$$\hat{g}(t)A^g_{\text{s.p.}} = A^g_{\text{s.p.}}\, g\hat{g}(t)$$

because the path picks up an additional g if the path is acted on by $A^g_{\text{s.p.}}$ before we measure it. Then if we wish to reverse this commutation relation, we have

$$A^g_{\text{s.p.}}\hat{g}(t) = g^{-1}\hat{g}(t)A^g_{\text{s.p.}}.$$

Then we can check whether the ribbon operator excites the vertex s.p. when acting on the ground state by applying the energy term $A_{\text{s.p.}}$ to the left of the ribbon operator. We see that

$$\begin{aligned} A_{\text{s.p.}}\hat{S}^R(t)|GS\rangle &= A_{\text{s.p.}}\sum_{g\in G} R(g)\delta(g, \hat{g}(t))|GS\rangle \\ &= \frac{1}{|G|}\sum_{x\in G} A^x_{\text{s.p.}}\sum_{g\in G} R(g)\delta(g, \hat{g}(t))|GS\rangle \\ &= \frac{1}{|G|}\sum_{x\in G}\sum_{g\in G} R(g)\delta(g, x^{-1}\hat{g}(t))A^x_{\text{s.p.}}|GS\rangle \\ &= \frac{1}{|G|}\sum_{x\in G}\sum_{g\in G} R(g)\delta(xg, \hat{g}(t))A^x_{\text{s.p.}}|GS\rangle. \end{aligned}$$

Then we can use the fact that $A^x_{\text{s.p.}}|GS\rangle = |GS\rangle$ as discussed in Sec. II to write this as

$$\begin{aligned} A_{\text{s.p.}}\hat{S}^R(t)|GS\rangle &= \frac{1}{|G|}\sum_{x\in G}\sum_{g\in G} R(g)\delta(xg, \hat{g}(t))|GS\rangle \\ &= \frac{1}{|G|}\sum_{x\in G}\sum_{g'=xg} R(x^{-1}g')\delta(g', \hat{g}(t))|GS\rangle \\ &= \left(\frac{1}{|G|}\sum_{x\in G} R(x^{-1})\right)\sum_{g'\in G} R(g')\delta(g', \hat{g}(t))|GS\rangle \\ &= \left(\frac{1}{|G|}\sum_{x\in G} R(x^{-1})\right)\hat{S}^R(t)|GS\rangle, \end{aligned}$$

where we used the fact that R is an irrep to split the contributions from x and g'. If R is a nontrivial irrep, this is zero by orthogonality of characters, and if R is the trivial irrep it is just $\hat{S}^R(t)|GS\rangle$. If $A_{\text{s.p.}}\hat{S}^R(t)|GS\rangle = 0$, the vertex is excited, so a nontrivial irrep gives an excited vertex at the start of the path. A similar calculation holds for the vertex transform at the end of the path and so that vertex is also excited if the irrep is nontrivial.

Next we consider the commutation relations of the ribbon operator with the edge transforms. The ribbon operator commutes with edge transforms for edges that are not on the path, but those transforms for edges on the path change the path label $\hat{g}(t)$. This is because, in addition to changing the plaquette labels, the edge transform $\mathcal{A}_i^e$ multiplies the label of the edge it acts on by $\partial(e)$. Then we have that

$$\hat{g}(t)\mathcal{A}_i^e = \mathcal{A}_i^e\partial(e)^{(\pm 1)}\hat{g}(t),$$

TABLE IV. The elements of the unitary irreps of $\mathbb{Z}_4$.

	1	i	-1	$-i$
1_{Rep}	1	1	1	1
-1_{Rep}	1	-1	1	-1
i_{Rep}	1	i	-1	$-i$
$-i_{\text{Rep}}$	1	$-i$	-1	i

where the plus or minus sign depends on the direction of the edge relative to the direction of t (+ if they are aligned, − if they are antialigned). This means that

$$\mathcal{A}_i^e \hat{g}(t) = \partial(e)^{(\mp 1)} \hat{g}(t) \mathcal{A}_i^e.$$

Therefore, if we act with the edge energy term $\mathcal{A}_i$ to the left of the ribbon operator, we have

$$\begin{aligned}\mathcal{A}_i \hat{S}^R(t)|GS\rangle &= \frac{1}{|E|}\sum_{e\in E}\mathcal{A}_i^e \sum_{g\in G} R(g)\delta(g, \hat{g}(t))|GS\rangle \\ &= \frac{1}{|E|}\sum_{e\in E}\sum_{g\in G} R(g)\delta(g, \partial(e)^{(\mp 1)}\hat{g}(t))\mathcal{A}_i^e|GS\rangle.\end{aligned}$$

As discussed in Sec. II, the ground states satisfy $\mathcal{A}_i^e|GS\rangle = |GS\rangle$, and so we can write this commutation relation as

$$\begin{aligned}\mathcal{A}_i \hat{S}^R(t)|GS\rangle &= \frac{1}{|E|}\sum_{e\in E}\sum_{g\in G} R(g)\delta(g, \partial(e)^{(\mp 1)}\hat{g}(t))|GS\rangle \\ &= \frac{1}{|E|}\sum_{e\in E}\sum_{g\in G} R(g)\delta(\partial(e)^{(\pm 1)}g, \hat{g}(t))|GS\rangle \\ &= \frac{1}{|E|}\sum_{e\in E}\sum_{g'=\partial(e)^{(\pm 1)}g} R(\partial(e)^{(\mp 1)}g')\delta(g', \hat{g}(t))|GS\rangle \\ &= \left(\frac{1}{|E|}\sum_{e\in E} R(\partial(e)^{(\mp 1)})\right)\sum_{g'\in G} R(g') \\ &\quad \times \delta(g', \hat{g}(t))|GS\rangle \\ &= \left(\frac{1}{|E|}\sum_{e\in E} R(\partial(e)^{(\mp 1)})\right)\hat{S}^R(t)|GS\rangle,\end{aligned}$$

where we used the fact that R is an irrep of G to separate the contribution from g' and $\partial(e)$. From this commutation relation, we see that whether the edge energy term is excited or not (i.e., whether the above expression is zero or not) depends on the expression $(\frac{1}{|E|}\sum_{e\in E} R(\partial(e)^{(\mp 1)}))$. This expression is zero if the irrep R is nontrivial in the subgroup $\partial(E) \subset G$. To see this, let us consider the irreps of G in this model. So far, our discussion of the electric ribbon operator has been valid for any crossed module with trivial $\triangleright$ and Abelian G. However, we now consider the specific groups $G = E = \mathbb{Z}_4$ and the map $\partial \to \mathbb{Z}_2$. For $\sum_{e\in E} R(\partial(e))$, we have

$$\begin{aligned}\sum_{e\in E} R(\partial(e)) &= R(\partial(1)) + R(\partial(-1)) + R(\partial(i)) + R(\partial(-i)) \\ &= R(1) + R(1) + R(-1) + R(-1) \\ &= 2R(1) + 2R(-1).\end{aligned}$$

If $R = \pm i_{\text{Rep}}$ [i.e., if R is one of the irreps sensitive to factors in $\partial(E)$], then $R(1) = 1$ and $R(-1) = -1$, implying that

$$\sum_{e\in E} R(\partial(e)) = 2 \cdot 1 + 2 \cdot -1 = 0.$$

This means that, in the case where $R = \pm i_{\text{Rep}}$, we have

$$\mathcal{A}_i \hat{S}^R(t)|GS\rangle = 0.$$

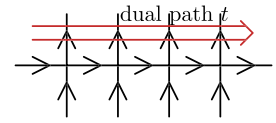

FIG. 30. An example of a dual path on our lattice. A magnetic ribbon operator acting on this dual path will produce excitations at the plaquettes at the two ends of the path.

This indicates that $\hat{S}^R(t)|GS\rangle$ is an eigenstate of $\mathcal{A}_i$ where the edge i is excited for all edges i on the path t. The string operator therefore costs one unit of energy per edge and so the corresponding excitations are confined.

On the other hand, the other two irreps satisfy $R[\partial(e)] = 1$. This means that for $R = \pm 1_{\text{Rep}}$,

$$\sum_{e\in E} R(\partial(e)) = 2 \cdot 1 + 2 \cdot 1 = 4,$$

so that

$$\frac{1}{|E|}\sum_{e\in E} R(\partial(e)) = 1,$$

and so

$$\mathcal{A}_i \hat{S}^R(t)|GS\rangle = \hat{S}^R(t)|GS\rangle.$$

Therefore, the electric ribbon operators labeled by these two irreps commute with the edge terms. This means that the edges are not excited by the ribbon operators, so the corresponding excitations are not confined. We can see that the ribbon operators labeled by irreps with trivial restriction to the image of ∂ (the irreps $\pm 1_{\text{Rep}}$) are not confined and those with nontrivial restriction ($\pm i_{\text{Rep}}$) are confined, similar to the general claim made in Sec. III A. Note that in the unconfined model, where $\partial(E) = \{1_G\}$, every irrep of the subgroup $\partial(E) \subset G$ is trivial, so that we have no confined excitations.

Next we consider the magnetic excitations (which we can find because $\triangleright$ is trivial). In order to construct a ribbon operator to produce these excitations, we first choose a path on the dual lattice, such as the one shown in Fig. 30. The magnetic ribbon operator $C^h(t)$ multiplies the edges cut by the dual path by either h or h^{-1} depending on the orientation of the edges. In the example shown in the figure, all of the cut edges point in the same direction, and so we multiply the label of these edges by the same element h, as shown in Fig. 31. Note that this particular form of the magnetic ribbon operator depends on the Abelian nature of $G = \mathbb{Z}_4$ and a more general case is given in Sec. III B (because G is Abelian we do not need to define a direct path for the ribbon, although we still need a convention for whether edges are multiplied by h or h^{-1}). Then we consider how this affects the plaquette terms near the ribbon. The internal plaquettes, which are those passed through by the dual path (i.e., those on the ribbon but not at

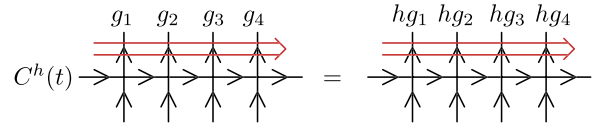

FIG. 31. An example of the action of the magnetic operator

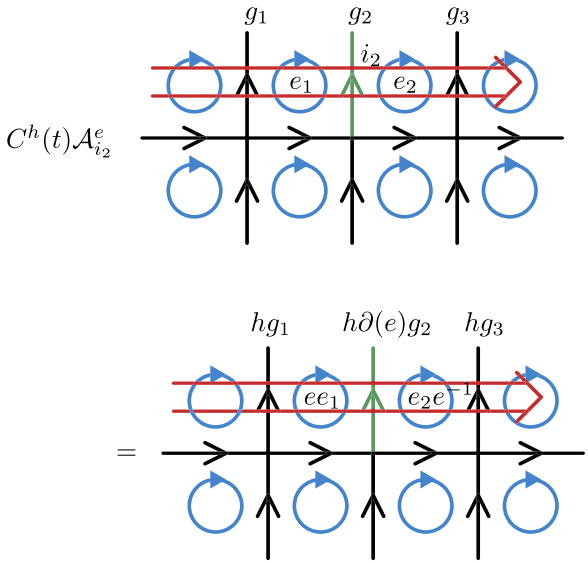

FIG. 32. An example of applying an edge transform followed by a magnetic ribbon operator. We apply the edge transform on the edge i_2 (green), initially labeled by the element g_2. The final label of i_2 is $h\partial(e)g_2$. If we applied the operators in the opposite order, the label would be $\partial(e)hg_2$, which is the same for this model.

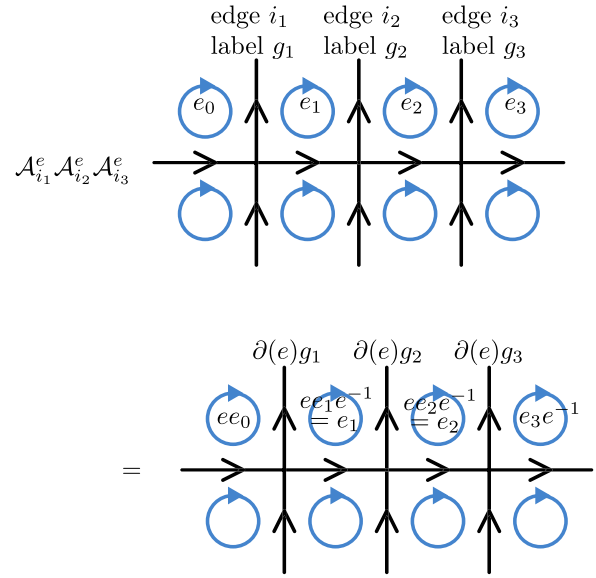

FIG. 33. Performing a series of edge transforms on the edges cut by the dual ribbon has a similar effect to the magnetic ribbon operator, changing the edge labels and leaving the internal plaquette labels (here e_1 and e_2) invariant. However, the two plaquettes at the ends of the ribbon (here initially labeled by e_0 and e_3) are affected by the edge transforms, whereas they are not affected by the magnetic ribbon operator. This difference between the action of the edge transforms and the action of the magnetic ribbon operator is equivalent to the action of local operators at the two ends of the ribbon.

the ends of the dual path), have two edges cut by the dual path. Each of these edges will gain a factor of h. However, one of these edges is aligned with the boundary of the plaquette, while the other is antialigned with the boundary. This means that the boundary of the plaquettes gains one factor of h and one factor of h^{-1}, which cancel. Therefore, the magnetic operator commutes with those internal plaquette operators. However, the end plaquettes gain only a factor of h or h^{-1}, so they are excited just as in Kitaev's quantum double model [37].

Taking the group G to be Abelian means that the magnetic ribbon operator commutes with all of the vertex transforms (again, just like in Kitaev's quantum double model [37]). This is because both the vertex and ribbon operators multiply a set of edges by fixed group elements (there is no configuration dependence, unlike in the non-Abelian case), and the Abelian nature of the group G means that the order in which this multiplication is done does not matter. The ribbon operator also commutes with the edge transforms for the same reason. We give an example of this commutation in Fig. 32, where we first apply an edge transform $\mathcal{A}^e_i$ on the edge labeled by g_2, then apply a magnetic ribbon operator $C^h(t)$. Under these operations, the edge label g_2 becomes $h\partial(e)g_2$, whereas applying the operators in the opposite order would give $\partial(e)hg_2$. However, $h\partial(e)g_2 = \partial(e)hg_2$ because G is Abelian, so the operators commute.

Having discussed all of the energy terms, we see that the magnetic ribbons only excite the two end plaquettes and commute with all of the other energy terms. In Sec. III B, we saw that for a general crossed module model the start-point vertex of the ribbon could be excited by the ribbon operator, but for this particular model the vertex is not excited because G is Abelian. Either way, just as in the more general $\triangleright$ trivial case, the magnetic excitations are not confined because excitations are only produced at the ends of the ribbon rather than along the length of the ribbon.

While none of the magnetic excitations are confined, some of them are "condensed." As we explained in Sec. III C, by condensed we mean that some of the excitations can be produced by local operators, acting only near the excitations themselves. This means that they cannot carry a nontrivial topological charge. To see which excitations are condensed, consider a ground state. Any ground state is an eigenstate of the edge terms with eigenvalue one and is unchanged by applying any edge transform $\mathcal{A}^e_i$. Therefore, we are free to apply these transforms without changing the state. The action of some of the magnetic ribbon operators is equivalent to a series of edge transforms (which act trivially on the ground state) and some local operators. To see this, consider applying an edge transform $\mathcal{A}^e_i$ on each edge cut by the dual path of the magnetic ribbon operator, as shown in Fig. 33. Apart from the action on the two end plaquettes, the action shown in Fig. 33 looks exactly like the action of a magnetic ribbon with label $\partial(e)$. In fact, we can turn this action into the action of the magnetic ribbon simply by applying *local* operators on the two end plaquettes to correct their labels. That is,

$$C^{\partial(e)}(t) = M^{e^{-1}}(p_0)M^e(p_3)\mathcal{A}^e_{i_1}\mathcal{A}^e_{i_2}\mathcal{A}^e_{i_3}, \tag{36}$$

where $M^e(p)$ multiplies the single plaquette p by e and is therefore local to the plaquette, and p_x refers to the plaquette initially labeled by e_x in Fig. 33. The operators $M^{e^{-1}}(p_0)$ and $M^e(p_3)$ are therefore local to the excitations produced at the two ends of the ribbon.

Then acting with both sides of Eq. (36) on a ground state gives us the equality

$$C^{\partial(e)}(t)|GS\rangle = M^{e^{-1}}(p_0)M^e(p_3)\mathcal{A}^e_{i_1}\mathcal{A}^e_{i_2}\mathcal{A}^e_{i_3}|GS\rangle$$
$$= M^{e^{-1}}(p_0)M^e(p_3)|GS\rangle,$$

where the second equality results from absorbing the $\mathcal{A}^e_i$ into the ground state as explained earlier. This equality means that the excitations produced by the magnetic operator can be reproduced by local operators acting on the ground state, so those excitations are not topological. That is, they are condensed. We see that the magnetic excitations produced by all magnetic operators with label in the image of ∂ are condensed. Furthermore, the fusion rule $C^g(t)C^h(t) = C^{gh}(t)$ means that $C^{g\partial(e)}(t)|GS\rangle = C^g(t)M^{e^{-1}}(p_1)M^e(p_4)|GS\rangle$, so that the g and $g\partial(e)$ excitations differ only by the application of local operators, and so must be in the same topological sector. Therefore, the magnetic topological sectors are not labeled by group elements, but instead by cosets $g\partial(E)$. A similar argument holds for any crossed module model where $\triangleright$ is trivial (although if G is non-Abelian the sectors are also widened by conjugation, as described in Sec. III B). For the particular crossed module considered in this section, we see that the elements 1 and -1 of G are in the image of ∂. Therefore, the magnetic excitation labeled by -1 is condensed (1 corresponds to no excitation, so we do not say that it is condensed) and the excitations labeled by i and $-i$ are in the same sector, but are not condensed.

Having considered the pointlike excitations of this example model, we next examine the looplike excitations. Thanks to $\triangleright$ being trivial and all of the plaquettes in the lattice having the same orientation, the membrane operators that produce these loop excitations are relatively simple. As discussed in Sec. III D, the membrane operators measure the total surface label of the membrane and assign a weight to each possible value. Because $\triangleright$ is trivial, when combining the plaquette labels into a total surface label we do not need to worry about defining base points and moving them around to ensure that these match. Combined with the fact that we have chosen all plaquettes to have the same orientation, this means that the total surface element of a surface made from multiple plaquettes becomes a simple product of the operators for the individual plaquettes. The expression $\delta(\hat{e}(m), e)$ from the membrane operator in the general case then becomes $\delta(\prod_{p\in m}\hat{e}_p, e)$, where $\hat{e}_p$ is the operator that measures the label of plaquette p. Furthermore, because the group E is Abelian we do not need to worry about the order of multiplication. As an example, consider a membrane made of four square plaquettes, shown in Fig. 34. The total surface label of this membrane is $e_4e_3e_2e_1$, where e_p is the plaquette label of plaquette p in the membrane and p runs from 1 to 4.

Now consider the commutation relations between the membrane operator and the energy terms. The operator $\delta(e, \hat{e}(m))$ clearly commutes with every vertex transform A^g_v because the vertex transform does not affect any plaquette labels when $\triangleright$ is trivial. Similarly, the operator $\delta(e, \hat{e}(m))$ commutes with the plaquettes terms B_p because both B_p and the surface measurement operator are diagonal in the element basis. The membrane operator also commutes with "internal" edge transforms. An internal edge is an edge where both plaquettes adjacent to that edge are within the membrane. For

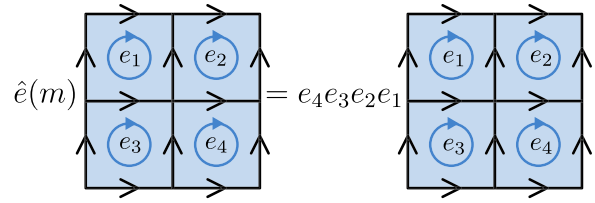

FIG. 34. The surface measurement operator $\hat{e}(m)$ is simplified when $\triangleright$ is trivial and the plaquettes all have the same orientation. For a surface m (shaded) formed from the combination of four plaquettes, the surface label is the product of the labels of each of these plaquettes, and the order of the product is irrelevant.

example, consider Fig. 35. In the figure, the red vertical edge (initially labeled by g_2) between the plaquettes labeled by e_1 and e_2 is an example of an internal edge because both adjacent plaquettes are within the surface m. In the case shown in the figure, we see that under the edge transform $\mathcal{A}^f_{i_2}$ the surface label $e(m)$ transforms as

$$e(m) = e_4e_3e_2e_1 \to e_4e_3e_2f^{-1}fe_1 = e_4e_3e_2e_1.$$

For any surface, the edge transform $\mathcal{A}^f_i$ on an edge wholly within that surface will generate a factor of f (from one of the plaquettes adjacent to that edge) and a factor of f^{-1} (from the other plaquette), which will cancel, leaving the surface label unchanged.

On the other hand, consider transforms on edges that are on the boundary of m (such as the one labeled by g_7 in Fig. 35).

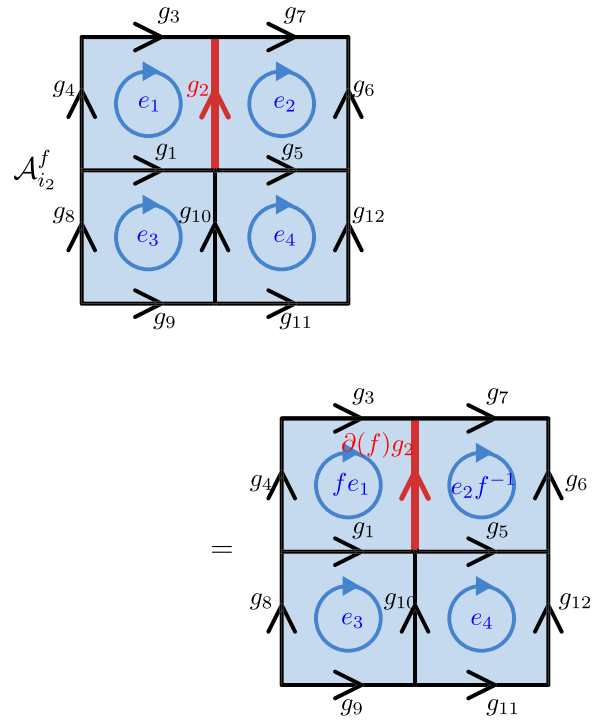

FIG. 35. An example of the action of an "internal" edge operator (applied on the thicker red edge with initial label g_2) acting on our combined surface. Note that one plaquette label gains a factor of f and another gains a factor of f^{-1}. These factors will cancel when we consider the total label of the surface.

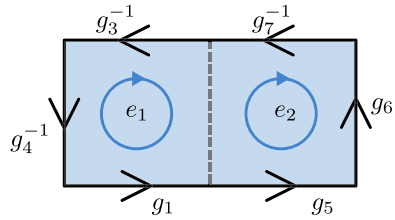

FIG. 36. The combination of the boundary of two plaquettes gives the boundary of the combined surface.

Of the two plaquettes adjacent to such an edge, only one plaquette is in m, so the surface label $e(m)$ gains a factor of f or f^{-1} from that plaquette (depending on the orientation of the edge) from an edge transform labeled by f, without the compensating factor from the other plaquette. This means that the edge transform does not generally commute with the membrane operator, and so the membrane operator may create edge excitations. When we construct basis membrane operators labeled by irreps of E, of the form

$$L^{\mu}(m) = \sum_{e \in E} \mu(e)\delta(\hat{e}(m), e)$$

for an irrep μ, the membrane operator then excites the boundary edges if the irrep μ is nontrivial. If the irrep μ is trivial, then the membrane operator is just the identity operator.

In Sec. III D, we explained that some of the loop excitations are condensed in the general case. We now wish to consider how this arises in our example model in more detail. Consider acting with a surface measurement operator $\hat{e}(m)$ on the (or a) ground state. The ground state satisfies fake flatness, which means that we can relate the plaquette labels to the labels of the path around the boundary of the plaquettes. This holds not only for individual plaquettes, but also for surfaces made up of multiple plaquettes. For example, considering Fig. 35, from fake flatness each plaquette label must satisfy $\partial(e_p) = g_{dp}^{-1}$, where g_{dp} is the label of the boundary of the plaquette. This means that

$$\begin{aligned}
\partial(e_1) &= g_2 g_3^{-1} g_4^{-1} g_1, \\
\partial(e_2) &= g_5 g_6 g_7^{-1} g_2^{-1} \\
\Rightarrow \partial(e_2 e_1) &= g_5 g_6 g_7^{-1} g_2^{-1} g_2 g_3^{-1} g_4^{-1} g_1 \\
&= g_5 g_6 g_7^{-1} g_3^{-1} g_4^{-1} g_1.
\end{aligned}$$

We can recognize the right-hand side of the final line as the label of the boundary of the combined surface of the two plaquettes (in reverse), as shown in Fig. 36.

Then we wish to combine this with the other plaquettes from Fig. 35. The labels of these plaquettes satisfy

$$\begin{aligned}
\partial(e_3) &= g_9 g_{10} g_1^{-1} g_8^{-1}, \\
\partial(e_4) &= g_{11} g_{12} g_5^{-1} g_{10}^{-1},
\end{aligned}$$

so that

$$\begin{aligned}
\partial(e_4 e_3 e_2 e_1) &= g_{11} g_{12} g_5^{-1} g_{10}^{-1} g_9 g_{10} g_1^{-1} g_8^{-1} g_5 g_6 g_7^{-1} g_3^{-1} g_4^{-1} g_1 \\
&= g_{11} g_{12} g_6 g_7^{-1} g_3^{-1} g_4^{-1} g_8^{-1} g_9,
\end{aligned}$$

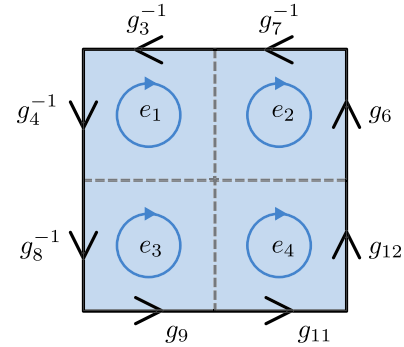

FIG. 37. The boundary of four combined plaquettes.

where we used the fact that G is Abelian to cancel group elements and their inverses (a similar result holds in the general case, but we have to make more careful use of the Peiffer conditions if G is non-Abelian). This is the label of the combined boundary of all four plaquettes (in reverse), indicating that the relationship between the boundary and surface label holds. The boundary for this combined surface is indicated in Fig. 37.

Now with this information in hand, consider the four membrane operators labeled by the irreps of the group $E = \mathbb{Z}_4$. The membrane operator $L^{\alpha}(m)$ labeled by an irrep α and applied on a membrane m is given by $L^{\alpha}(m) = \sum_{e \in E} \alpha(e)\delta(e, \hat{e}(m))$. Then we have

$$\begin{aligned}
L^{1_{\mathrm{Rep}}}(m) &= \delta(\hat{e}(m), 1) + \delta(\hat{e}(m), -1) + \delta(\hat{e}(m), i) \\
&\quad + \delta(\hat{e}(m), -i) \\
&= 1, \\
L^{-1_{\mathrm{Rep}}}(m) &= \delta(\hat{e}(m), 1) + \delta(\hat{e}(m), -1) - \delta(\hat{e}(m), i) \\
&\quad - \delta(\hat{e}(m), -i), \\
L^{i_{\mathrm{Rep}}}(m) &= \delta(\hat{e}(m), 1) - \delta(\hat{e}(m), -1) + i\delta(\hat{e}(m), i) \\
&\quad - i\delta(\hat{e}(m), -i), \\
L^{-i_{\mathrm{Rep}}}(m) &= \delta(\hat{e}(m), 1) + \delta(\hat{e}(m), -1) - i\delta(\hat{e}(m), i) \\
&\quad + i\delta(\hat{e}(m), -i).
\end{aligned}$$

We see that the membrane operator labeled by the trivial irrep is just the identity operator because summing over all of the Kronecker delta just gives one. The membrane operator labeled by -1_{Rep} can also be written in a simpler form by combining different Kronecker deltas. Noting that $\partial(1) = \partial(-1) = 1$ and $\partial(i) = \partial(-i) = -1$, we can see that

$$\delta(\hat{e}(m), 1) + \delta(\hat{e}(m), -1) = \delta(\partial(\hat{e}(m)), 1)$$

and

$$\delta(\hat{e}(m), i) + \delta(\hat{e}(m), -i) = \delta(\partial(\hat{e}(m)), -1).$$

Therefore

$$L^{-1_{\mathrm{Rep}}}(m) = \delta(\partial(\hat{e}(m)), 1) - \delta(\partial(\hat{e}(m)), -1).$$

That is, we can write this membrane operator entirely in terms of $\partial(\hat{e}(m))$, which is not sensitive to elements in the kernel of ∂. In the ground state, the surface label is related to the label of the boundary of that surface, as we have seen

previously:

$$\partial(\hat{e}(m))|GS\rangle = \hat{g}_{dm}^{-1}|GS\rangle,$$

where we label the boundary element for membrane m by g_{dm}. This means that, when acting on the ground state, the membrane operator labeled by -1_{Rep} gives

$$L^{-1_{\text{Rep}}}(m)|GS\rangle = \left[\delta\left(\hat{g}_{dm}^{-1}, 1\right) - \delta\left(\hat{g}_{dm}^{-1}, -1\right)\right]|GS\rangle.$$

However, the operator

$$\left[\delta\left(\hat{g}_{dm}^{-1}, 1\right) - \delta\left(\hat{g}_{dm}^{-1}, -1\right)\right]$$

is simply an electric ribbon operator applied around the closed loop that forms the boundary of m (specifically a confined electric operator, as we require from the fact that the boundary edges are excited). This indicates that we can replicate the action of the *surface* operator by a *path* operator applied on the boundary of the surface. This path is local to the excitation (which lies on the boundary of the surface), and so the excitation is condensed and cannot be a domain wall.

On the other hand, consider the last two membrane operators $L^{i_{\text{Rep}}}(m)$ and $L^{-i_{\text{Rep}}}(m)$. The action of these operators on the ground state cannot be written in terms of the path operator $\hat{g}_{dm}$, so these membrane operators are not condensed. We note that restricting the irreps that label these operators to the kernel of ∂, we have $\pm i_{\text{Rep}}(1) = 1$ and $\pm i_{\text{Rep}}(-1) = -1$. We therefore see that the noncondensed excitations are labeled by irreps with nontrivial restriction to the kernel, as we expect from our more general claim in Sec. III E.

This pattern of condensation is reflected in the fusion rules of the looplike excitations. These excitations satisfy a similar fusion rule to the magnetic excitations, as we showed more generally in Sec. III D. Given two membrane operators labeled by irreps α_1 and α_2 of E, the fusion rule is

$$\begin{aligned} L^{\alpha_1}(m)L^{\alpha_2}(m) &= \sum_{e_1,e_2\in E} \alpha_1(e_1)\delta(e_1, \hat{e}(m))\alpha_2(e_2)\delta(e_2, \hat{e}(m)) \\ &= \sum_{e_1,e_2\in E} \alpha_1(e_1)\alpha_2(e_2)\delta(e_1, e_2)\delta(e_1, \hat{e}(m)) \\ &= \sum_{e_1\in E} \alpha_1(e_1)\alpha_2(e_1)\delta(e_1, \hat{e}(m)), \end{aligned}$$

so that two membrane operators labeled by irreps α_1 and α_2 fuse to one operator labeled by the irrep $\alpha_1\alpha_2$, defined by $\alpha_1\alpha_2(e) = \alpha_1(e)\alpha_2(e)$. From this rule, along with the definition of the irreps given in Table IV, we can see that the condensed membrane operator (labeled by -1_{Rep}), together with the trivial operator (labeled by 1_{Rep}), form a closed subset of the membrane operators under fusion, as we may expect. We can also see that the membrane operator labeled by i_{Rep} is related to the membrane operator labeled by $-i_{\text{Rep}}$ by fusion with the condensed membrane operator -1_{Rep}, and so can be regarded as belonging to the same sector of excitations. We therefore have two sectors of looplike excitation, with all of the condensed excitations belonging to the same sector and all of the noncondensed excitations belonging to another sector in this case.

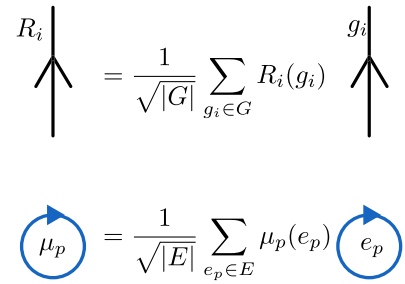

FIG. 38. In order to examine the ground states, we change basis from states where the edges and plaquettes are labeled by elements of G and E to states where they are labeled by irreps of those same groups.

2. *Ground states in the irrep basis*

Having considered each of the excitations, we now consider the ground states and ground-state degeneracy. To do this, it will be simplest to change basis from elements of the groups G and E to irreps of the groups. This change of basis for the edge elements and surface elements is shown in Fig. 38.

We then consider how the energy terms act in this new basis, starting with the vertex terms. We use the shorthand notation shown in Fig. 39 for a state with given edge elements around the vertex in question. After some simple algebra performed (for a more general case) in Sec. S-VI in the Supplemental Material [45], we find that the vertex terms act in the irrep basis according to

$$\begin{aligned} &A_v|R_1, R_2, R_3, R_4\rangle \\ &\quad = \delta\left(\left(R_1^{-1}R_2R_3R_4^{-1}\right), 1_{\text{Rep}}\right)|R_1, R_2, R_3, R_4\rangle. \end{aligned} \tag{37}$$

We can see that the vertex term ensures that the irreps labeling the surrounding edges fuse to the identity irrep at the vertex in the ground state (with inverses on some of the irreps to account for the orientation of the edges). Equivalently, the irreps labeling the edges entering the vertex fuse to the same channel as the irreps of the edges leaving the vertex.

Next consider the edge terms in this irrep basis. Again we define a shorthand for the state of the labels around an edge, shown in Fig. 40.

Then (again omitting algebraic steps described in Sec. S-VI in the Supplemental Material [45]) the edge term acts on the

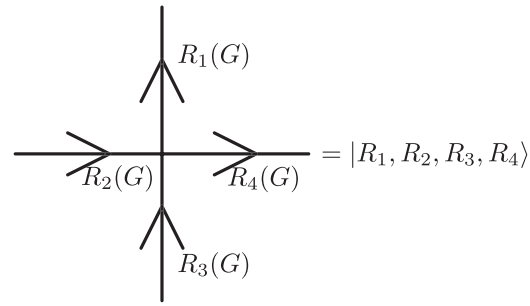

FIG. 39. It is convenient to introduce a shorthand for the state of the edges around a vertex.

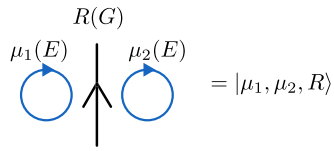

FIG. 40. We introduce a shorthand for the labels around an edge. μ_1 and μ_2 here label the plaquettes adjacent to the edge.

edge and surrounding plaquettes as

$$\mathcal{A}_i|\mu_1, \mu_2, R\rangle = \delta\big((\mu_1^{-1}\mu_2)(E), \mu^R(E)\big)|\mu_1, \mu_2, R\rangle, \quad (38)$$

where μ^R is defined by

$$\mu^R(e) = R(\partial(e)), \quad (39)$$

for all $e \in E$ and is itself an irrep of E. The representation μ^R derived from the label of the separating edge is called the defect label for the representation R of that edge. In the particular case considered in this section, the irreps $R = \pm 1_{\text{Rep}}$ have a defect label given by the identity irrep and the irreps $R = \pm i_{\text{Rep}}$ have -1_{Rep} as the defect label. From Eq. (38) we see that the edge energy terms enforce a fusion rule, that two neighboring plaquettes fuse with the edge separating them (or rather, with the defect label derived from the edge) to give the identity representation. This is also true for the horizontal edges, which act in an equivalent way to the vertical edge transforms (just consider rotating Fig. 40 90° clockwise and applying the same mathematics). We say that two neighboring plaquettes separated by an edge are linked, with the dual path between the two plaquettes called the link. In the ground state, two linked plaquettes must be related by the fusion rule derived in Eq. (38). For example, given the link shown in Fig. 41, the edge term enforces that, in the ground state

$$\mu_2 \overset{!}{=} \mu_1\mu^R. \quad (40)$$

Finally, consider the plaquette term in this new basis. Once again, we define a shorthand for the labels of the degrees of freedom near the plaquette, as shown in Fig. 42. After some algebra, we find that

$$B_p|R_1, R_2, R_3, R_4, \mu\rangle = \frac{1}{|G|}\sum_{\substack{\text{irreps } R \\ \text{of } G}} |RR_1, RR_2, R^{-1}R_3, R^{-1}R_4, \mu^R\mu\rangle, \quad (41)$$

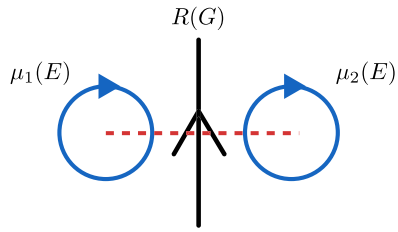

FIG. 41. We can consider the plaquettes on either side of an edge as being linked by the edge (just as adjacent vertices are linked by an edge). Here the link is represented by the dashed line, which can be obtained by rotating the edge by 90°.

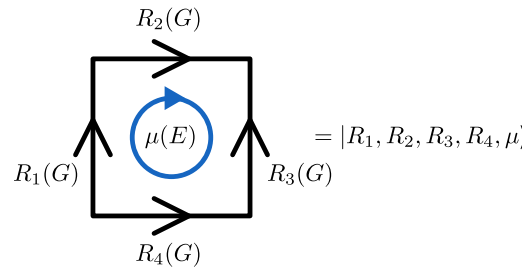

FIG. 42. The final energy term to consider is the plaquette term. We use a shorthand for the state of labels near a plaquette which are acted on by the plaquette energy term.

where (as described earlier in the section), μ^R is the irrep of E defined by $\mu^R(e) = R[\partial(e)]$ for irrep R of G. We can see from Eq. (41) that we can split the plaquette energy term into a sum of terms, one per irrep R, each of which fluctuates the labels of the edges around the plaquette by R and the label of the plaquette itself by μ^R. We call these individual terms plaquette transforms and write the transform corresponding to irrep R as B_p^R. Then $B_p = \frac{1}{|G|}\sum_{\text{irreps } R} B_p^R$. Because of the group structure of the 1D irreps, these plaquette transforms satisfy a similar algebra to the vertex transforms:

$$B_p^{R_1}B_p^{R_2} = B_p^{R_1R_2},$$

as can be directly verified from Eq. (41). In particular, this algebra means that a plaquette transform can be absorbed into the corresponding plaquette term (just as for vertex transforms):

$$B_p^R B_p = B_p.$$

This implies that plaquette transforms have no effect on the ground state because the ground state is an eigenstate of each plaquette term with eigenvalue one, and so

$$B_p^R|GS\rangle = B_p^R B_p|GS\rangle = B_p|GS\rangle = |GS\rangle.$$

Having considered the energy terms of the model in this irrep basis, we can now examine the ground states of the model. To construct a ground state, we first find a configuration in the irrep basis that satisfies all of the vertex and edge constraints, then we apply the plaquette terms to produce a suitable superposition of these. We first pick an edge configuration (in the irrep basis) that satisfies the vertex terms. These vertex terms are the same here as in Kitaev's quantum double model (when that model is treated in the irrep basis), and so any irrep configurations which satisfy the vertex terms of Kitaev's quantum double model will also satisfy the vertex conditions of this model.

The next step in finding the ground states is to choose plaquette labels that satisfy the edge terms, given the edge labels. In a path-connected manifold (where each pair of plaquettes is connected by a dual path made of a series of links) the choice of any single plaquette label (along with the previously determined edge labels) fixes the labels of the other plaquettes. To see how this occurs, consider two plaquettes on the lattice, such as the heavily shaded blue and orange plaquettes in Fig. 43. Because the lattice is path connected, we can construct a path on the dual lattice between the two plaquettes (through the lightly shaded green plaquettes in the

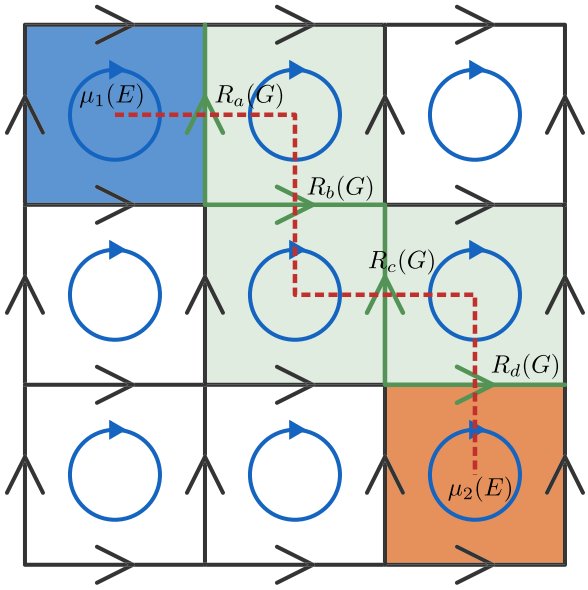

FIG. 43. Given two plaquettes that can be connected by a path in the dual lattice, the labels of the two plaquettes in the ground state are related due to the conditions imposed by the edge energy terms. For example, here the heavily shaded (blue and orange) plaquettes are connected by a dual path through the lightly shaded (green) plaquettes, represented by the (red) dashed line. The edge terms on the green edges that intersect with this line then enforce that the irrep μ_2 of the orange plaquette must be related to the irrep μ_1 of the blue plaquette by $\mu_2 = \mu_1 \mu^{R_a} \mu^{R_b} \mu^{R_c} \mu^{R_d}$ in the ground state, where the R_x are the irreps labeling the edges intersected by the dual path.

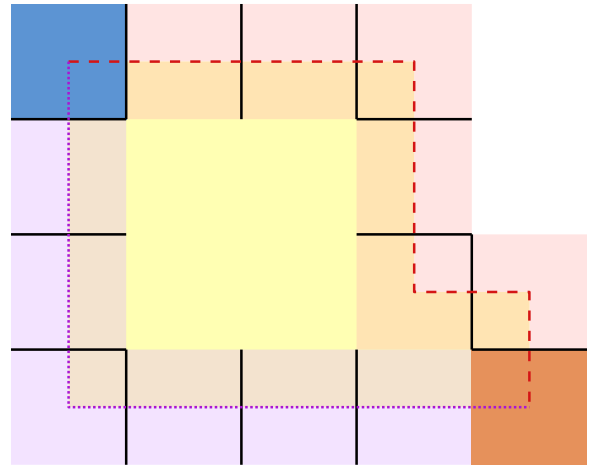

FIG. 44. There may be many dual paths that connect any two plaquettes. For example, both the red dashed line and purple dotted line connect the two heavily shaded (blue and orange) plaquettes and so both of these paths give constraints on the labels of the two plaquettes (as described in Fig. 43). If the two paths can be deformed into one another, then they enclose a contractible surface (the yellow region in this figure). The vertex terms in this region enforce fusion rules, so that the total charge carried in or out of the region by the black edges is trivial, and this ensures that the two paths agree (carry the same defect label) in the ground state. This guarantees that both paths give consistent relations between the two plaquettes in the ground state.

example in Fig. 43). By rotating the edges cut by the dual path by 90° in order to form links, we obtain a path of links that connect the two plaquettes (the red dashed lines in Fig. 43). The edge term [as given in Eq. (38)] forces the label of two adjacent plaquettes to be related by fusion of the defect label of the link connecting them (i.e., of the edge separating the plaquettes). This means that choosing the label of the first plaquette in the dual path fixes the label of the next in the path and so on, until we reach the end of the path. This means that once we have set the label of one plaquette, the label of any other plaquette connected to that one by a dual path is also fixed.

For example, in Fig. 43 the blue plaquette, with label μ_1, is separated from the next plaquette along the path by an edge with label R_a. Considering the action of the edge term applied on that edge, which enforces the relation shown in Fig. 41 in the ground state, the label of the next plaquette on the path must be $\mu_1 \mu^{R_a}$, where μ^{R_a} is defined in terms of R_a by Eq. (39). We can repeat this for the next plaquette in the path, and the next, until we reach the final plaquette. This tells us that the label of the orange plaquette, the last plaquette on the path, is $\mu_2 = \mu_1 \mu^{R_a} \mu^{R_b} \mu^{R_c} \mu^{R_d}$. This is equivalent to $\mu_2 = \mu_1 \mu^{R_a R_b R_c R_d}$. We can imagine taking the edges intersected by the dual path and rotating them by 90° (clockwise), to form a path connecting the blue and orange plaquettes (shown as a red dashed line). Then $R_a R_b R_c R_d$ is the irrep that we would obtain from fusing the labels of the rotated edges along that path. We see that the label of the orange plaquette is obtained by fusing the label of the blue plaquette with the defect label of the dual path connecting the two plaquettes (where μ^R is the defect label corresponding to a label of R). In this example, the direction of each rotated edge matches the direction of the path. If a rotated edge pointed against the dual path, that edge would instead contribute the inverse irrep to the dual path (in a similar way to how edges on the lattice contribute to a direct path), which matches the inverse that would appear in the condition imposed by the corresponding edge term on the adjacent plaquette labels due to the orientation of the edge being reversed.

While on a generic path-connected manifold any two plaquettes can be connected by links in this way, this does not guarantee that we can assign the second plaquette a label in a consistent way. Two plaquettes may be connected by many different such dual paths, and it is not guaranteed that these different paths will give a consistent label for the second plaquette. However, if we consider a simply connected manifold, the various different paths can all be deformed into one another, which means that they differ only by a closed contractible path on the dual lattice. This closed dual path will enclose some region of the lattice, as shown in the example in Fig. 44, and all of the edges that point into or out of this region (the black edges in Fig. 44) will be cut by the dual path. However, the vertex terms in that region enforce that the edges coming into or out of the region must fuse to the identity [individual vertex terms enforce that the edges coming in and out of the vertex fuse to the identity, as indicated by Eq. (37)]. This means that the path label (in the irrep basis) associated to the closed dual path must be trivial. In turn, this means that the two possible dual paths between the two plaquettes

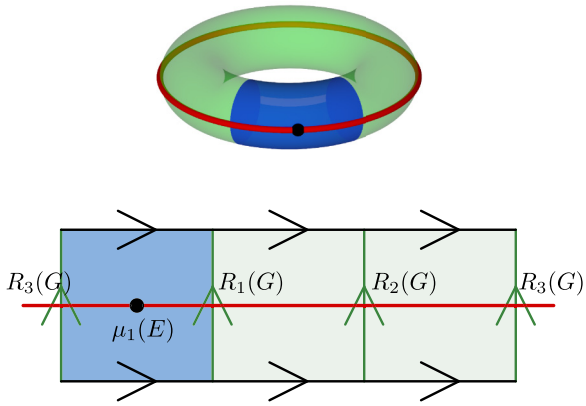

FIG. 45. We consider an example of a manifold that is not simply connected, namely, the torus in the upper part of the figure. The torus can be represented by a rectangle with its opposite sides identified, as in the lower part of the figure. As we described in Fig. 43, any two plaquettes connected by a path in the dual lattice must have their labels related by fusion with the defect label of the dual path, if the edges crossed by the dual path are unexcited. This means that the blue (dark gray in grayscale) plaquette in this figure must have a label that is related to itself by fusion with the defect label of the closed dual path shown here. In the case shown in the lower part of the figure, this means that $\mu_1(E) = \mu_1(E)\mu^{R_1(G)R_2(G)R_3(G)}$. More generally if the closed dual path is t and its defect label is $\mu^{R(t)}$, then we must have $\mu_1 = \mu_1\mu^{R(t)}$. This means that the label of the closed dual path around the cycle of the torus must satisfy $\mu^{R(t)} = 1_{\text{Rep}}$ in the ground state.

(which together form the closed path) have the same labels, and so guarantees that the different paths will give consistent answers for the label of the second plaquette.

On the other hand, if the manifold is not simply connected, then we cannot guarantee this consistency, and so some sets of edge labels may not generate a ground state (i.e., edge excitations may be inevitable for some otherwise valid sets of edge labels, which is only revealed when trying to find appropriate plaquette labels). For example, consider the case of a torus, such as the one shown in Fig. 45. Suppose that the label of one of the plaquettes is given by $\mu_1(E)$. Then, just as we did in Fig. 43, we can see what labels any other plaquette should have (if the edges are all unexcited) by fusing this plaquette label with the defect label of the dual path connecting the two plaquettes. If the path is t, with defect label $\mu^{R(t)}$ (the general version of $\mu^{R_a}\mu^{R_b}\mu^{R_c}\mu^{R_d}$ from Fig. 43), then the label μ_2 of the second plaquette must satisfy $\mu_2 = \mu_1\mu^{R(t)}$. Now consider a noncontractible closed cycle connecting the first plaquette to itself, such as the cycle of the torus shown in Fig. 45 (the red cycle), so that $\mu_2 = \mu_1$. This gives us the condition $\mu_1 = \mu_1\mu^{R(t)}$. That is, in order to be consistent with the edge energy terms, the label of the plaquette must be the same as the label obtained by fusing the plaquette label with the defect label of the dual path. If it is not, then there is a contradiction and so the edge energy terms cannot all be satisfied. This means that the edge labels are only consistent with the edge energy terms when $\mu^{R(t)} = 1_{\text{Rep}}$ (irrespective of the label of the plaquette itself), which is true when the dual path is labeled by $R(t) = \pm 1_{\text{Rep}}$. This tells us that the ground state (which must satisfy the edge energy terms) can only have certain quantum numbers wrapping the cycles of the torus (it can only have irreps that have trivial defect labels).

Once we have chosen consistent plaquette and edge configurations in the irrep basis (i.e., a set of irrep labels that satisfy the vertex and edge energy terms), a ground state is acquired by applying the plaquette energy terms to fluctuate the configurations. Knowing that all of the different allowed edge configurations for a spherical manifold are connected by the fluctuations from the plaquette term (because Kitaev's quantum double model [37] has a unique ground state on the sphere), we would expect the ground-state degeneracy to arise from the different choices for the label of the first plaquette. This would suggest a ground-state degeneracy of four on the sphere, with one state per irrep of E that we can take as our choice for the first plaquette. However, this value for the ground-state degeneracy is not quite correct. If we perform a plaquette transform B_p^R on each plaquette, it affects each edge twice in a way that cancels out. This is because each edge is aligned with one adjacent plaquette and so the edge label gains a factor of R from the transform associated to that plaquette, but the edge is antialigned with another plaquette and so the edge label gains a factor of R^{-1} from that plaquette, which cancels with the first factor. On the other hand, each plaquette label is only affected by one transform and so the series of plaquette transforms changes the label of each plaquette by μ^R. Because these plaquette transforms must leave the ground state invariant (analogous to the behavior of vertex and edge transforms on the ground state), the state resulting from applying this series of plaquette transforms must appear with equal weight as the original state in the ground state.

This means that an initial choice for the first plaquette label of irrep β is not an independent choice from choosing $\mu^R\beta$ instead. The initial choice of irrep should only be considered modulo the possible μ^R. In this example model, the only nontrivial irrep that can be expressed as $\mu^R(e) = R[\partial(e)]$ for some irrep R of G is the -1_{Rep} representation. This means that our initial choice of plaquette label is defined only up to multiplication by the -1_{Rep} irrep, i.e., up to a minus sign. Therefore, the only independent choices are 1_{Rep} and i_{Rep}. This implies that the ground-state degeneracy should be two on the sphere, which matches the general formula given in Ref. [1]. Note that this degeneracy is the same as the number of sectors of loop excitations, and the noncondensed loop excitations will form domain walls between different regions that look like the different ground states. As with the ($\mathbb{Z}_2$, $\mathbb{Z}_3$) model considered in Sec. VI A, these ground states are locally distinguishable rather than being topologically protected. Unlike for the ($\mathbb{Z}_2$, $\mathbb{Z}_3$) model, these ground states are related by a spontaneously broken symmetry. We mentioned that multiplying each plaquette irrep by -1_{Rep} must leave the ground state invariant. This is a global symmetry, although it is not spontaneously broken. On the other hand we could also multiply each plaquette irrep by $\pm i_{\text{Rep}}$. This is also a symmetry, although it is spontaneously broken in the ground-state space. In other words, there is a $\mathbb{Z}_4$ symmetry that is spontaneously broken down to $\mathbb{Z}_2$, with the broken symmetry resulting in a nontopological degeneracy and the unbroken part giving a symmetry-enriched topological phase (as we discuss further in Sec. VIII). We will discuss this idea

in more detail in Sec. VII, where we consider the more general $\triangleright$ trivial case.

VII. THE $\triangleright$ TRIVIAL CASE IN THE IRREP BASIS

In Sec. VI B 2 we saw that, at least for a particular example of a higher-lattice gauge theory model, changing the basis for our Hilbert space allowed us to reveal information about the ground-state structure of the model. Specifically, it was useful to change from a basis where the edges and plaquettes were labeled by group elements of G and E to one where they were labeled by irreducible representations of those groups. In this section we will take the more general class of higher-lattice gauge theory models in (2+1)D for which $\triangleright$ is trivial and apply the same change of basis. We will then examine the various energy terms in this basis and discuss the ground states in particular. This change of basis is motivated by work from Ref. [49], which mapped Kitaev's quantum double model [37] to another set of models for (2+1)D topological phases, called string-net models [30]. In Sec. VIII, we will show that this change of basis similarly allows us to map some of the higher-lattice gauge theory models to a construction for symmetry-enriched topological phases described in Ref. [16].

We start by defining our change of basis, which is a generalization of the one used in Sec. VI B 2. Consider a single edge of our lattice. In our usual basis, we describe this edge with a group label. For example, if the edge is labeled by $g \in G$, we could denote the state of the edge by $|g\rangle$. However, we can construct an alternate basis, where the edge is instead labeled by an irrep of G and the matrix indices for that irrep. For an irrep R and matrix indices a and b, we define the state [49]

$$|R, a, b\rangle = \sqrt{\frac{|R|}{|G|}} \sum_{g \in G} [D^R(g)]_{ab} |g\rangle, \tag{42}$$

where $|R|$ is the dimension of the irrep R and $[D^R(g)]$ is the matrix representing g in the irrep R. This is the same change of basis we used in Sec. VI B 2, except that because G may be non-Abelian we must include matrix indices for the representations in the change of basis. We can apply a similar change of basis to the plaquette labels, but because E is Abelian when $\triangleright$ is trivial, all of the irreps are one dimensional. Therefore, for an irrep μ of E we can write the corresponding plaquette state as

$$|\mu\rangle = \sqrt{\frac{1}{|E|}} \sum_{e \in E} \mu(e) |e\rangle, \tag{43}$$

where $|e\rangle$ is the state in which the plaquette is labeled by the group element $e \in E$ and $\mu(e)$ is the phase representing e in the 1D irrep (or equivalently is the character of the irrep).

Having defined our new basis for each degree of freedom, with the basis for the entire lattice made from tensor products of these individual basis elements, we can see how the energy terms of our model act in this new basis. This will again be similar to the results that we found for the example model in Sec. VI B 2, except for features arising from the possibility of G being non-Abelian. We will also not restrict to a particular lattice, such as the square lattice used in Sec. VI B. We start by considering the vertex energy term. As described in Sec. II, a vertex transform A_v^x acts on each edge attached to that vertex (and when $\triangleright$ is trivial the transform acts on no other degrees of freedom). For an edge i with label g_i attached to v, this action is

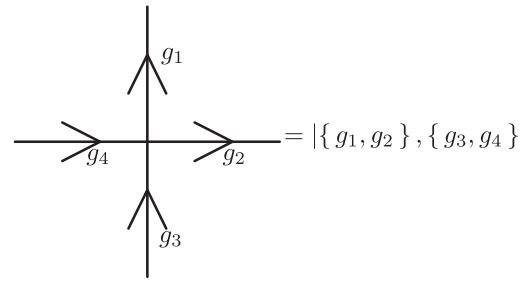

FIG. 46. The vertex transform acts on the edges adjacent to that vertex in a way that depends on whether those edges point towards or away from the vertex. We therefore need to differentiate between the inwards and outwards edges in the state, which we do by collecting their labels in separate sets when we write the state.

$$A_v^x : g_i = \begin{cases} x g_i & \text{if } i \text{ points away from } v, \\ g_i x^{-1} & \text{if } i \text{ points towards } v. \end{cases} \tag{44}$$

In order to describe the action of the vertex transform on all of the surrounding edges simultaneously, we denote the state of the adjacent edges by $|\{ g_i \}_{\text{out}}, \{ g_j \}_{\text{in}}\rangle$, where the subscript "in" denotes the inwards pointing edges and the subscript "out" refers to the outwards pointing ones. For example, in Fig. 46 we would denote the state of the edges around the vertex by $|\{ g_1, g_2 \}, \{ g_3, g_4 \}\rangle$. The action of the vertex transform A_v^x on the state $|\{ g_i \}_{\text{out}}, \{ g_j \}_{\text{in}}\rangle$ can then be written as

$$A_v^x |\{ g_i \}_{\text{out}}, \{ g_j \}_{\text{in}}\rangle = |\{ x g_i \}_{\text{out}}, \{ g_j x^{-1} \}_{\text{in}}\rangle. \tag{45}$$

The vertex energy term A_v is then given by $A_v = \frac{1}{|G|} \sum_{x \in G} A_v^x$. In order to apply this term in our new basis, we define a state

$$\begin{aligned} &|\{ R_i, a_i, b_i \}_{\text{out}}, \{ R_j, a_j, b_j \}_{\text{in}}\rangle \\ &= \sum_{\{ g_i \}_{\text{out}}} \sum_{\{ g_j \}_{\text{in}}} \left(\prod_{\substack{\text{outgoing} \\ \text{edges } i}} \sqrt{\frac{|R|}{|G|}} [D^{R_i}(g_i)]_{a_i b_i} \right) \\ &\quad \times \left(\prod_{\substack{\text{incoming} \\ \text{edges } j}} \sqrt{\frac{|R|}{|G|}} [D^{R_j}(g_j)]_{a_j b_j} \right) |\{ g_i \}_{\text{out}}, \{ g_j \}_{\text{in}}\rangle, \end{aligned}$$

where $\sum_{\{ g_i \}_{\text{out}}}$ sums over each element of G for each outgoing edge and $\sum_{\{ g_j \}_{\text{in}}}$ does the same for each incoming edge. Then we can apply the vertex energy term to this state. By applying some algebraic manipulations, given in Sec. S-VI of

the Supplemental Material [45], we find that

$$\begin{aligned} &A_v|\{R_i, a_i, b_i\}_{\text{out}}, \{R_j, a_j, b_j\}_{\text{in}}\rangle \\ &= \frac{1}{|G|}\sum_{x\in G}\sum_{\{c_i\}}\sum_{\{c_j\}}\left(\prod_{\substack{\text{outgoing}\\ \text{edges } i}}[D^{\overline{R}_i}(x)]_{c_i a_i}\right) \\ &\quad\times\left(\prod_{\substack{\text{incoming}\\ \text{edges } j}}[D^{R_j}(x)]_{c_j b_j}\right) \\ &\quad\times|\{R_i, c_i, b_i\}_{\text{out}}, \{R_j, a_j, c_j\}_{\text{in}}\rangle, \end{aligned} \tag{46}$$

where $\overline{R}$ is the representation of G conjugate to R, which satisfies

$$[D^{\overline{R}_i}(x)]_{c_i a_i} = [D^{R_i}(x)]^*_{c_i a_i}.$$

The product

$$\left(\prod_{\substack{\text{outgoing}\\ \text{edges } i}}[D^{\overline{R}_i}(x)]_{c_i a_i}\right)\left(\prod_{\substack{\text{incoming}\\ \text{edges } j}}[D^{R_j}(x)]_{c_j b_j}\right)$$

is itself a matrix element of a (generally reducible) representation of G formed from the combination of the individual representations. Because of the grand orthogonality theorem for representations, summing this over the elements $x \in G$ projects to the identity representation. The vertex energy term therefore energetically penalizes states for which the irreps around the vertex do not fuse to the identity (with the direction of the edge with respect the vertex accounted for by using the original irrep or the conjugate irrep). For example, in the Abelian case, where the irreps are all one dimensional and so we do not need to consider matrix indices, the action of the vertex term on a basis state becomes

$$\begin{aligned} &A_v|\{R_i\}_{\text{out}}, \{R_j\}_{\text{in}}\rangle \\ &= \delta\left(\left(\prod_{\substack{\text{outgoing}\\ \text{edges } i}}\overline{R}_i\right)\left(\prod_{\substack{\text{incoming}\\ \text{edges } j}}R_j\right), 1_{\text{Rep}}\right) \\ &\quad\times|\{R_i\}_{\text{out}}, \{R_j\}_{\text{in}}\rangle. \end{aligned} \tag{47}$$

Next we consider the edge term. An edge transform $\mathcal{A}^e_i$ acts on the edge i itself and the two adjacent plaquettes. If the edge is initially labeled by g_i, then the edge transform acts on the edges as $\mathcal{A}^e_i : g_i = \partial(e)g_i$. For an adjacent plaquette p, with initial label e_p, the action of the transform is

$$\mathcal{A}^e_i : e_p = \begin{cases} e_p e^{-1} & \text{if the circulation of } p \text{ matches} \\ & \text{the orientation of } i, \\ e e_p & \text{if the circulation of } p \text{ opposes} \\ & \text{the orientation of } i. \end{cases}$$

Because E is Abelian when $\triangleright$ is trivial, we can simplify the notation here by neglecting the order of multiplication and writing

$$\mathcal{A}^e_i : e_p = e_p e^{\sigma_p},$$

where σ_p is -1 if the circulation of p aligns with the orientation of i and is 1 otherwise.

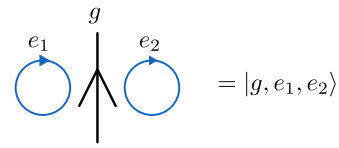

FIG. 47. The edge transform affects the edge itself and the two neighboring plaquettes. We wish to introduce a labeling scheme for the state of the degrees of freedom associated to the edge and these plaquettes. If the label of the edge is g, the label of the plaquette to the left of the edge (with respect to the orientation of the edge) is e_1 and the label of the right plaquette is e_2, then we denote the state by $|g, e_1, e_2\rangle$.

Now we wish to consider the action of the edge transform in the irrep basis. As illustrated in Fig. 47, we denote the initial state of the three degrees of freedom (the edge and the two adjacent plaquettes) in the group element basis by $|g, e_1, e_2\rangle$, where e_1 labels the plaquette to the left of the edge, while e_2 labels the plaquette to the right of the edge. Then to implement the change of basis to the irrep basis, we define

$$\begin{aligned} |\{R, a, b\}, \mu_1, \mu_2\rangle = &\sqrt{\frac{|R|}{|G|}}\sum_{g\in G}\frac{1}{|E|}\sum_{e_1,e_2\in E}[D^R(g)]_{ab} \\ &\times\ \mu_1(e_1)\mu_2(e_2)|g, e_1, e_2\rangle, \end{aligned}$$

where we have used greek letters to represent the irreps of E to distinguish them from the irreps of G. Then in the new basis, the action of the edge transform is given by

$$\begin{aligned} \mathcal{A}^e_i|\{R, a, b\}, \mu_1, \mu_2\rangle = &\sum_{c=1}^{|R|}\{D^R[\partial(e)^{-1}]\}_{ac}\mu_1(e^{-\sigma_1})\mu_2(e^{-\sigma_2}) \\ &\times\ |\{R, c, b\}, \mu_1, \mu_2\rangle, \end{aligned} \tag{48}$$

as proven in Sec. S-VI in the Supplemental Material [45] (where σ_p is 1 if the plaquette p is antialigned with the edge and is -1 otherwise). We now wish to consider the object $\{D^R[\partial(e)^{-1}]\}_{ac}$ in closer detail. While R is an irrep of G, the argument $\partial(e)$ is only ever in the subgroup $\partial(E)$ of G. Just as we discussed previously in Sec. III A (in the context of electric ribbon operators), the fact that $\partial(E)$ is a subgroup in the center of G means that R branches to multiple copies of the same irrep of $\partial(E)$, due to Clifford's theorem [50]. We can also see this from Schur's lemma, which tells us that the matrices of irrep R that represent elements in $\partial(E)$ are scalar multiples of the identity, with the scalar being a 1D irrep of $\partial(E)$, which we will denote by $R^{\text{irr.}}_\partial$. Then we have

$$[D^R(\partial(e)^{-1})]_{ac} = \delta_{ac}R^{\text{irr.}}_\partial(\partial(e)^{-1}).$$

Furthermore, we can use this irrep of $\partial(E)$ to define an irrep of E, which we call μ^R, by $\mu^R(e) = R^{\text{irr.}}_\partial(\partial(e))$. This is a representation of E due to the fact that ∂ is a group homomorphism, and it is an irrep because it is a 1D representation. Substituting these results into Eq. (48) gives us

$$\begin{aligned} &\mathcal{A}^e_i|\{R, a, b\}, \mu_1, \mu_2\rangle \\ &\quad= \mu^R(e^{-1})\mu_1(e^{-\sigma_1})\mu_2(e^{-\sigma_2})|\{R, a, b\}, \mu_1, \mu_2\rangle. \end{aligned}$$

We now consider the energy term, which is an average over all of the edge transforms on i: $\mathcal{A}_i = \frac{1}{|E|}\sum_{e\in E}\mathcal{A}^e_i$. Defining

$\mu^{-1}(e) = \mu^*(e) = \mu(e^{-1})$, we find from the grand orthogonality theorem that

$$\mathcal{A}_i|\{R, a, b\}, \mu_1, \mu_2\rangle = \delta\big(\mu^R \mu_1^{\sigma_1} \mu_2^{\sigma_2}, 1_{\mathrm{Rep}(E)}\big)|\{R, a, b\}, \mu_1, \mu_2\rangle. \tag{49}$$

We can see that this edge term checks that the irreps of the two plaquettes on either side of the edge are compatible with the irrep labeling the edge. This idea becomes more clear if we take a fixed orientation for the two plaquettes. For example, we can take the case in Fig. 47, where the two plaquettes have the same orientation (clockwise). Then with this orientation, the plaquette on the left is aligned against the direction of the edge, while the plaquette on the right is aligned with the edge. This means that the energy term becomes

$$\begin{aligned}\mathcal{A}_i|\{R, a, b\}, \mu_1, \mu_2\rangle \\ \delta\big(\mu^R \mu_1 \mu_2^{-1}, 1_{\mathrm{Rep}(E)}\big)|\{R, a, b\}, \mu_1, \mu_2\rangle \\ = \delta(\mu^R \mu_1, \mu_2)|\{R, a, b\}, \mu_1, \mu_2\rangle.\end{aligned} \tag{50}$$

Then it is clear that the edge term enforces that the irreps labeling the two plaquettes differ by the irrep μ^R derived from the irrep R labeling the edge. We note that, because $\mu^R(e) = R^{\mathrm{irr.}}_{\partial}[\partial(e)]$, the irrep μ^R is trivial in the kernel of ∂. That is, for an element e_k satisfying $\partial(e_k) = 1_G$, we have $\mu^R(e_k) = R^{\mathrm{irr.}}_{\partial}(1_G) = 1$. This means that the Kronecker delta in Eq. (50) enforces that $\mu_1(e_k) = \mu_2(e_k)$, so the two plaquettes must carry the same irrep of the kernel of ∂.

Finally, we consider the plaquette terms. The plaquette term B^p acts in the group element basis according to $B^p|\psi\rangle = \delta(\partial(e_p)g_p, 1_G)$, where e_p is the label of the plaquette and g_p is the path element corresponding to the boundary of the plaquette. This path element can be expressed as

$$g_p = \prod_{\substack{\text{edge } i \text{ in} \\ \text{boundary}(p)}} g_i^{\sigma_i},$$

where σ_i is 1 if the edge i is oriented along the boundary and -1 if it is oriented against it. The product is taken in the order of the boundary, so that the first edge on the boundary is on the left of the product. We can denote the state of the plaquette and the edges on the boundary by $|e_p, \{g_i\}\rangle$. Then we can write the action of the plaquette operator on this state as

$$B_p|e_p, \{g_i\}\rangle = \delta\left(\partial(e_p) \prod_{\substack{\text{edge } i \text{ in} \\ \text{boundary}(p)}} g_i^{\sigma_i}, 1_G\right)|e_p, \{g_i\}\rangle.$$

Now we wish to consider the action of the plaquette term in the irrep basis. We define the irrep basis states by

$$|\mu, \{R_i, a_i, b_i\}\rangle = \sum_{\{g_i\}} \left(\prod_i \sqrt{\frac{|R_i|}{|G|}}[D^{R_i}(g_i)]_{a_i,b_i}\right) \times \sum_{e_p \in E} \sqrt{\frac{1}{|E|}}\mu(e_p)|e_p, \{g_i\}\rangle.$$

We find that the action of the plaquette operator on this basis state is (as shown in Sec. S-VI of the Supplemental Material [45])

$$\begin{aligned}B_p|\mu, \{R_i, a_i, b_i\}\rangle \\ = \sum_{\text{irreps } R \text{ of } G} \sum_{\{c_i\}} \sum_{\{g_i\}} \frac{|R|}{|G|} \\ \times \left(\prod_i \sqrt{\frac{|R_i|}{|G|}}[D^{R_i}(g_i)]_{a_i,b_i}[D^R(g_i^{\sigma_i})]_{c_i c_{i+1}}\right) \\ \times \sum_{e_p \in E} \sqrt{\frac{1}{|E|}}\mu(e_p)\mu^R(e_p)|e_p, \{g_i\}\rangle.\end{aligned} \tag{51}$$

We can split the plaquette term into a sum of terms, where each term corresponds to one irrep R on the right-hand side of Eq. (51). That is, we write

$$B_p = \sum_{\text{irreps } R \text{ of } G} \frac{|R|}{|G|} B_p^R, \tag{52}$$

where

$$\begin{aligned}B_p^R|\mu, \{R_i, a_i, b_i\}\rangle \\ = \sum_{\{c_i\}} \sum_{\{g_i\}} \left(\prod_i \sqrt{\frac{|R_i|}{|G|}}[D^{R_i}(g_i)]_{a_i,b_i}[D^R(g_i^{\sigma_i})]_{c_i c_{i+1}}\right) \\ \times \sum_{e_p \in E} \sqrt{\frac{1}{|E|}}\mu(e_p)\mu^R(e_p)|e_p, \{g_i\}\rangle \\ = \sum_{\{c_i\}} \sum_{\{g_i\}} \left(\prod_i \sqrt{\frac{|R_i|}{|G|}}[D^{R_i}(g_i)]_{a_i,b_i}[D^R(g_i^{\sigma_i})]_{c_i c_{i+1}}\right) \\ \times |\mu \cdot \mu^R, \{g_i\}\rangle.\end{aligned}$$

We see that B_p^R acts by fusing the irrep R into the edges along the boundary of the plaquette (with an inverse if the edge is antialigned with the boundary) and fusing the irrep μ^R into the plaquette. For example, when G is Abelian this becomes

$$\begin{aligned}B_p^R|\mu, \{R_i\}\rangle = \sum_{\{g_i\}} \left(\prod_i \sqrt{\frac{1}{|G|}}R_i(g_i)R\big(g_i^{\sigma_i}\big)\right) \\ \times \sum_{e_p \in E} \sqrt{\frac{1}{|E|}}\mu(e_p)\mu^R(e_p)|e_p, \{g_i\}\rangle \\ = \sum_{\{g_i\}} \left(\prod_i \sqrt{\frac{1}{|G|}}(R_i R^{\sigma_i})(g_i)\right) \\ \times \sum_{e_p \in E} \sqrt{\frac{1}{|E|}}(\mu\mu^R)(e_p)|e_p, \{g_i\}\rangle \\ = |\mu\mu^R, \{R_i R^{\sigma_i}\}\rangle,\end{aligned}$$

where $R^{\sigma_i}(g) = R(g^{\sigma_i})$. The total plaquette term B_p then fluctuates the irreps of the edges and plaquette by averaging over

the irreps fused into the edges and plaquette:

$$B_p|\mu, \{R_i\}\rangle = \sum_{\text{irreps } R \text{ of } G} \frac{1}{|G|}|\mu\mu^R, \{R_i R^{\sigma_i}\}\rangle. \tag{53}$$

We note that the plaquette labels resulting from the action of the plaquette term have the form $\mu\mu^R$, where

$$\mu^R(e) = R^{\text{irr.}}_{\partial}(\partial(e)). \tag{54}$$

This means that when we restrict the irrep to the kernel of ∂, by considering elements e_k in the kernel, we have

$$(\mu\mu^R)(e_k) = \mu(e_k)R^{\text{irr.}}_{\partial}(\partial(e_k)) = \mu(e_k)R^{\text{irr.}}_{\partial}(1_G) = \mu(e_k),$$

so that the resulting irrep that labels the plaquette has the same restriction to the kernel of ∂ as the original irrep label.

Having considered the action of the different energy terms in the irrep basis in some detail, we now wish to consider what this means for the energy eigenstates and in particular the ground states. In the group element basis, the vertex term and the edge term both fluctuate the group elements around the edge or vertex, while the plaquette term puts constraints on what elements are allowed in the ground state. On the other hand, in the irrep basis this is reversed. The vertex and edge terms enforce fusion rules on the irreps in the ground states, while the plaquette term fluctuates the labels on and around the plaquette. In order to construct a ground state, we can first choose a set of edge irrep labels which satisfies the rules enforced by the vertex terms, which only act on the edge labels. Then we can pick a set of plaquette irrep labels that satisfy the edge terms, given our choice of edge labels. Finally, we apply the plaquette terms to fluctuate these degrees of freedom and produce the ground states, which are linear combinations of various irrep configurations satisfying the fusion rules. For those readers familiar with Kitaev's quantum double model, the first step is equivalent to how we would consider the ground states in that model in the irrep basis because the vertex term is the same in both models. However, it is interesting to consider the last two steps in more detail because these involve the plaquette labels.

First, we want to choose plaquette labels that satisfy the edge terms. Recall that the edge term acts on an edge i and the two adjacent plaquettes according to

$$\mathcal{A}_i|\{R_i, a, b\}, \mu_1, \mu_2\rangle = \delta(\mu^{R_i}\mu_1, \mu_2)|\{R_i, a, b\}, \mu_1, \mu_2\rangle,$$

provided that the plaquettes have the same clockwise orientation, where μ_1 is the initial label of the left plaquette and μ_2 is the label of the right plaquette, as indicated in Fig. 47. This enforces that the two irreps of E differ by multiplication by an irrep derived from the edge label R_i. This does not fix the label of either plaquette, but instead ensures that they are related by a factor. Once μ_1 and R_i are chosen, the irrep μ_2 is set. As explained in Sec. VI B 2, where we considered a particular example model, if the manifold represented by our lattice is simply connected, this means that choosing the label of one plaquette will fix the value of all other plaquettes on the lattice. In addition, because μ^{R_i} has a trivial restriction to the kernel of ∂, every plaquette label will have the same restriction to the kernel of ∂ (if we choose all of the plaquettes to have the same orientation, otherwise some will have the conjugate irrep of the kernel). Keeping this in mind, we now consider applying the plaquette terms. These fluctuate the values of the edge and plaquette labels, so that the ground state is not a simple product state. However, the plaquette term only fluctuates the plaquette labels by irreps μ^R which have trivial restriction to the kernel of ∂. This means that the restriction of the plaquette labels to the kernel of ∂ is unaffected by the application of the plaquette terms. Given that this restriction of the irrep labeling a plaquette to the kernel is also the same for each plaquette due to the edge terms, this means that this restriction of the plaquette label to the kernel of ∂ is a property of the overall ground state constructed in this way. This means (on a simply connected manifold) that we will have one ground state or ground-state sector for each possible irrep of the kernel of ∂, and so there are multiple ground states even on the 2-sphere. This ground-state degeneracy does not arise due to topological concerns, as we can tell from the fact that the ground state can be determined locally by measuring the label of a single plaquette. Instead, for these models with $\triangleright$ trivial, there is a symmetry that results in this ground-state degeneracy.

We claim that, if all of the plaquettes are oriented in the same way, this symmetry is given by multiplication of each plaquette's irrep label by the same irrep μ of E (if a plaquette is oriented in the opposite way, we should instead multiply its label by the inverse irrep). We denote the operator that does this by U^μ, where we have one such operator for each irrep μ of E. In order to be a symmetry of the model, this operator must commute with the energy terms. The symmetry operator clearly commutes with the vertex term because the vertex term does not act on the plaquette labels. However, we can also show that the symmetry operator commutes with the other energy terms. Recall that, when the plaquettes all have the same orientation, the edge energy term checks that the two plaquettes on either side of the edge have labels related by multiplication by an irrep associated to the edge. Because the 1D irreps of E form an Abelian group, multiplying the irreps of both plaquettes by a common irrep μ does not change the relationship between the two irreps and so preserves this condition. That is, given an initial state $|R, a, b, \mu_1, \mu_2\rangle$, acting first with the edge term and then the symmetry operator gives us

$$\begin{aligned} U^\nu\mathcal{A}_i|R, a, b, \mu_1, \mu_2\rangle &= U^\nu\delta(\mu^{R_i}\mu_1, \mu_2)|\{R_i, a, b\}, \mu_1, \mu_2\rangle \\ &= \delta(\mu^{R_i}\mu_1, \mu_2)|\{R_i, a, b\}, \nu\mu_1, \nu\mu_2\rangle. \end{aligned}$$

On the other hand, for the other order of operations we have

$$\begin{aligned} &\mathcal{A}_i U^\nu|R, a, b, \mu_1, \mu_2\rangle \\ &\quad= \mathcal{A}_i|\{R_i, a, b\}, \nu\mu_1, \nu\mu_2\rangle \\ &\quad= \delta(\mu^{R_i}\nu\mu_1, \nu\mu_2)|\{R_i, a, b\}, \nu\mu_1, \nu\mu_2\rangle \\ &\quad= \delta(\mu^{R_i}\mu_1, \mu_2)|\{R_i, a, b\}, \nu\mu_1, \nu\mu_2\rangle, \end{aligned}$$

where in the last line we used the fact that the irreps of E form an Abelian group to remove the common factor of ν in each term of the Kronecker delta. This indicates that the symmetry operator does indeed commute with the edge terms. While we assumed that the plaquettes all have the same orientation, the same result holds generally [the symmetry operator then multiplies the plaquettes with the opposite orientation by the

inverse irrep ν^{-1}, but this inverse cancels with an inverse in the action of the edge term described by Eq. (49)].

Lastly, we must consider the commutation between the plaquette terms and the symmetry. The plaquette term is made of a sum of operators B_p^R which interact with the plaquette labels by multiplying them by an irrep μ^R, but because the group of irreps of E is Abelian this multiplication always commutes with the multiplication from the symmetry operator. Therefore, the symmetry operator commutes with the plaquette terms. Combining this with our previous results, we see that the symmetry operator commutes with all of the energy terms, as required. We have defined a symmetry operator U^μ for all irreps of E, but we mentioned earlier that the ground states were labeled by irreps of the kernel of ∂. The presence of degenerate ground states, even on a spherical manifold, suggests that the symmetry is spontaneously broken, but the fact that the ground states are labeled by irreps of the kernel of ∂ rather than irreps of the full group E suggests that the symmetry is only partially broken, as we will see later in this section.

Having constructed this symmetry operator by utilizing the irrep basis for our model, it is enlightening to consider how this symmetry operator acts in our original basis. Consider a state $|\{\mu_p\}\rangle$, where $\{\mu_p\}$ denotes the irrep labels μ_p of each plaquette p and we do not need to consider the edge labels. The action of the symmetry operator U^ν on this state is (assuming that all of the plaquettes have the same orientation)

$$U^\nu|\{\mu_p\}\rangle = |\{\nu\mu_p\}\rangle.$$

Now we can use our change of basis to see how this operator acts in the original basis. A state $|\{e_p\}\rangle$, where each plaquette is labeled by a group element e_p, is given in terms of the irrep basis states by

$$|\{e_p\}\rangle = \sum_{\{\mu_p\}} \left(\prod_p \sqrt{\frac{1}{|E|}} \mu_p(e_p)^{-1} \right) |\{\mu_p\}\rangle,$$

where $\sum_{\{\mu_p\}}$ sums over all irreps μ_p of E for each plaquette p [this can directly be verified as the inverse transformation of Eq. (43) for each plaquette]. Then the symmetry operator U^ν acting on this state is

$$\begin{aligned} U^\nu|\{e_p\}\rangle &= \sum_{\{\mu_p\}} \left(\prod_p \sqrt{\frac{1}{|E|}} \mu_p(e_p)^{-1} \right) U^\nu|\{\mu_p\}\rangle \\ &= \sum_{\{\mu_p\}} \left(\prod_p \sqrt{\frac{1}{|E|}} \mu_p(e_p)^{-1} \right) |\{\nu\mu_p\}\rangle. \end{aligned}$$

Now because the 1D irreps of E form a group, we may replace the dummy index μ_p with $\mu'_p = \nu\mu_p$ in the sum for each p. This gives us

$$\begin{aligned} U^\nu|\{e_p\}\rangle &= \sum_{\{\mu'_p = \nu\mu_p\}} \left(\prod_p \sqrt{\frac{1}{|E|}} (\nu^{-1}\mu'_p)(e_p)^{-1} \right) |\{\mu'_p\}\rangle \\ &= \sum_{\{\mu'_p\}} \left(\prod_p \sqrt{\frac{1}{|E|}} \nu(e_p)\mu'_p(e_p)^{-1} \right) |\{\mu'_p\}\rangle \\ &= \left(\prod_p \nu(e_p) \right) \sum_{\{\mu'_p\}} \left(\prod_p \sqrt{\frac{1}{|E|}} \mu'_p(e_p)^{-1} \right) |\{\mu'_p\}\rangle \\ &= \left(\prod_p \nu(e_p) \right) |\{e_p\}\rangle \\ &= \nu\left(\prod_p e_p \right) |\{e_p\}\rangle. \end{aligned}$$

Given that the plaquettes all have the same orientation, $\prod_p e_p$ is just the total surface element of the lattice. Writing this total surface element as $e(L)$, we see that the symmetry operator acts as

$$U^\nu|\{e_p\}\rangle = \nu(e(L))|\{e_p\}\rangle$$

on a basis element. We can then write the operator acting on an arbitrary state $|\psi\rangle$ as

$$U^\nu|\psi\rangle = \sum_{e\in E} \nu(e)\delta(\hat{e}(L), e)|\psi\rangle, \tag{55}$$

where $\hat{e}(L)$ is the operator that measures the total surface element. We note that, if $|\psi\rangle$ is a ground state, then fake flatness implies that $\partial(\hat{e}(L))$ must be related to the path element $\hat{g}(L)$ corresponding to the path around the boundary of the lattice by $\partial(\hat{e}(L))\hat{g}(L) = 1_G$. If our manifold is a sphere then the boundary is trivial, and so we have $\partial(\hat{e}(L)) = 1_G$. This implies that, for a ground state $|GS\rangle$ on the sphere, only the labels e in the kernel of ∂ contribute, so that

$$\begin{aligned} U^\nu|GS\rangle &= \sum_{e\in E} \nu(e)\delta(\hat{e}(L), e)|GS\rangle \\ &= \sum_{e\in \ker(\partial)} \nu(e)\delta(\hat{e}(L), e)|GS\rangle. \end{aligned}$$

This tells us that the action of the symmetry operator U^ν only depends on the restriction of ν to the kernel, and in particular is trivial if the restriction to the kernel is trivial. Therefore, the symmetries labeled by irreps with such trivial restrictions are unbroken in the ground states, which further explains (in the case of the 2-sphere) why the ground states are labeled by irreps of the kernel and not by general irreps of E.

For a more general manifold, the picture is slightly more complicated. We can use the fake-flatness condition to write

$$|GS\rangle = \delta(\partial(\hat{e}(L)), \hat{g}(L)^{-1})|GS\rangle.$$

This allows us to write

$$U^\nu|GS\rangle = \sum_{e\in E} \nu(e)\delta(\hat{e}(L), e)\delta(\partial(\hat{e}(L)), \hat{g}(L)^{-1})|GS\rangle.$$

We can use $\delta(\hat{e}(L), e)$ to replace the operator $\hat{e}(L)$ in the fake-flatness condition with the variable e:

$$U^\nu|GS\rangle = \sum_{e\in E} \nu(e)\delta(\hat{e}(L), e)\delta(\partial(e), \hat{g}(L)^{-1})|GS\rangle.$$

We can represent an element $e \in E$ as a product $e_k q$, where e_k is in the kernel of ∂ and q is a representative of an element of the quotient group $E/\ker(\partial)$ [so that each coset of $\ker(\partial)$ in E is represented by a unique element q]. Denoting the set

of representatives of this quotient group by Q_∂, we can write the sum over $e \in E$ as

$$\sum_{e\in E} = \sum_{e_k\in\ker(\partial)} \sum_{q\in Q_\partial}.$$

This allows us to write the action of the symmetry operator as

$$\begin{aligned} U^\nu|GS\rangle &= \sum_{e\in E} \nu(e)\delta(\hat{e}(L), e)\delta(\partial(e), \hat{g}(L)^{-1})|GS\rangle \\ &= \sum_{e_k\in\ker(\partial)} \sum_{q\in Q_\partial} \nu(e_k q)\delta(\hat{e}(L), e_k q) \\ &\quad \times \delta(\partial(e_k q), \hat{g}(L)^{-1})|GS\rangle. \end{aligned}$$

We can then use a defining property of representations to write $\nu(e_k q) = \nu(e_k)\nu(q)$. Furthermore, e_k is in the kernel of ∂, and so $\partial(e_k q) = \partial(q)$. This gives us

$$\begin{aligned} U^\nu|GS\rangle = &\sum_{e_k\in\ker(\partial)} \sum_{q\in Q_\partial} \nu(e_k)\nu(q)\delta(\hat{e}(L), e_k q) \\ &\times \delta(\partial(q), \hat{g}(L)^{-1})|GS\rangle. \end{aligned}$$

Because the $q \in Q_\partial$ are unique representatives of the cosets of $\ker(\partial)$ in E, there is a unique q satisfying $\partial(q) = \hat{g}(L)^{-1}$. Denoting this value of q (which is generally an operator) by $\hat{q}_L$, this allows us to remove the sum over $q \in Q_\partial$ and the Kronecker delta enforcing fake flatness:

$$U^\nu|GS\rangle = \sum_{e_k\in\ker(\partial)} \nu(e_k)\nu(\hat{q}_L)\delta(\hat{e}(L), e_k\hat{q}_L)|GS\rangle.$$

Then, even if ν is trivial in $\ker(\partial)$, so that $\nu(e_k) = 1$ for all e_k, the action of the symmetry operator may still be nontrivial. When ν is trivial in the kernel, we have

$$U^\nu|GS\rangle = \nu(\hat{q}_L) \sum_{e_k\in\ker(\partial)} \delta(\hat{e}(L), e_k\hat{q}_L)|GS\rangle.$$

Fake flatness ensures that

$$\sum_{e_k\in\ker(\partial)} \delta(\hat{e}(L), e_k\hat{q}_L)|GS\rangle = |GS\rangle$$

[from the fact that $\partial(\hat{q}_L) = \hat{g}(L)^{-1}$], and so this action becomes

$$U^\nu|GS\rangle = \nu(\hat{q}_L)|GS\rangle,$$

which is a simple phase if $|GS\rangle$ is an eigenstate of $\hat{q}_L$ (i.e., has a well-defined boundary label) but can be a more complicated transformation if $|GS\rangle$ is a linear combination of such states.

The action of the symmetry operators given in Eq. (55) also reveals additional information about the model and in particular its excitations. We can see that the action of the symmetry operator is exactly the same as the action of an E-valued membrane operator

$$L^\nu(m) = \sum_{e\in E} \nu(e)\delta(\hat{e}(m), e),$$

applied over the entire lattice (see Sec. III D). This means that when we apply an E-valued membrane operator on part of the lattice it is the same as applying a symmetry operator over that section of the lattice. This means that we are changing which irrep that part of the lattice corresponds to, while leaving the rest of the lattice untouched. This creates a domain corresponding to a different ground state, and so we see that the looplike excitation on the boundary of the membrane is in fact a domain wall between these different domains, just as we discussed for an example model in Sec. VI B 2. This idea can also give us an alternative interpretation of the condensed loop excitations. The condensed E-valued membrane operators, which we found to be equivalent to a confined electric ribbon operator around the boundary of the membrane, are labeled by irreps with trivial restriction to the kernel of ∂. As we saw earlier, such irreps correspond to unbroken symmetries, which do not change the ground state when applied on the entire lattice (for a sphere). Therefore, it seems that these condensed membrane operators do not produce a domain corresponding to a different ground state compared to the rest of the lattice, which agrees with the idea that these operators act equivalently on the ground state to electric ribbon operators around the boundary of the membrane (because such local operators cannot make domains).

Next we consider how to construct projectors to the various ground-state sectors. All of the plaquettes in a given basis ground state are labeled by irreps which have the same restriction to the kernel of ∂ (assuming the plaquettes all have the same orientation, otherwise plaquettes with the opposite orientation will restrict to the inverse irrep). This means that if we are in the space of ground states, we can determine which sector we are in by measuring this quantity for a single plaquette. Consider a plaquette p, with state $|\mu_p\rangle = \sqrt{\frac{1}{|E|}} \sum_{e_p\in E} \mu_p(e_p)|e_p\rangle$. Now consider applying a single-plaquette multiplication operator $M^e(p)$ to this plaquette, which just multiplies the group label of the plaquette by e. Then we have

$$\begin{aligned} M^e(p)|\mu_p\rangle &= \sqrt{\frac{1}{|E|}} \sum_{e_p\in E} \mu_p(e_p)|ee_p\rangle \\ &= \sqrt{\frac{1}{|E|}} \sum_{e'_p=ee_p\in E} \mu_p(e^{-1}e'_p)|e'_p\rangle \\ &= \sqrt{\frac{1}{|E|}} \sum_{e'_p\in E} \mu_p(e^{-1})\mu_p(e'_p)|e'_p\rangle \\ &= \mu_p(e^{-1})|\mu_p\rangle, \end{aligned}$$

so that the result is the accumulation of a phase $\mu_p(e^{-1})$. Then for each irrep ν of the kernel of ∂ we can construct an operator

$$P^\nu = \frac{1}{|\ker(\partial)|} \sum_{e\in\ker(\partial)} \nu(e)M^e(p).$$

Applying this operator to the state $|\mu_p\rangle$ gives us

$$\begin{aligned} P^\nu|\mu_p\rangle &= \frac{1}{|\ker(\partial)|} \sum_{e\in\ker(\partial)} \nu(e)M^e(p)|\mu_p\rangle \\ &= \frac{1}{|\ker(\partial)|} \sum_{e\in\ker(\partial)} \nu(e)\mu_p(e^{-1})|\mu_p\rangle \\ &= \frac{1}{|\ker(\partial)|} \sum_{e\in\ker(\partial)} \nu(e)\mu_p(e)^*|\mu_p\rangle. \end{aligned}$$

From μ_p we can define an irrep $\mu_p^{\ker}$ of $\ker(\partial)$ by restricting μ_p to the kernel of ∂, so that $\mu_p^{\ker}(e) = \mu_p(e)$ for e in the kernel of ∂. We can therefore apply the grand orthogonality theorem to write

$$\frac{1}{|\ker(\partial)|}\sum_{e\in\ker(\partial)} \nu(e)\mu_p(e)^* = \delta\big(\nu, \mu_p^{\ker}\big),$$

so that

$$P^\nu|\mu_p\rangle = \delta\big(\nu, \mu_p^{\ker}\big)|\mu_p\rangle.$$

That is, the operator P^ν projects onto states for which the plaquette p is labeled by irreps of E that restrict to the irrep ν of the kernel. We saw earlier that we can construct a basis for the ground states that is labeled by these irreps for the kernel, so that each plaquette in the ground state has the same restriction to the kernel. This means that, when applied in the space of ground states, the projection operator P^ν projects onto the ground state sector labeled by the irrep ν of the kernel of ∂.

In this section we have demonstrated that the (2+1)D higher-lattice gauge theory model possesses a global symmetry when $\triangleright$ is trivial, indicating that it describes some kind of symmetry-enriched topological (SET) phase. It is therefore interesting to relate this model to other constructions for SET phases. In the following section we will do exactly this for one such construction, known as symmetry-enriched string nets.

VIII. MAPPING THE (2+1)D HIGHER-LATTICE GAUGE THEORY MODEL TO THE SYMMETRY-ENRICHED STRING-NET CONSTRUCTION

A. Symmetry-enriched string nets

The higher-lattice gauge theory model in (2+1)D can be considered as a generalization of Kitaev's quantum double model [37]. It is known that Kitaev's quantum double model can be mapped to a subset of another class of models for topological phases, known as the string-net models [49]. In the same way, we can map the $\triangleright$ trivial (2+1)D higher-lattice gauge theory model to a subset of a class of string-net-like models, known as symmetry-enriched string nets [16]. In order to explain this connection, we will first give a summary of the symmetry-enriched string-net models from Ref. [16].

The symmetry-enriched string-net model is considered on a honeycomb lattice (though it can be generalized to any trivalent lattice) [16]. The plaquettes of the lattice are labeled by group elements in some group H. The (directed) edges of the lattice are labeled by objects in an H *extension* of a *unitary fusion category* $\mathcal{C}$. For the purposes of this work, we can just consider a fusion category as a collection of objects with some fusion rules that describe how we can combine them. For example, given two objects a and b, which can fuse to objects c or d, we write $a \times b = c + d$. More generally, we write that $a \times b = \sum_c N_{ab}^c c$, where N_{ab}^c are called fusion multiplicities. There must also be an identity (or vacuum) object which fuses trivially with the other objects. A familiar example of a category is the collection of representations of some finite group X, where the simple objects are the irreps of the group. These irreps can be fused (by considering a tensor product of the matrices from each representation) and the result of this fusion can be decomposed into a sum of irreps. There are other important components for a fusion category, such as the so-called F matrices, which encode associativity relations on the fusion of multiple objects [16]. These are important for the explicit construction of string-net models [30], but we will not need to consider them in detail here.

Given a unitary fusion category $\mathcal{C}$, an H extension of that category is another fusion category $\mathcal{D}$ which contains $\mathcal{C}$ and which has a property known as H grading [16]. Each object of the new category $\mathcal{D}$ is associated to a group element $h \in H$. This divides the category into parts $\mathcal{D}_h$ such that $\mathcal{D} = \oplus_{h\in H}\mathcal{D}_h$, with each part satisfying $\mathcal{D}_x \times \mathcal{D}_y \subset \mathcal{D}_{xy}$. That is, given an object in $\mathcal{D}_x$ and an object in $\mathcal{D}_y$, their fusion products must be in $\mathcal{D}_{xy}$. Furthermore, the part of $\mathcal{D}$ corresponding to the identity element of H is $\mathcal{C}$, so that $\mathcal{D}_{1_H} = \mathcal{C}$ [16].

Now that we have considered the objects labeling the directed edges (objects in the category $\mathcal{D}$) and plaquettes (elements of the symmetry group H) of the honeycomb lattice, we must consider the Hamiltonian. The Hamiltonian is a sum of commuting projector operators, where we have operators for the vertices, edges, and plaquettes of the model, just as we do in the higher-lattice gauge theory model. The Hamiltonian is then given by [16]

$$H = -\sum_{\text{vertices } v} Q_v - \sum_{\text{edges } l} P_l - \sum_{\text{plaquettes } p} B_p, \qquad (56)$$

where we will now define each of these terms. The first operator Q_v is associated to a vertex v of the lattice, and projects onto states where the three edges adjacent to that vertex obey the fusion rules (so if two edges go into the vertex and one comes out, the labels of the two incoming edges must fuse to the label of the outgoing edge) [16].

The operator P_l, acting on an edge l, checks that the labels of the two plaquettes separated by that edge "agree" with the label of the edge, in the following sense [16]. The edge is labeled by an object s in $\mathcal{D}$. This object is associated to a group element h_s such that $s \in \mathcal{D}_{h_s}$. Then the operator P_l projects onto the case where the group elements of the plaquettes on either side of the link differ by multiplication by this element h_s. For example, in the situation shown in Fig. 48, where we have an edge l bordered by plaquette p and p', the projector P_l is one if $h_{p'}^{-1}h_p = h_s$ and zero otherwise. Which plaquette should play the role of p' in this expression is determined by the orientation of the edge: when the edge is rotated by 90° anticlockwise it should point from p to p'.

Finally, consider the plaquette term B_p. This is made of a sum of terms corresponding to the different object types in the category $\mathcal{D}$. We have

$$B_p = \sum_{s\in\mathcal{D}} a_s B_p^s \tilde{U}_p^{h_s}.$$

Here B_p^s acts by fusing a closed string of object s into the edges of plaquette p, while $\tilde{U}_p^{h_s}$ right multiplies the plaquette label h_p by h_s, where h_s is the group label associated to object s. We have described B_p^s qualitatively here, but it is the same as the string-net term B_p^s from Ref. [30], for those familiar with the string-net model.

While the input to the symmetry-enriched string-net model is an H extension of a category $\mathcal{C}$, the output topological phase

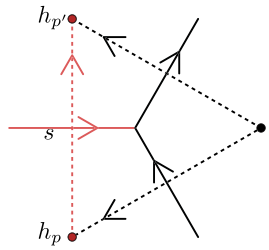

FIG. 48. In this diagram, adapted from Fig. 9 of Ref. [16], we consider the energy term associated to the edges of the lattice in the symmetry-enriched string-net model. Each edge (solid arrows in this figure) separates two plaquettes (whose centers are represented by the dots). Then the edge can be associated to an edge in the dual lattice by rotating it 90° anticlockwise (obtaining the dashed arrows which connect the plaquettes). The edge term then checks that the plaquette labels at the two ends of the dual edge differ by a label h_s, where s is the label of the edge and h_s is the group element associated to that label. For example, considering the red edge (labeled by s), the adjacent plaquettes p and p' are labeled by h_p and $h_{p'}$, respectively. The dual edge corresponding to the red edge (the red dashed arrow) points from p to p' and so the edge term gives one if $h_{p'}^{-1}h_p = h_s$ and zero otherwise.

is described by a braided H-crossed extension of $\mathcal{Z}(\mathcal{C})$ [16], where $\mathcal{Z}(\mathcal{C})$ is the Drinfeld center of (C) (i.e., the output from a standard string-net model). This category describes the fusion and braiding statistics of the topological excitations of the model, while the symmetry group is given by H.

B. Mapping from the higher-lattice gauge theory model

We will now consider how we can map from the higher-lattice gauge theory model in (2+1)D (with $\triangleright$ trivial) to these symmetry-enriched string-net models. In Sec. VII, we took the (2+1)D higher-lattice gauge theory model in the case where $\triangleright$ is trivial, and we expressed each energy term in a new basis. In this new basis, each edge and plaquette is labeled by an irreducible representation (and matrix indices, for non-Abelian groups) of G and E, respectively. In this section we will show that we can use this basis to relate the higher-lattice gauge theory models (with $\triangleright$ trivial) to the symmetry-enriched string-net models. To do so, we consider placing the higher-lattice gauge theory model on a honeycomb lattice, so that it is on the same lattice as the symmetry-enriched string-net model. However, there is still some difference in the decoration of the lattice in the two cases. In the higher-lattice gauge theory model, the plaquettes have an orientation, whereas they do not in the symmetry-enriched string-net model. In order to address this, we simply choose all plaquettes to have the same orientation (clockwise) for the higher-lattice gauge theory model.

Having fixed the lattice, we now consider the labels of the edges and plaquettes in the two models. In the higher-lattice gauge theory model, the edges and plaquettes are typically labeled by elements of the two groups G and E, respectively. However, in the irrep basis introduced in Sec. VII, the edges of this lattice are labeled by irreps of G (and their matrix indices), while the plaquettes are labeled by irreps of E. Because E is Abelian, the irreps of E are 1D and form a group. We claim that this group of irreps corresponds to the symmetry group H whose elements label the plaquettes in the symmetry-enriched string-net model. On the other hand, the labels of the edges are given by irreps of G and their matrix indices in our irrep basis for the higher-lattice gauge theory model, while the edges in the symmetry-enriched string-net model are labeled by objects in a fusion category. The irreps of a group form a fusion category and we claim that this is the category $\mathcal{D}$ whose objects label the edges in the symmetry-enriched string-net model. We note that this identification is the same as the one used in Ref. [49], where Kitaev's quantum double was mapped to the (nonenriched) string nets. The mapping between the edge labels is the same whether we are considering a map from the quantum double model to the string-net model or a map from the higher-lattice gauge theory model to the symmetry-enriched string-net model. This is because when we omit the plaquette labels (by making the labels belong to the trivial group), the symmetry-enriched string-net model becomes an ordinary string-net model and the higher-lattice gauge theory model becomes Kitaev's quantum double model.

One subtlety with the identification of the edge labels in the two models is that, in the irrep basis of the higher-lattice gauge theory model, the edges are not only labeled by the irreps, which are the objects of $\mathcal{D}$, but also the matrix indices for those irreps (when G is non-Abelian). As described in Ref. [49], the matrix indices of the edges in Kitaev's quantum double model, and so in the higher-lattice gauge theory model, can be associated to the vertices at the two ends of the edge. These additional degrees of freedom are fixed when the vertex terms are applied, with the indices being contracted to ensure appropriate fusion [49]. This means that, even if the two models have different Hilbert spaces when G is non-Abelian, the ground states of the models are equivalent.

So far, we have only considered the labels of the edges in the symmetry-enriched string-net model as belonging to a fusion category. However, the category $\mathcal{D}$ whose objects label the edges in the symmetry-enriched string-net model has additional structure, which is important for further discussion of the mapping. That is, $\mathcal{D}$ is an H extension of another category $\mathcal{C}$, where H is the group whose elements label the plaquettes. This means that each object s in $\mathcal{D}$ is associated with a group element h_s, and the objects in $\mathcal{D}$ that correspond to the identity of H are the objects of $\mathcal{C}$, as discussed in Sec. VIII A (and in more detail in Ref. [16]). How is this reflected in the higher-lattice gauge theory model? We have identified $\mathcal{D}$ as Rep(G), the category formed from the irreps of G. Given an irrep R of G, it is associated to a 1D irrep $R_\partial^{\text{irr.}}$ of the subgroup $\partial(E)$, where $R_\partial^{\text{irr.}}(\partial(e)) = [D^R(\partial(e))]_{11}$, as we described in Sec. VII when we first considered the irrep basis. This irrep $R_\partial^{\text{irr.}}$ is in turn associated to an irrep μ^R of E, satisfying $R_\partial^{\text{irr.}}(\partial(e)) = \mu^R(e)$. This is the irrep of E that we called the defect label of R in Sec. VI B 2. We claim that this irrep μ^R is the group element associated to the object R (recall that we have identified the symmetry group H from the symmetry-enriched string-net model with the group formed by the irreps of E). That is, if R is the object s of $\mathcal{D}$, then μ^R is the group element h_s of H associated to that object. In particular, this means that the objects of $\mathcal{C} = \mathcal{D}_{1_H}$ are the irreps with trivial restriction to $\partial(E)$, which are equivalent to

TABLE V. The group $\mathbb{Z}_4$ has four irreps, which are one dimensional. In each row, we give the phase representing each group element for a particular irrep (which is equivalently the character for that irrep).

	1_G	i_G	-1_G	$-i_G$
1_R	1	1	1	1
-1_R	1	-1	1	-1
i_R	1	i	-1	$-i$
$-i_R$	1	$-i$	-1	i

irreps of the quotient group $G/\partial(E)$ [note that $\partial(E)$ is central in G for $\triangleright$ trivial].

There is a small subtletly in that, while μ^R is an irrep of E, it is not a generic irrep of E. This is because it is only sensitive to $\partial(e)$ and not to e itself, which means that it acts trivially on the kernel of ∂. This means that some of the group elements $h \in H$ (which are irreps of E), specifically the irreps of E with a nontrivial restriction to the kernel, cannot be written as $h = \mu^R$ for some irrep R of G and so have no objects associated to them. This means that some of the parts $\mathcal{D}_h$ of the graded category $\mathcal{D}$ are empty. Reference [16] specifically does not study cases with such empty parts of the graded category, and so for the sake of this mapping we will restrict to the case where the kernel of ∂ is trivial from here on [so that E and $\partial(E)$ are isomorphic]. From Sec. VII, we know that the different ground states of the sphere are labeled by the irreps of the kernel, and so under this restriction we will not have degenerate ground states on the sphere (we do not have spontaneous symmetry breaking).

Before we compare the Hamiltonians of the two models, we introduce a simple example to help describe the identification of the objects in the two models, which we will use throughout this section to explain features of the mapping. Consider the crossed module $(G = \mathbb{Z}_4, E = \mathbb{Z}_2, \partial \to \mathbb{Z}_2, \triangleright \to \mathrm{id})$, where ∂ maps the elements of $E = \mathbb{Z}_2$ to the $\mathbb{Z}_2$ subgroup of $\mathbb{Z}_4$. If we write the elements of G as 1_G, i_G, -1_G, and $-i_G$, and the elements of E as 1_E and -1_E, then we have $\partial(1_E) = 1_G$ and $\partial(-1_E) = -1_G$, which is a group homomorphism as required. This crossed module (as required) obeys the Peiffer condition (1) because for any $g \in G$ and $e \in E$, $\partial(g \triangleright e) = \partial(e)$ from $\triangleright$ being trivial, and $\partial(e) = g\partial(e)g^{-1}$ because of the Abelian nature of G, so that $\partial(g \triangleright e) = g\partial(e)g^{-1}$. It also obeys the second Peiffer condition, Eq. (2), because for any pair $e, f \in E$ we have $\partial(e) \triangleright f = f$ from $\triangleright$ being trivial, and $f = efe^{-1}$ from E being Abelian, so that $\partial(e) \triangleright f = efe^{-1}$.

Having satisfied ourselves that $(G = \mathbb{Z}_4, E = \mathbb{Z}_2, \partial \to \mathbb{Z}_2, \triangleright \to \mathrm{id})$ is indeed a valid crossed module, we can find the corresponding symmetry-enriched string-net model. The category $\mathcal{D}$ of this string-net model is given by $\mathrm{Rep}(G = \mathbb{Z}_4)$, whose objects are the four (unitary) irreps of $\mathbb{Z}_4$, which we describe in Table V below. Meanwhile, the symmetry group H of the symmetry-enriched string net is the group of irreps of E, i.e., the irreps of $\mathbb{Z}_2$, where multiplication for this group is defined by $(\alpha_1\alpha_2)(e) = \alpha_1(e)\alpha_2(e)$ for any two irreps α_1, α_2. The resulting group is itself a copy of $\mathbb{Z}_2$. As described in Sec. VIII A, in the symmetry-enriched string-net model each object from the category is associated to an element of this symmetry group (the category has a G grading). The group element associated to an irrep of G (which is an object in the category) is the irrep of E obtained by restricting that irrep of G to the subgroup $\partial(E)$ of G [note that for the mapping we restrict to cases where $\partial(E)$ is isomorphic to E]. Considering the irreps of $\mathbb{Z}_4$, as defined in Table V, we see that the irreps 1_R and -1_R of $G = \mathbb{Z}_4$ restrict to the trivial irrep of $\mathbb{Z}_2 = \partial(E)$ [because $\pm 1_R(1_G) = \pm 1_R(-1_G) = 1$]. This means that these two irreps belong to $\mathcal{D}_{1_H}$, the part of $\mathcal{D}$ associated to the identity element of the symmetry group. On the other hand, the irreps $\pm i_R$ restrict to the nontrivial irrep of the $\mathbb{Z}_2$ subgroup [because $\pm i_R(1_G) = 1$ and $\pm i_R(-1_G) = -1$], and so belong to the other part of the category $\mathcal{D}_{-1_H}$, associated to the nontrivial symmetry element.

Next we wish to compare the Hamiltonians of the two models. We will show that the energy terms of the higher-lattice gauge theory model are equivalent, in the irrep basis, to those of the symmetry-enriched string-net model. First, we consider the vertex terms. In Sec. VII we showed that the vertex term acts on neighboring edges in the irrep basis by checking that the irreps fuse to the identity (if all of the edges point towards the vertex). This is equivalent to the term Q_v from the symmetry-enriched string-net model [16], which checks that the edges around the vertex obey fusion rules (so that if they all point inwards, they fuse to the identity). This is explained in more detail in Ref. [49] for the mapping between Kitaev's quantum double model and the string-net model (the vertex terms for the quantum double model are the same as those for higher-lattice gauge theory when $\triangleright$ is trivial, and similarly the vertex terms for the string-net model are the same as those for the symmetry-enriched string-net model, so the mapping works the same in either case). In the case of the example model, where the group $G = \mathbb{Z}_4$ is Abelian, this term is simple because fusion of two irreps R_1 and R_2 is just given by multiplication of the irreps defined by $(R_1R_2)(g) = R_1(g)R_2(g)$ (note that the irreps form a group under this multiplication). Therefore, the vertex term just checks that the irreps (which are the natural labels for the edges in the symmetry-enriched string-net model, and which become the labels of the edges in the higher-lattice gauge theory model after a change of basis) multiply to give the identity irrep.

The second energy term to consider is the edge term. In the symmetry-enriched string-net model, the edge term checks that the two plaquettes separated by that edge have labels that agree with the edge label. If the two plaquettes p and p' have labels h_p and $h_{p'}$, while the edge l has label s_l, then the energy term P_l gives zero if $h_{p'}^{-1}h_p = h_{s_l}$ (where if we rotate the edge 90° anticlockwise, it points from p to p' as shown in Fig. 48). In Sec. VII we saw that the edge term in the higher-lattice gauge theory model in the irrep basis enforces that, for two plaquettes 1 and 2, labeled by irreps μ_1 and μ_2, that are separated by an edge l with label R_l, the labels satisfy $\mu^{R_l}\mu_1 = \mu_2$. Here plaquette 1 is the plaquette to the left of the edge and plaquette 2 is to the right (with respect to the orientation of the edge, as shown in Fig. 49). This is equivalent to saying that if we rotate the edge by 90° anticlockwise, it points from plaquette 2 to plaquette 1. That is, in the language

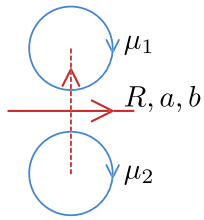

FIG. 49. For the higher-lattice gauge theory model in the irrep basis, the vertex term applied on the (red) edge enforces that the labels of the two adjacent plaquettes differ by an irrep μ^R, where R is the irrep of G labeling the edge and μ^R is an irrep of E derived from R. This has the same form as the edge term in the symmetry-enriched string-net model, once we identify R with an object of the category $\mathcal{D}$ and μ^R with the associated element of the symmetry group.

of the string-net model, plaquette 1 is p' and plaquette 2 is p. This means that the condition $\mu^{R_l}\mu_1 = \mu_2$, which can also be written as $\mu^{R_l} = \mu_1^{-1}\mu_2$ (using the fact that the group of 1D irreps is Abelian to swap the order of multiplication), is equivalent to the $h_{s_l} = h_{p'}^{-1}h_p$ condition from the symmetry-enriched string-net model. μ^{R_l} is the irrep of E associated to irrep R_l of G in the same way that h_{s_l} is the group element of H associated to object s_l in the symmetry-enriched string-net model. Therefore, the edge terms are the same in the two models.

To understand this better, consider our example model. In this simple model, the plaquettes have two basis states, described by the identity irrep and the nontrivial irrep of $\mathbb{Z}_2$. Then we can distinguish between two types of edge: ones where the plaquette label changes across the edge (i.e., the two plaquettes on either side of the edge have different labels) and ones where it stays the same. The two situations allow different edge labels when the edge term is satisfied. If the plaquette label changes across the edge, then the edge term tells us that the edge label must correspond to the nontrivial element of the symmetry group, i.e., the nontrivial irrep of $\mathbb{Z}_2$, in order to satisfy $\mu^{R_l}\mu_1 = \mu_2$. From our previous discussion, we know that the irreps of $G = \mathbb{Z}_4$ corresponding to this nontrivial irrep of $\mathbb{Z}_2$ are $\pm i_R$. Therefore, the edge labels that can separate two different plaquette labels are $\pm i_R$. On the other hand, if the plaquette label does not change across the edge, then the edge must correspond to a trivial irrep of $\mathbb{Z}_2$ (μ^{R_l} must be the trivial irrep), so the edge must be labeled by one of the irreps $\pm 1_R$ of $G = \mathbb{Z}_4$. In the general case, where the plaquette label can take more than two values, we have different kinds of transition of the plaquette label across the edge, and these must be consistent with the label of the edge, as described earlier.

The final energy term to consider is the plaquette term. In the symmetry-enriched string-net model, the plaquette term B_p is given by

$$B_p = \sum_{s\in\mathcal{D}} a_s \tilde{B}_p^s \tilde{U}_p^{h_s},$$

where $\tilde{B}_p^s$ is the same as the plaquette term from the ordinary string-net model (it acts by fusing a string of label s around the plaquette) and $\tilde{U}_p^{h_s}$ right multiplies the plaquette label by h_s. Note that we have added a tilde to $\tilde{B}_p^s$ in order to differentiate it from a similar operator in the higher-lattice gauge theory model. For the class of these symmetry-enriched string-net models that we are mapping to, the objects are irreps of the group G. We can therefore write the plaquette term in these cases as

$$B_p = \sum_{\text{irreps } R \text{ of } G} a_R \tilde{B}_p^R \tilde{U}_p^{h_R}.$$

As we saw in Sec. VII, we can write the plaquette term for the higher-lattice gauge theory model as

$$B_p = \sum_{\text{irreps } R \text{ of } G} \frac{|R|}{|G|} B_p^R,$$

where the effect of B_p^R is to fuse the irrep R into the edges of the plaquette and also to multiply the plaquette label by μ^R. This action on the edges is the same as the action of the plaquette term in Kitaev's quantum double model and therefore the same as the action of the ordinary string-net plaquette term $\tilde{B}_p^s$ (as indicated by the mapping discussed in Ref. [49]). As noted in Ref. [49] for the mapping from the quantum double model to the string-net model, there is a subtlety in that the plaquette term in the string-net model is ill defined if the fusion rules are not satisfied at adjacent vertices, and is typically chosen to be zero, whereas for the quantum double model the plaquette terms are always well defined. However, this does not affect the ground state because the fusion rules are satisfied in the ground state. The same thing is true for the mapping from the higher-lattice gauge theory model to the symmetry-enriched string-net models.

In addition to the plaquette terms from the two models acting the same on the edges, the plaquette terms also have equivalent action on the plaquettes. The plaquette transform B_p^R multiplies the plaquette term by μ^R, while the $\tilde{U}_p^{h_R}$ term from the symmetry-enriched string-net model multiplies the plaquette label by h_R. As we established earlier, the group element h_R associated to object R is μ^R, so these are the same. When we include the action on both the edges and the plaquettes, we see that the operator B_p^R from the higher-lattice gauge theory model is equivalent to $\tilde{B}_p^R\tilde{U}_p^{h_R}$ from the symmetry-enriched string-net model. Therefore, the plaquette term of the higher-lattice gauge theory model maps onto the plaquette term of the symmetry-enriched string-net model when we take $a_R = |R|/|G|$. While these coefficients a_R can be chosen freely to define different string-net models [30], they are usually taken to be $a_R = d_R/D^2$, where d_R is the so-called quantum dimension of R and D^2 is the sum of the squared quantum dimensions of all of the objects: $D^2 = \sum_{s\in\mathcal{D}} d_s^2$. This choice of coefficients ensures that the string-net model is associated to a topological phase with a smooth continuum limit and that the energy terms are projectors [30]. Indeed, these coefficients were used in Ref. [16] for the symmetry-enriched string-net construction. We should therefore check that these coefficients also agree between the symmetry-enriched string-net model and the higher-lattice gauge theory model. Identifying the quantum dimension of irrep R as $|R|$ [49], the total quantum dimension is given by $D^2 = \sum_{\text{irrep } R} |R|^2 = |G|$. This means that $d_R/D^2 = |R|/|G|$. Therefore, the coefficients a_R for which the two plaquette terms match are the standard coefficients used for string-net models. Combining this with our results

for the other energy terms, we see that all of the energy terms match between the two models.

Now let us consider the plaquette term in our simple example model. In this case the plaquette term involves a sum over the four irreps of $G = \mathbb{Z}_4$. Because these irreps are all one dimensional, the coefficient $a_R = |R|/|G|$ for these irreps is equal to $\frac{1}{4}$. Writing the plaquette term with the symmetry-enriched string-net notation, we have

$$B_p = \frac{1}{4} \sum_{\text{irreps } R \text{ of } G} \tilde{B}_p^R \tilde{U}_p^{h_R},$$

where h_R is the symmetry element associated to the irrep (or object, in the string-net language) R. Knowing that the irreps $\pm 1_R$ are associated to the identity element of the symmetry group, which we denote by 1_H, while the irreps $\pm i_R$ are associated to the nontrivial element, which we denote by -1_H, the plaquette term can be written as

$$B_p = \tfrac{1}{4}\big(\tilde{B}_p^{1_R} + \tilde{B}_p^{-1_R}\big)\tilde{U}_p^{1_H} + \tfrac{1}{4}\big(\tilde{B}_p^{i_R} + \tilde{B}_p^{-i_R}\big)\tilde{U}_p^{-1_H}.$$

Noting that the action of $\tilde{U}_p^{h_R}$ is to multiply the plaquette label by h_R, we can see that $\tilde{U}_p^{1_H}$ is just the identity operator. Furthermore, $\tilde{B}_p^{1_R}$ just fuses the vacuum string around the plaquette, so this is also the identity operator. This allows us to simplify our expression for the plaquette term to

$$B_p = \tfrac{1}{4}\big(1 + \tilde{B}_p^{-1_R}\big) + \tfrac{1}{4}\big(\tilde{B}_p^{i_R} + \tilde{B}_p^{-i_R}\big)\tilde{U}_p^{-1_H}.$$

By using the understanding of the ground state that we gained by examining the edge terms, we can see why the plaquette term requires the additional action of $\tilde{U}_p^{h_R}$ on the plaquette label itself when compared to the ordinary string-net model. The edge term enforces that a string of label 1_R or -1_R must separate plaquettes with the same symmetry label, while a string of label $\pm i_R$ must separate plaquettes with different labels. If we were to fuse a string of label $\pm i_R$ around a plaquette without changing the plaquette label itself, this would violate that rule. For example, if the plaquette was originally surrounded by a single string of label 1_R, its label must agree with all of the surrounding plaquettes' labels. But then when we fuse a string of label i_R around the plaquette, the edge terms then require that the plaquette label must disagree with the surrounding plaquettes. In order to satisfy this rule, when we fuse the string around the plaquette we must also change the label of the plaquette.

We have therefore shown that there is an equivalence between a subset of the higher-lattice gauge theory models and a subset of the symmetry-enriched string-net models. Specifically, we considered a higher-lattice gauge theory model described by the crossed module $(G, E, \partial, \triangleright)$, where $\triangleright$ is trivial ($g \triangleright e = e$ for all $g \in G$ and $e \in E$) and $\ker(\partial)$ is just the identity element 1_E. We saw that such a model is equivalent to the symmetry-enriched string-net model labeled by a group $H = \mathrm{Rep}(E)$ and an H-graded fusion category $\mathrm{Rep}(G)$. This means that the topological phase described by the two models is the same, allowing us to identify the SET phase realized by the higher-lattice gauge theory model as described by a braided $\mathrm{Rep}(E)$-crossed extension of $\mathcal{Z}[\mathrm{Rep}(\mathcal{G}/\partial(\mathcal{E}))]$. While we assumed that E and $\partial(E)$ were isomorphic for this mapping, the fact that a nontrivial $\ker(\partial)$ introduces spontaneous symmetry breaking described by irreps of the kernel (as we discussed in Sec. VII) suggests that a similar result holds for nontrivial $\ker(\partial)$, but with $H = \mathrm{Rep}[E/\ker(\partial)]$ as the unbroken part of the symmetry instead of the full symmetry [note that the properties of the electric and magnetic excitations are unaffected by changing E while keeping $\partial(E)$ fixed].

We can also use this correspondence between Hamiltonians to identify features in the two models. For example, in the higher-lattice gauge theory model we know that we obtain looplike excitations labeled by irreps of E. However, we also know that these looplike excitations are equivalent to confined electric excitations (at least, in the absence of other excitations) if the irrep labeling them is not sensitive to the kernel of E. Because we took the kernel of ∂ to be trivial when we mapped to the symmetry-enriched string-net model, this means that all of these looplike excitations are of this type. We therefore expect the presence of confined excitations in the symmetry-enriched string-net models, but not uncondensed loop excitations (which correspond to domain walls between different ground states). In the higher-lattice gauge theory model, the confined electric excitations are labeled by irreps of G which have nontrivial restriction to $\partial(E)$. In the language of the symmetry-enriched string-net models, the confined electric excitations should be those whose label is associated to a nontrivial group element of H, meaning those labeled by objects that are not in the category $\mathcal{C}$ of which $\mathcal{D}$ is a group extension. We expect this to hold outside of the small subset of symmetry-enriched string nets that we can map to directly. This is because in Ref. [16] it is stated that the anyonic excitations are the same as those produced by an ordinary string-net model with $\mathcal{C}$ as an input category, and so any extra excitations (such as the extra electric excitations we find in the higher-lattice gauge theory model) must be either confined or condensed.

As an example of the confined and condensed excitations, consider the simple model $(\mathbb{Z}_4, \mathbb{Z}_2, \partial, \triangleright \to \mathrm{id})$ we have been looking at throughout this section. From our general results for higher-lattice gauge theory models (see Sec. III), we know that there are four electric ribbon operators labeled by the different irreps of $G = \mathbb{Z}_4$. However, the excitations produced by the ribbon operators labeled by irreps with nontrivial restriction to the image of ∂, i.e., to the $\mathbb{Z}_2$ subgroup of $\mathbb{Z}_4$, are confined. Therefore, the excitations labeled by the irreps $\pm i_R$ are confined. These are the same irreps that are associated to the nontrivial symmetry group element (the nontrivial irrep of E), as we expect from the general discussion above. This just leaves the ribbon operators labeled by the irreps 1_R and -1_R, of which the one labeled by 1_R is the trivial operator. We also know that there are four purely magnetic ribbon operators, labeled by the group elements of $G = \mathbb{Z}_4$, but the operators labeled by elements in $\partial(E)$ correspond to condensed excitations. The ribbon operator labeled by the identity element is always trivial, but we also see that the excitation labeled by -1_G is condensed (which also means that the two remaining magnetic excitations belong to the same topological sector). These confined electric and condensed magnetic excitations (and excitations built from fusion with them) would not be counted towards the excitations described in Ref. [16] because the authors of that work were only interested in distinct types of (unconfined) anyons. This leaves us with only one unconfined electric excitation and one distinct magnetic excitation,

along with their fusion product and the trivial charge. These are the same excitations we would expect for the toric code. This matches the prediction from Ref. [16] because the category $\mathcal{C}$ of objects with trivial symmetry group label contains the irreps 1_R and -1_R, and so the excitations should be the same as those from the $C = \mathrm{Rep}(\mathbb{Z}_2)$ string-net model (which is the toric code).

Another important feature in both models is the presence of a symmetry. In Sec. VII, we saw that the higher-lattice gauge theory model (with $\triangleright$ trivial) has a symmetry under multiplying each plaquette label (in the irrep basis) by an irrep ν of E. This is equivalent to the symmetry of the symmetry-enriched string-net models of Ref. [16] under multiplication of each plaquette label by a group element h of H. This symmetry exists for all of the symmetry-enriched string-net models, not just the ones we can map to from the higher-lattice gauge theory model. In the symmetry-enriched string-net model, this symmetry can permute the excitation types (for instance, an example is given in Ref. [16] where the symmetry swaps between the electric and magnetic excitations of the toric code). In the case of the higher-lattice gauge theory models, however, the ribbon operators that produce the electric and magnetic excitations do not act on the plaquette labels and so these excitations are not affected by the symmetry.

IX. TOPOLOGICAL CHARGE FROM CLOSED RIBBON OPERATORS WHEN $\triangleright$ IS TRIVIAL

Now that we have looked at the excitations and their properties, it will be useful to discuss the conserved topological charge carried by the excitations in more detail, particularly to illustrate the ideas of confinement and condensation. The topological charge contained in a region of the lattice cannot be changed, except by moving some charge into or out of the region by using an operator that connects the interior and exterior of the region. That is, the charge cannot be changed by any local operator, where by local we here mean an operator entirely contained within the region. This means that any operator that changes the topological charge within a region will move charge through the boundary of that region and so can be detected by an operator on the boundary of the region. Indeed, the topological charge within a region can be measured by an operator on the boundary of the region. Because the topological charge is conserved in this sense, rather than being conserved by the action of the Hamiltonian, the charges are really properties of the Hilbert space. However, the Hamiltonian determines which particular set of charges are relevant for the particular model. The ground state acts as the topological vacuum for that set of charges, meaning that the ground state has trivial topological charge in all regions. This enforces additional properties for the topological charge realized by the topological model. First, smoothly deforming the boundary within which we measure the charge should not change the value of charge measured, as long as the boundary does not cross any excitations in doing so (thereby including or excluding additional excitations in or from the region of interest). This is because deforming the surface will just include more or less of the vacuum, which has trivial topological charge. Second, the Hamiltonian does not produce or move excitations, so we require that the topological charge within a surface be conserved under the action of the Hamiltonian. In addition to these properties, we require some way to combine the charge in two regions to get a total topological charge, in order to reproduce the fusion rules of anyon theories.

Given these properties, we look for measurement operators that would detect such a charge. Following Ref. [36], we wish to construct these operators from the ribbon operators of our model. The ribbon operators (apart from the confined ones) have many of the properties that we require. They can freely be deformed, provided that we leave the end points fixed. Furthermore, the ribbon operators form a complete set of operators, once we also include the E-valued membrane operators and single-plaquette multiplication operators. To see this, note that we can apply each operator on a single edge or plaquette by choosing the associated ribbon or membrane appropriately. The electric ribbon operator then measures the value of an edge, while the magnetic operator allows us to multiply an edge by any element of G. Combining these therefore allows us to freely measure and control the state of an individual edge. Similarly, the E-valued membrane operator allows us to measure the state of an individual plaquette and the single-plaquette multiplication operator allows us to multiply the plaquette label by any element of E. To produce any operator, we can use the measurement operators on every edge and plaquette to fix which state in our Hilbert space we act on and then use the other operators to control the action on that state. Then summing over each possible state in our Hilbert space with a different action for each state will give us a general operator. We can therefore create any operator as a combination of ribbon and membrane operators (along with the single-plaquette multiplication operators). However, the ribbon operators will generally produce excitations, with only closed ribbon operators potentially producing no excitations. Therefore, we must restrict to operators that can be produced by combining closed ribbon operators (and single-plaquette multiplication operators or E-valued membrane operators, although these correspond to the symmetry content of the theory and we will only use these operators in a limited way, as we describe later). Some of the closed ribbon operators do still produce excitations where they join onto themselves (i.e., at the start of the ribbon, which is also the end), and so we must further restrict to closed ribbon operators that do not create such excitations. This is required to make operators that simply measure the topological charge, without moving said charge. These closed ribbon operators will then form an algebra, from which we can produce our charge measurement operators.

In order to produce the charge measurement operators, we first choose a region whose topological charge we want to measure. We then consider applying a general electric and magnetic closed ribbon operator around the boundary of that surface. We choose the labels of these ribbon operators, and take linear combinations of them, to ensure that this closed ribbon operator does not produce any excitations. As we will see later, we may also need to apply a single-plaquette multiplication operator to ensure that the magnetic ribbon operator does not produce an excitation at the start (which is also the end) of the ribbon. Apart from this, we do not use any single-plaquette multiplication operators or E-valued membrane operators. This is because these operators either

correspond to the symmetry content of the model, or are related to condensed versions of the ribbon operators. The single-plaquette measurement operators in the kernel of ∂ distinguish between the symmetry-related ground states, while the E-valued membrane operators locally perform the symmetry transformation, as we discussed in Sec. VII. Therefore, we regard two valid measurement operators that differ only by these operators as equivalent when considering the topological content of the model.

For the higher-lattice gauge theory models with $\triangleright$ trivial, we can construct the charge measurement operators explicitly. These charge measurement operators will be useful for considering condensation and confinement. During condensation, a charge from the original uncondensed model joins the ground state of the new model (after condensation). Therefore, the expectation value of the charge measurement operator of the old model should be nonzero when applied to the ground state of the new model [36]. Because of this fact, it is useful to first construct the charge measurement operators in the uncondensed higher-lattice gauge theory models. We explained in Sec. III E that, given a model described by the crossed module $(G, E, \partial, \triangleright \to \mathrm{id})$, we can construct another crossed module $(G, E, \partial \to 1_G, \triangleright \to \mathrm{id})$, with $\partial(e) = 1_G \ \forall\, e \in E$. Because the groups G and E are the same as in the original model, the Hilbert spaces of the models based on the two crossed modules are the same. However, in the new model the image of ∂ is $\partial(E) = \{\, 1_G \,\}$ and the kernel is $\ker(\partial) = E$. This indicates (from our analysis on the ribbons in Sec. III) that there should be no condensation or confinement. In this unconfined model E and G completely decouple in the energy terms. The vertex term and plaquette terms become the equivalent terms from Kitaev's quantum double model [37]. In addition, the edge transform now only affects the surface labels. We can therefore consider this model as a copy of Kitaev's quantum double model describing the edge elements combined with an independent model describing the surface elements. The surface elements are fluctuated by the edge transforms. Following the arguments in Sec. VI B 2, but taking $\partial \to 1_G$, the edge terms project to states where the plaquettes are all labeled by the same irrep of E in the irrep basis, with the choice of that irrep describing the various ground states on the sphere.

Because of this decoupling of the surface and edge elements, the G-valued excitations (the electric and magnetic excitations) are exactly the same as in Kitaev's quantum double model [37], with no confinement. In particular, the ribbon algebra is the same and the ribbons only fail to commute with vertex and plaquette terms at the end sites of the ribbon. Then, following the methods of Bombin and Martin-Delgado [36], we can find the measurement operators that detect the charges labeled by objects in G. As we show in Sec. S-V B in the Supplemental Material [45], the relevant closed ribbon projectors are labeled by two quantities. The first label is a conjugacy class C of G. Given such a conjugacy class, we choose a representative r_C. We can then construct the centralizer N_C of that representative, which is the subgroup formed by elements that commute with r_C. The centralizers of different representatives of the conjugacy class are isomorphic, so the choice of representative is not significant. Then we can construct irreps of this centralizer. The irrep R of the centralizer is the second label for our projector. The measurement operators on a closed ribbon σ are then given by

$$K_\sigma^{RC} := \frac{|R|}{|N_C|} \sum_{D \in (N_C)_{cj}} \overline{\chi}_R(D) K_\sigma^{DC}, \tag{57}$$

where

$$K_\sigma^{DC} := \sum_{q \in Q_C} \sum_{d \in D} F_\sigma^{qdq^{-1}, q r_C q^{-1}}, \tag{58}$$

just like the equivalent operators for the quantum double model found in Ref. [36]. Here $(N_C)_{cj}$ is the set of conjugacy classes of the centralizer N_C, $|N_C|$ is the size of N_C, χ_R is the character of irrep R, and Q_C is a set of representatives of the quotient group G/N_C, so that for each $c_i \in C$ there is a unique $q_i \in Q_C$ such that $c_i = q_i r_C q_i^{-1}$. $F_\sigma^{h,g}$ is the combined electric and magnetic ribbon that we defined at the end of Sec. III B (where the first argument in the superscript corresponds to the magnetic part and the second argument corresponds to the electric part). Then, substituting the expression for K_σ^{DC} into the one for K_σ^{RC}, we see that

$$K_\sigma^{RC} = \frac{|R|}{|N_C|} \sum_{D \in (N_C)_{cj}} \overline{\chi}_R(D) \sum_{q \in Q_C} \sum_{d \in D} F_\sigma^{qdq^{-1}, q r_C q^{-1}}. \tag{59}$$

The set of these operators over each conjugacy class and irrep of the centralizer of that conjugacy class (defined as the centralizer of the fixed representative) form a set of orthogonal projectors that make up a resolution of the identity, as described in Ref. [36].

From the fact that both the braiding (as described in Sec. V A) and the topological charge projectors match those from Kitaev's quantum double model in the uncondensed case when $\triangleright$ is trivial, we infer that the phase described by the uncondensed model is the same as the quantum double model with group G, albeit with an additional symmetry described by the group E.

A. Condensation

We have now constructed the topological charges for our uncondensed model. We can then use these charge measurement operators to see which of these charges condense in our original model (where ∂ need not be trivial, though we still require $\triangleright$ to be trivial). Because the ground state is the topological vacuum of the model, any charges which are present in the ground state of the condensed model must have (at least partially) condensed. Therefore, we must calculate the expectation value of the charge measurement operators to see which charges have condensed. That is, we must work out

$$\left\langle K_\sigma^{RC} \right\rangle := \langle GS | K_\sigma^{RC} | GS \rangle,$$

where K_σ^{RC} is a measurement operator in the uncondensed model and $|GS\rangle$ is a ground state of the condensed model.

We have

$$\begin{aligned}&\langle GS|K_\sigma^{RC}|GS\rangle\\&= \langle GS|\frac{|R|}{|N_C|}\sum_{D\in(N_C)_{cj}}\overline{\chi}_R(D)\sum_{q\in Q_C}\sum_{d\in D}F_\sigma^{qdq^{-1},qr_Cq^{-1}}|GS\rangle\\&= \langle GS|\frac{|R|}{|N_C|}\sum_{D\in(N_C)_{cj}}\overline{\chi}_R(D)\sum_{q\in Q_C}\sum_{d\in D}C^{qdq^{-1}}(\sigma)\\&\quad\times\delta(g(\sigma),qr_Cq^{-1})|GS\rangle.\end{aligned}$$

Then we use the fact that $C^h(\sigma)|GS\rangle = |GS\rangle$ for a closed, contractible ribbon, as established in Sec. S-II B of the Supplemental Material [45], to write

$$\begin{aligned}&\langle GS|K_\sigma^{RC}|GS\rangle\\&= \langle GS|\frac{|R|}{|N_C|}\sum_{D\in(N_C)_{cj}}\overline{\chi}_R(D)\sum_{q\in Q_C}\sum_{d\in D}\delta(g(\sigma),qr_Cq^{-1})|GS\rangle\\&= \frac{|R|}{|N_C|}\sum_{D\in(N_C)_{cj}}\overline{\chi}_R(D)\sum_{q\in Q_C}\sum_{d\in D}\langle GS|\delta(g(\sigma),qr_Cq^{-1})|GS\rangle.\end{aligned}$$

Because σ is a contractible closed path, $g(\sigma)$ must be in $\partial(E)$ in the ground state due to fake flatness. Indeed, because the edge terms fluctuate the path element by all of the elements in $\partial(E)$, $g(\sigma)$ is equally likely to be any element of this subgroup. Therefore,

$$\langle GS|\delta(g(\sigma),qr_Cq^{-1})|GS\rangle = \frac{1}{|\partial(E)|}\delta(r_C\in\partial(E)).$$

The expectation value of the measurement operator is then

$$\begin{aligned}&\langle GS|K_\sigma^{RC}|GS\rangle\\&= \frac{|R|}{|N_C|}\sum_{D\in(N_C)_{cj}}\overline{\chi}_R(D)\sum_{q\in Q_C}\sum_{d\in D}\frac{1}{|\partial(E)|}\delta(r_C\in\partial(E)).\end{aligned}$$

When r_C is in $\partial(E)$, all elements of G commute with it [because $\partial(E)$ is in the center of G when $\triangleright$ is trivial] and so N_C is just G. This also means that Q_C is trivial and just includes the identity element. Therefore,

$$\begin{aligned}\langle GS|K_\sigma^{RC}|GS\rangle &= \frac{|R|}{|G|}\sum_{d\in G}\overline{\chi}_R(d)\frac{1}{|\partial(E)|}\delta(r_C\in\partial(E))\\&= \delta_{R,1_R}\frac{1}{|\partial(E)|}\delta(r_C\in\partial(E)),\end{aligned}$$

where in the last line we used the orthogonality of characters. The condensed charges are those for which this quantity is nonzero. Therefore, we see that the condensed charges are those where R is trivial and C is a subset of the image of ∂. If C is in $\partial(E)$, then C only contains a single element $\partial(e)$ because $\partial(E)$ is in the center of G. This means that the charge measurement operators for the condensed charges can be written in a simpler way as $K_\sigma^{1_{\text{Rep}},\{\partial(e)\}} = \frac{1}{|G|}\sum_{d\in G}F_\sigma^{d,\partial(e)}$. Consider how this measurement operator acts when it encloses an excitation (produced by some open ribbon operator). It checks that the path of the measurement operator (the closed ribbon operator) has a path element of $\partial(e)$. This isolates the case where the excitation has a magnetic label in $\partial(E)$. The closed ribbon operator also acts with an equal superposition of every magnetic operator. This checks that the electric part of the excitation is trivial, so that the excitation is pure magnetic. Then the condensed magnetic excitations, those measured by the closed ribbon operators with nonzero expectation in the ground state, are the pure magnetic ones with label in the image of ∂. This agrees with our discussion in Sec. III C, where we came to the same conclusion based on the ribbon operators that produce the corresponding excitations.

B. Confinement

In the previous section, we put the measurement operators of the uncondensed model into the condensed model to see which of the charges were condensed in the latter model. In this section, we look at the charges of the condensed model and see which of those are confined. To construct the topological charge measurement operators for the condensed model, we first throw out the ribbon operators that fail to commute with the edge terms. This is because our measurement operators must commute with all of the energy terms. We find that the remaining measurement operators are labeled by two objects, C and R. When we discussed the charge measurement operators for the uncondensed model, the appropriate label C was a conjugacy class of G. However, for a general model, the appropriate label C indicates a union of cosets, the "conjugacy class of cosets" that was discussed earlier in Sec. III C. Specifically, C labels a union of cosets $g\partial(E)$ for each g within a conjugacy class of G. We can also define the classes C with the following equivalence relation: $g \sim x\partial(e)gx^{-1}\ \forall\, x\in G,\ e\in E$. We choose for each such class a representative element $r_C \in G$. Then the second label of the measurement operator R is an irrep of the group N_C', where N_C' is the subgroup of G made up of elements g such that $gr_Cg^{-1}r_C^{-1}\in\partial(E)$. That is, N_C' is the subgroup of elements that commute with r_C up to an element of $\partial(E)$.

The measurement operator also depends on the symmetry state of the plaquette at the start and end of the ribbon. In Sec. VII, we discussed how there is a spontaneously broken symmetry, and the plaquettes in the different states correspond to different irreps of the kernel of ∂. If the plaquette is labeled by the trivial irrep, then the projectors to definite topological charge are defined by

$$K_\sigma^{RC} := \frac{|R|}{|N_C'|}\sum_{D\in(N_C')_{\text{cj}}}\overline{\chi}_R(D)K_\sigma^{DC}, \tag{60}$$

where $(N_C')_{\text{cj}}$ is the set of conjugacy classes of N_C' (so that each D is a conjugacy class), $|R|$ is the dimension of irrep R, and K_σ^{DC} is given by

$$\begin{aligned}K_\sigma^{DC} := &\sum_{q\in Q_C}\sum_{d\in D}\sum_{h\in\partial(E)}F_\sigma^{qdq^{-1},qr_Cq^{-1}h}M^{f(r_C,d)^{-1}}(p)\\&\times\frac{1}{|\ker(\partial)|}\sum_{e_k\in\ker(\partial)}M^{e_k}(p).\end{aligned} \tag{61}$$

Here Q_C is a set of representatives of the quotient group G/N_C', and conjugating r_C by each element $q\in Q_C$ generates all elements of the equivalence class C up to factors in $\partial(E)$. $M^{f(r_C,d)^{-1}}(p)$ is a single-plaquette multiplication operator that multiplies the first plaquette on the ribbon p (the start and end

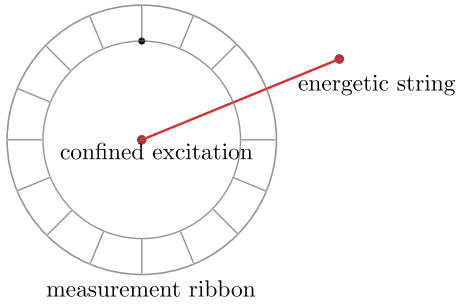

FIG. 50. If our measurement operator encloses a confined excitation (or multiple such excitations), the energetic string dragged by this excitation will pass through our measurement ribbon and cause an edge to be excited.

plaquettes for the closed ribbon) by an element $f(r_C, d)^{-1}$ such that $\partial(f(r_C, d)) = r_C d r_C^{-1} d^{-1}$. This means that the topological charge projector labeled by union C of cosets and irrep R of N'_C is given by the following:

Topological charge projectors

$$K_\sigma^{RC} = \frac{|R|}{|N'_C|} \sum_{D\in(N'_C)_{\text{cj}}} \overline{\chi}_R(D) \sum_{q\in Q_C} \sum_{d\in D} \sum_{h\in\partial(E)} F_\sigma^{qdq^{-1}, qr_Cq^{-1}h} \times M^{f(r_C,d)^{-1}}(p) \frac{1}{|\ker(\partial)|} \sum_{e_k\in\ker(\partial)} M^{e_k}(p). \tag{62}$$

In Sec. S-V B of the Supplemental Material [45], we prove that these are indeed orthogonal projectors. In addition, we construct the projectors corresponding to other symmetry states of the plaquette p (by applying the symmetry operators U^ν from Sec. VII).

Having found the projectors to definite topological charge, we want to consider which charges are confined. When we measure a confined charge, there will always be a violation of one or more energy terms on the measurement ribbon, due to the presence of the confining string. Given that we expect confinement to be due to the edge terms (from our discussion of the ribbon operators), we expect that at least one of the outward-pointing edges on our ribbon should be violated in the measured state. An example situation is shown in Fig. 50.

We can therefore check whether a charge is confined by applying a product of all of the edge terms cut by the dual path of the ribbon σ. For a confined charge, at least one of the edges must be excited and so the state must be an eigenstate where one of the edge terms has eigenvalue zero. This means that the product of edge terms will give zero. That is, whenever the state being measured has definite topological charge labeled by R and C, so that $K_\sigma^{RC}|\psi\rangle = |\psi\rangle$, if R and C correspond to a confined charge we must have $\prod_{i\in\sigma} \mathcal{A}_i|\psi\rangle = 0$. This means that the product of operators $\prod_{i\in\sigma} \mathcal{A}_i K_\sigma^{RC}$ must give zero because K_σ^{RC} projects to states for which the product of edge terms gives zero (and the edge terms commute with the measurement operator). On the other hand, if a charge is not confined, then a state $|\psi\rangle$ with that charge enclosed by the ribbon (and no other excitations near the ribbon) will satisfy

$$\prod_{i\in\sigma} \mathcal{A}_i|\psi\rangle = |\psi\rangle$$

because the edges will not be excited. Instead of considering a product of the edge terms, we can consider a product of edge transforms, which also leaves the state invariant when the edges are unexcited (because any edge transforms on unexcited edges leave the state invariant). We consider the product

$$\prod_{i\in\sigma} \mathcal{A}_i^e,$$

where we assume that all of the edges i point outwards (we would simply replace e with e^{-1} for any edge that pointed inwards). Then the state $|\psi\rangle$ corresponding to an unconfined charge within σ must satisfy

$$\prod_{i\in\sigma} \mathcal{A}_i^e|\psi\rangle = |\psi\rangle.$$

This implies that for an arbitrary state $|\psi\rangle$ we must have

$$\prod_{i\in\sigma} \mathcal{A}_i^e K_\sigma^{RC}|\psi\rangle = K_\sigma^{RC}|\psi\rangle,$$

where R and C label an unconfined charge, because K_σ^{RC} projects to states which correspond to that unconfined charge.

We now wish to use this fact to identify the confined charges. As we prove in Sec. S-III in the Supplemental Material [45], any magnetic ribbon with label in $\partial(E)$ can be written as a product of edge transforms, multiplied by two operators at the ends of the ribbon that change the labels of the plaquettes at each end. In that section, we consider open ribbons. However, for closed ribbons, the two end plaquettes are at the same place and the two single-plaquette multiplication operators will cancel out. This means that any closed magnetic ribbon operator with label in $\partial(E)$ can be expressed simply as a product of edge transforms. The converse is also true, and a product of edge transforms along the dual path of a ribbon can be written as a condensed closed magnetic ribbon operator. That is, given a closed ribbon σ where all of the edges cut by the dual path of the ribbon point outwards (away from the direct path of the ribbon), we have

$$C^{\partial(e)}(\sigma) = \prod_{i\in\sigma} \mathcal{A}_i^e. \tag{63}$$

If some of the edges instead pointed inwards (towards the direct path), we would simply have to change the label e to e^{-1} for those edges in the right-hand side of this equation. We can use this result to write the condition for the unconfined charges as

$$C^{\partial(e)}(\sigma) K_\sigma^{RC}|\psi\rangle = K_\sigma^{RC}|\psi\rangle.$$

Writing the condition in this way is useful because we can combine $C^{\partial(e)}(\sigma)$ with K_σ^{RC}, using our algebra of operators, to

obtain a condition on K_σ^{RC} itself. We have

$$C^{\partial(e)}(\sigma)K_\sigma^{RC} = \frac{|R|}{|N_C'|}\sum_{D\in(N_C')_{\mathrm{cj}}}\overline{\chi}_R(D)\sum_{q\in Q_C}\sum_{d\in D}\sum_{h\in\partial(E)} C^{\partial(e)}(\sigma)F_\sigma^{qdq^{-1},qr_Cq^{-1}h}M^{f(r_C,d)^{-1}}(p)\frac{1}{|\ker(\partial)|}\sum_{e_k\in\ker(\partial)}M^{e_k}(p)$$
$$= \frac{|R|}{|N_C'|}\sum_{d\in N_C'}\overline{\chi}_R(d)\sum_{q\in Q_C}\sum_{h\in\partial(E)} F_\sigma^{\partial(e)qdq^{-1},qr_Cq^{-1}h}M^{f(r_C,d)^{-1}}(p)\frac{1}{|\ker(\partial)|}\sum_{e_k\in\ker(\partial)}M^{e_k}(p),$$

where for convenience we replaced the sum over conjugacy classes D of N_C' and elements d in that conjugacy class with a single sum over elements of N_C'. Because $\partial(E)$ is in the center of G (due to $\triangleright$ being trivial), we can commute $\partial(e)$ next to d in the label of $F_\sigma^{\partial(e)qdq^{-1},qr_Cq^{-1}h}$. Then we can replace the dummy variable d with $d' = \partial(e)d$ [because $\partial(e)$ is in the center of G, d' will also be in N_C'], to obtain $F_\sigma^{qd'q^{-1},qr_Cq^{-1}h}$. The fact that $\partial(e)$ commutes with all elements of G also means that $f(r_C,d)$ can be chosen to be the same as $f(r_C,d')$ (recall that $f(r_C,d)$ satisfies $\partial(f(r_C,d)) = r_Cdr_C^{-1}d^{-1}$, which is the same as $r_Cd'r_C^{-1}d'^{-1}$). This gives us

$$C^{\partial(e)}(\sigma)K_\sigma^{RC} = \frac{|R|}{|N_C'|}\sum_{d'=\partial(e)d\in N_C'}\overline{\chi}_R(\partial(e)^{-1}d')\sum_{q\in Q_C}\sum_{h\in\partial(E)} F_\sigma^{qd'q^{-1},qr_Cq^{-1}h}M^{f(r_C,d')^{-1}}(p)\frac{1}{|\ker(\partial)|}\sum_{e_k\in\ker(\partial)}M^{e_k}(p).$$

We can split the character $\overline{\chi}_R(\partial(e)^{-1}d')$ into the contributions from $\partial(e)$ and d':

$$\overline{\chi}_R(\partial(e)^{-1}d') = \sum_{c=1}^{|R|}[D^R(\partial(e)^{-1}d')]_{cc}^* = \sum_{c=1}^{|R|}\sum_{a=1}^{|R|}[D^R(\partial(e)^{-1})]_{ca}^*[D^R(d')]_{ac}^*.$$

We can then use the fact that $\partial(E)$ is in the center of G (which also means that it is always in N_C') to simplify this expression. From Schur's lemma,

$$[D^R(\partial(e)^{-1})]_{ac}^* = \delta_{ac}[D^R(\partial(e)^{-1})]_{11}^*$$

(because the matrix must be a scalar multiple of the identity). We can then define an irrep of $\partial(E)$, $R_\partial^{\mathrm{irr.}}$, by

$$R_\partial^{\mathrm{irr.}}(\partial(e)) = [D^R(\partial(e))]_{11},$$

as we have before in Sec. III A when discussing the electric excitations. We then have

$$\overline{\chi}_R(\partial(e)^{-1}d') = \sum_{c=1}^{|R|}\sum_{a=1}^{|R|}R_\partial^{\mathrm{irr.}}(\partial(e^{-1}))^*\delta_{ac}(D^R(d'))_{ac}^* = R_\partial^{\mathrm{irr.}}(\partial(e^{-1}))^*\sum_{c=1}^{|R|}(D^R(d'))_{cc}^* = R_\partial^{\mathrm{irr.}}(\partial(e))\overline{\chi}_R(d').$$

This then implies that

$$C^{\partial(e)}(\sigma)K_\sigma^{RC} = \frac{|R|}{|N_C'|}\sum_{d'=\partial(e)d\in N_C'}\overline{\chi}_R(\partial(e)^{-1}d')\sum_{q\in Q_C}\sum_{h\in\partial(E)} F_\sigma^{qd'q^{-1},qr_Cq^{-1}h}M^{f(r_C,d')^{-1}}(p)\frac{1}{|\ker(\partial)|}\sum_{e_k\in\ker(\partial)}M^{e_k}(p)$$
$$= R_\partial^{\mathrm{irr.}}(\partial(e))\frac{|R|}{|N_C'|}\sum_{d'\in N_C'}\overline{\chi}_R(d')\sum_{q\in Q_C}\sum_{h\in\partial(E)} F_\sigma^{qd'q^{-1},qr_Cq^{-1}h}M^{f(r_C,d')^{-1}}(p)\frac{1}{|\ker(\partial)|}\sum_{e_k\in\ker(\partial)}M^{e_k}(p)$$
$$= R_\partial^{\mathrm{irr.}}(\partial(e))K_\sigma^{RC}. \tag{64}$$

We see that K_σ^{RC} is left invariant, and so the charge labeled by the pair R and C is unconfined, when $R_\partial^{\mathrm{irr.}}(\partial(e)) = 1$ for each $e\in E$, i.e., when the irrep $R_\partial^{\mathrm{irr.}}$ is trivial. This gives us a simple way to check, from the label of a charge, that the charge is unconfined.

From the above argument, we may expect that charges with irrep label R corresponding to a nontrivial irrep $R_\partial^{\mathrm{irr.}}$ of $\partial(E)$ are confined. We can check this directly to make sure that the charges are always definitely confined or definitely unconfined (rather than confinement depending on some internal space of the charge) as we expect. As discussed previously, for a confined charge applying the edge terms on each of the edges surrounding the measurement region will give us zero because at least one of the outwards edges must be excited. That is, $\prod_{i\in\sigma}\mathcal{A}_iK_\sigma^{RC} = 0$. We know that we can extract from the edge term $\mathcal{A}_i$ any edge transform: $\mathcal{A}_i = \mathcal{A}_i\mathcal{A}_i^e$. Therefore, our operator to check whether any of the edges of our ribbon are excited can be written as

$$\prod_{i\in\sigma}\mathcal{A}_i = \prod_{i\in\sigma}\mathcal{A}_i\prod_{i'\in\sigma}\mathcal{A}_{i'}^e = \frac{1}{|E|}\sum_{e\in E}\prod_{i\in\sigma}\mathcal{A}_i\prod_{i'\in\sigma}\mathcal{A}_{i'}^e.$$

Then using this form and Eq. (63), we see that

$$\prod_{i\in\sigma}\mathcal{A}_iK_\sigma^{RC} = \prod_{i\in\sigma}\mathcal{A}_i\frac{1}{|E|}\sum_{e\in E}\prod_{i'\in\sigma}\mathcal{A}_{i'}^eK_\sigma^{RC}$$
$$= \prod_{i\in\sigma}\mathcal{A}_i\frac{1}{|E|}\sum_{e\in E}C^{\partial(e)}(\sigma)K_\sigma^{RC}$$
$$= \prod_{i\in\sigma}\mathcal{A}_i\frac{1}{|E|}\frac{|E|}{|\partial(E)|}\sum_{h\in\partial(E)}C^h(\sigma)K_\sigma^{RC}.$$

Using Eq. (64), this implies that

$$\prod_{i\in\sigma}\mathcal{A}_i K_\sigma^{RC} = \prod_{i\in\sigma}\mathcal{A}_i \frac{1}{|\partial(E)|}\sum_{h\in\partial(E)} R_\partial^{\text{irr.}}(h^{-1})K_\sigma^{RC}$$
$$= 0 \text{ iff } R_\partial^{\text{irr.}} \text{ is not the trivial irrep.}$$

This indicates that the charges with nontrivial irreps of $\partial(E)$ are confined, as we expect from our discussion of ribbon operators in Sec. III A, where we saw that electric ribbon operators labeled by such irreps are confined.

So far we have not related the labels of the ribbon operators to the labels of the topological charge carried by the excitations they produce. However, in Sec. S-V C in the Supplemental Material [45], we use the charge measurement operators to verify our intuition about the charge carried by electric and magnetic excitations. For example, by applying the measurement operator around an excitation produced by a pure electric ribbon labeled by irrep R_x of G, and matrix indices a and b, we find that such an excitation has label C given by the class containing the identity 1_G (this class is the image of ∂). We then find that the second label R is R_x or $\overline{R_x}$ depending on whether we measure the excitation at the start or the end of the ribbon. This matches our intuition that the irrep, and not the matrix indices a and b, should label the topological charge.

X. CONCLUSION

The (2+1)D higher-lattice gauge theory model is interesting, in that it contains features outside those from the more heavily studied string-net and Kitaev quantum double models. Here we have been able to study many of these properties in two cases: one where $\triangleright$ is trivial and one where we restrict to fake-flat configurations. By constructing the ribbon operators that produce the pointlike excitations, we found that these particles are analogous to the electric and magnetic excitations from Kitaev's quantum double model [37]. Unlike the excitations in the quantum double model, however, some of the anyons in the higher-lattice gauge theory model are confined, and others are condensed, in a similar way to the excitations from Ref. [36]. In the $\triangleright$ trivial case, we were able to discuss this in terms of a condensation-confinement transition, just as we did for the (3+1)D case in Ref. [44]. We also used the ribbon operators to find the braiding relations of these pointlike excitations, which are analogous to those for Kitaev's model [37], and to construct the projectors to definite topological charge (following the method used in Ref. [36]).

One intriguing feature of the (2+1)D higher-lattice gauge theory model is that, despite being in (2+1)D, there are looplike excitations that are produced by membrane operators. We found that, when $\triangleright$ is trivial, these looplike excitations can be interpreted in terms of two distinct phenomena. First, some of the loop excitations correspond to confined versions of the electric excitations which are produced pairwise and separated, before being recombined, thereby dragging an energetic string which connects into a loop. More interestingly, some of the looplike excitations can be interpreted as domain walls between patches of lattice corresponding to different ground states (with general looplike excitations made from a combination of the two types). This revealed the presence of a symmetry, which leads to multiple ground states even on a spherical spatial manifold. Therefore, at least under certain circumstances, the lattice model represents a symmetry-enriched topological phase (SET phase). We further confirmed this by mapping a subset of the higher-lattice gauge theory models (where $\triangleright$ is trivial and we further make ∂ injective) to a subset of the symmetry-enriched string-net models from Ref. [16]. However, unlike in the wider class of symmetry-enriched string-net models, the symmetry in the higher-lattice gauge theory models never permutes the anyon types (at least in the cases we were able to study in detail).

This leads us to an interesting avenue for potential further study: We have found a tidy interpretation of the higher-lattice gauge theory model in (2+1)D in terms of a SET phase only when $\triangleright$ is trivial. It would be interesting to further study the case where $\triangleright$ is nontrivial (beyond the examples considered in Sec. VI A, as well as Sec. S-VII of the Supplemental Material [45]), if a method for dealing with the inconsistency under changes to the branching structure can be found. Furthermore, the fact that the symmetry in the cases where $\triangleright$ is trivial does not permute the anyon types raises the question of whether there is an extension to this model which does allow the symmetry to permute anyon type.

In compliance with EPSRC policy framework on research data, this publication is theoretical work that does not require supporting research data.

ACKNOWLEDGMENTS

We would like to thank J. Faria Martins and A. Bullivant for informative discussions about the higher-lattice gauge theory model. We are also grateful to P. Fendley for advice on the preparation of this series of papers. We acknowledge support from EPSRC Grant No. EP/S020527/1.

[1] A. Bullivant, M. Calcada, Z. Kadar, P. Martin, and J. F. Martins, Topological phases from higher gauge symmetry in 3+1D, Phys. Rev. B **95**, 155118 (2017).

[2] A. Bullivant, J. F. Martins, and P. Martin, Representations of the loop braid group and Aharonov-Bohm like effects in discrete (3+1)-dimensional higher gauge theory, Adv. Theor. Math. Phys. **23**, 1685 (2019).

[3] A. Bullivant and C. Delcamp, Excitations in strict 2-group higher gauge models of topological phases, J. High Energy Phys. 01 (2019) 107.

[4] A. Bullivant, M. Calcada, Z. Kadar, P. Martin, and J. Faria Martins, Higher lattices, discrete two-dimensional holonomy and topological phases in (3+1)D with higher gauge symmetry, Rev. Math. Phys. **32**, 2050011 (2020).

[5] C. Delcamp and A. Tiwari, From gauge to higher gauge models of topological phases, J. High Energy Phys. 10 (2018) 049.

[6] C. Delcamp and A. Tiwari, On 2-form gauge models of topological phases, J. High Energy Phys. 05 (2019) 064.

[7] V. Koppen, J. F. Martins, and P. P. Martin, Exactly solvable models for 2+1D topological phases derived from crossed modules of semisimple Hopf algebras, arXiv:2104.02766.

[8] S. Gukov and A. Kapustin, Topological quantum field theory, nonlocal operators, and gapped phases of gauge theories, arXiv:1307.4793.

[9] A. Kapustin and R. Thorngren, Topological field theory on a lattice, discrete theta-angles and confinement, Adv. Theor. Math. Phys. **18**, 1233 (2014).

[10] A. Kapustin and R. Thorngren, Higher symmetry and gapped phases of gauge theories, in *Algebra, Geometry, and Physics in the 21st Century: Kontsevich Festschrift*, edited by D. Auroux, L. Katzarkov, T. Pantev, Y. Soibelman, and Y. Tschinkel (Springer, Cham, 2017), pp. 177–202.

[11] A. Mesaros and Y. Ran, Classification of symmetry enriched topological phases with exactly solvable models, Phys. Rev. B **87**, 155115 (2013).

[12] X. Chen, Z.-C. Gu, Z.-X. Liu, and X.-G. Wen, Symmetry protected topological orders and the group cohomology of their symmetry group, Phys. Rev. B **87**, 155114 (2013).

[13] X. Chen, Z.-C. Gu, and X.-G. Wen, Local unitary transformation, long-range quantum entanglement, wave function renormalization, and topological order, Phys. Rev. B **82**, 155138 (2010).

[14] X.-G. Wen, Quantum orders and symmetric spin liquids, Phys. Rev. B **65**, 165113 (2002).

[15] M. Barkeshli, P. Bonderson, M. Cheng, and Z. Wang, Symmetry fractionalization, defects, and gauging of topological phases, Phys. Rev. B **100**, 115147 (2019).

[16] C. Heinrich, F. Burnell, L. Fidkowski, and M. Levin, Symmetry enriched string-nets: Exactly solvable models for SET phases, Phys. Rev. B **94**, 235136 (2016).

[17] Y.-M. Lu and A. Vishwanath, Classification and properties of symmetry-enriched topological phases: Chern-Simons approach with applications to Z_2 spin liquids, Phys. Rev. B **93**, 155121 (2016).

[18] J. Maciejko, X.-L. Qi, A. Karch, and S.-C. Zhang, Fractional topological insulators in three dimensions, Phys. Rev. Lett. **105**, 246809 (2010).

[19] B. Swingle, M. Barkeshli, J. McGreevy, and T. Senthil, Correlated topological insulators and the fractional magnetoelectric effect, Phys. Rev. B **83**, 195139 (2011).

[20] M. Levin and A. Stern, Classification and analysis of two-dimensional Abelian fractional topological insulators, Phys. Rev. B **86**, 115131 (2012).

[21] A. M. Essin and M. Hermele, Classifying fractionalization: Symmetry classification of gapped $\mathbb{Z}_2$ spin liquids in two dimensions, Phys. Rev. B **87**, 104406 (2013).

[22] J. C. Y. Teo, T. L. Hughes, and E. Fradkin, Theory of twist liquids: Gauging an anyonic symmetry, Ann. Phys. **360**, 349 (2015).

[23] N. Tarantino, N. H. Lindner, and L. Fidkowski, Symmetry fractionalization and twist defects, New J. Phys. **18**, 035006 (2016).

[24] L. Chang, M. Cheng, S. X. Cui, Y. Hu, W. Jin, R. Movassagh, P. Naaijkens, Z. Wang, and A. Young, On enriching the Levin–Wen model with symmetry, J. Phys. A: Math. Theor. **48**, 12FT01 (2015).

[25] M. Hermele, String flux mechanism for fractionalization in topologically ordered phases, Phys. Rev. B **90**, 184418 (2014).

[26] T. Lan, L. Kong, and X.-G. Wen, Classification of (2+1)-dimensional topological order and symmetry-protected topological order for bosonic and fermionic systems with on-site symmetries, Phys. Rev. B **95**, 235140 (2017).

[27] X.-G. Wen, Colloquium: Zoo of quantum-topological phases of matter, Rev. Mod. Phys. **89**, 041004 (2017).

[28] L.-Y. Hung and X.-G. Wen, Quantized topological terms in weak-coupling gauge theories with a global symmetry and their connection to symmetry-enriched topological phases, Phys. Rev. B **87**, 165107 (2013).

[29] L. Y. Hung and Y. Wan, K matrix construction of symmetry-enriched phases of matter, Phys. Rev. B **87**, 195103 (2013).

[30] M. A. Levin and X.-G. Wen, String-net condensation: A physical mechanism for topological phases, Phys. Rev. B **71**, 045110 (2005).

[31] F. A. Bais and J. K. Slingerland, Condensate induced transitions between topologically ordered phases, Phys. Rev. B **79**, 045316 (2009).

[32] F. J. Burnell, Anyon condensation and its applications, Annu. Rev. Condens. Matter Phys. **9**, 307 (2018).

[33] T. Neupert, H. He, C. von Keyserlingk, G. Sierra, and B. A. Bernevig, Boson condensation in topologically ordered quantum liquids, Phys. Rev. B **93**, 115103 (2016).

[34] F. A. Bais, B. J. Schroers, and J. K. Slingerland, Hopf symmetry breaking and confinement in (2+1)-dimensional gauge theory, J. High Energy Phys. 05 (2003) 068.

[35] I. S. Eliëns, J. C. Romers, and F. A. Bais, Diagrammatics for Bose condensation in anyon theories, Phys. Rev. B **90**, 195130 (2014).

[36] H. Bombin and M. A. Martin-Delgado, Family of non-Abelian Kitaev models on a lattice: Topological condensation and confinement, Phys. Rev. B **78**, 115421 (2008).

[37] A. Y. Kitaev, Fault-tolerant quantum computation by anyons, Ann. Phys. **303**, 2 (2003).

[38] D. C. Tsui, H. L. Stormer, and A. C. Gossard, Two-dimensional magnetotransport in the extreme quantum limit, Phys. Rev. Lett. **48**, 1559 (1982).

[39] X.-G. Wen and Q. Niu, Ground state degeneracy of the FQH states in presence of random potential and on high genus Riemann surfaces, Phys. Rev. B **41**, 9377 (1990).

[40] A. Stern, Anyons and the quantum Hall effect - A pedagogical review, Ann. Phys. **323**, 204 (2008).

[41] T. Chakraborty and P. Pietlinen, *The Quantum Hall Effects: Integral and Fractional*, 2nd ed., Springer Series in Solid-State Sciences (Springer, New York, 1995).

[42] S. D. Sarma and A. Pinczuk, *Perspectives in Quantum Hall Effects: Novel Quantum Liquids in Low-dimensional Semiconductor Structures* (Wiley, New York, 1997).

[43] K. J. Satzinger, Y. Liu, A. Smith, C. Knapp, M. Newman, C. Jones, Z. Chen, C. Quintana, X. Mi, A. Dunsworth *et al.*, Realizing topologically ordered states on a quantum processor, Science **374**, 1237 (2021).

[44] J. Huxford and S. H. Simon, preceding paper, Excitations in the higher-lattice gauge theory model for topological phases. I. Overview, Phys. Rev. B **108**, 245132 (2023).

[45] See Supplemental Material at http://link.aps.org/supplemental/10.1103/PhysRevB.108.245133 for various algebraic proofs that support the main text, in addition to a discussion of some cases where the magnetic excitations can be constructed even with a nontrivial map $\triangleright$.
[46] J. C. Baez, Higher Yang–Mills theory, arXiv:hep-th/0206130.
[47] H. Pfeiffer, Higher gauge theory and a non-Abelian generalization of 2-form electrodynamics, Ann. Phys. **308**, 447 (2003).
[48] A. Y. Kitaev, Anyons in an exactly solved model and beyond, Ann. Phys. **321**, 2 (2006).
[49] O. Buerschaper and M. Aguado, Mapping Kitaev's quantum double lattice models to Levin and Wen's string-net models, Phys. Rev. B **80**, 155136 (2009).
[50] A. H. Clifford, Representations induced in an invariant subgroup, Ann. Math. **38**, 533 (1937).
[51] J. Huxford and S. H. Simon, Excitations in the higher-lattice gauge theory model for topological phases III: The (3+1)D case, arXiv:2202.08294.
[52] J. M. Leinaas and J. Myrheim, On the theory of identical particles, Nuovo Cimento B **37**, 1 (1977).
[53] F. Wilczek, Magnetic flux, angular momentum, and statistics, Phys. Rev. Lett. **48**, 1144 (1982).
[54] S. Rao, An anyon primer, arXiv:hep-th/9209066.
[55] M. G. Alford, K.-M. Lee, J. March-Russell, and J. Preskill, Quantum field theory of non-abelian strings and vortices, Nucl. Phys. B **384**, 251 (1992).